

**Comment R2.1:** *This study analyses the global relationship between  $ET_o$  annual maps obtained by means of three different methods (ASCE PM, P-T and H-S), with the purpose of determining the accuracy of the methods based on poor data availability (P-T and H-S). In addition, the manuscript includes a calibration exercise to obtain revised coefficients at the global scale for P-T and H-S equations based on the obtained ASCE PM data. The research topic is highly relevant given the relevance of estimating the atmospheric evaporative demand (AED) with accuracy since AED is an important hydroclimatic variable with strong implications in aridity conditions and climate change processes. The manuscript is in general well written, the figures show high quality and it has a good structure. The authors use a high amount of data for analysis and validation, including gridded datasets and meteorological networks in California and Australia. The manuscript is a bit long and sometimes it is difficult to follow but independently of formal issues I find major methodological problems in the manuscript, which are related to the treatment of the data used, the spatial resolution of the gridded products and the assessment of the uncertainty in the  $ET_o$  estimations. I am including some detailed issues below about these issues.*

**Response:** We would like to thank the reviewer for the precise comments related to methodological problems since he gave us the opportunity to provide more justifications, clarifications and details about the methods and data used in this work. We carefully considered all the comments and we followed all his recommendations in order to improve the manuscript and reduce any uncertainties related to methodological issues about the spatial resolutions. More details are given to the responses of the following specific comments. We also suggest the reviewer to check carefully the responses to the comments of Reviewer 1, since his suggestions led to substantial changes in the manuscript.

**Comment R2.2:** *I would recommend the authors to work at coarser spatial resolution to reduce the strong uncertainty associated to the selected high resolution (1 km) of final products. Page 4: I find highly problematic to interpolate the low resolution  $0.5^\circ$  data for wind speed, humidity and solar radiation to 1 km. The results of the bilinear interpolation of the  $0.5^\circ$  data does not really increase the necessary spatial resolution of these variables to be compared with the high resolution of  $t_{max}$  and  $t_{min}$  data (in any case high resolution temperature data from the global dataset used is also affected by spatial errors and uncertainties, which should be also taken into account). The 1 km interpolated wind speed, humidity and solar radiation has a spatial resolution completely unreal. These variables are essential to be taken into account to estimate  $ET_o$  spatial patterns since  $ET_o$  is usually more sensitive to these variables than to temperature (McVicar et al., 2012a and b). For this reason, I consider that 1 km gridded maps generated in this study show high uncertainty, which is not quantified/provided in this study. The authors are computing  $ET_o$  by PM equation as reference to be compared with H-S and P-T methods, but there is not any assessment of the error in the PM estimations related to the data inaccuracies and the poor resolution of the input climate data. I think these problems would be solved (not completely since an assessment of uncertainty should be taken into account) if authors consider to focus at coarse ( $0.5^\circ$ ) spatial resolution, which avoids unnecessary interpolation of wind speed, radiation and humidity variables and the outputs would be useful for continental to global assessments. Thus, the results of figures 8-10 confirms that interpolation of low resolution variables have strong influence on the comparability of different  $ET_o$  estimations, which can be associated to the poor interpolation approach applied to the coarse climate variables.*

**Response:** We agree with the reviewer that the bilinear interpolation method may not be the most appropriate method to increase the resolution of wind speed, solar radiation and humidity data and we also agree that 1 km raster resolutions are in general an exaggeration for describing climatic variables. The basic reason that led us to show the results of both  $\sim 1$  km (30 arc-sec) and  $0.5$  deg was to cover the complete range of resolutions observed in the initial data. In addition, the aim was to provide  $ET_o$  rasters of 1 km for comparative purposes with other studies, which have also provided 1 km resolutions of global  $ET_o$  for the same period using other methods and the same sources of data. For example, Zomer et al. (2008) provided 1 km resolution maps using the Hargreaves-Samani method based on the temperature data of Hijmans et al. (2005). The bilinear interpolation used for global solar radiation, specific humidity and wind speed data of Sheffield et al. (2006) provided insignificant improvement but allowed to develop 1 km rasters of exact spatial arrangement with the 1 km rasters of temperature, especially in the coastlines and small islands. This has provided an improvement of  $\sim 4\%$  in the RMSE

of ASCE- $ET_o$  estimations obtained from the map, when compared with the respective values of stations (Fig.R1a,b). This improvement seems negligible for the total validation dataset, but it was significant when it was examined for some individual stations located in regions of 0.5 degree pixels with high internal topographic-temperature variability. In order to avoid any criticism about the interpolation method used for increasing the resolution of solar radiation, humidity and wind speed data, we decided to remove any results and discussion about the finer resolutions keeping only the results for 0.5 degree resolution. For this reason all the results and all the maps and tables presented in the revised version correspond only to the 0.5 deg resolution.

The comparisons between the  $ET_o$  values of rasters (0.5 degree) and stations for both reference crops were added in the supplementary material (see Fig.S2g,h) and their reference in the text can be found in Page 10, lines 25-26.

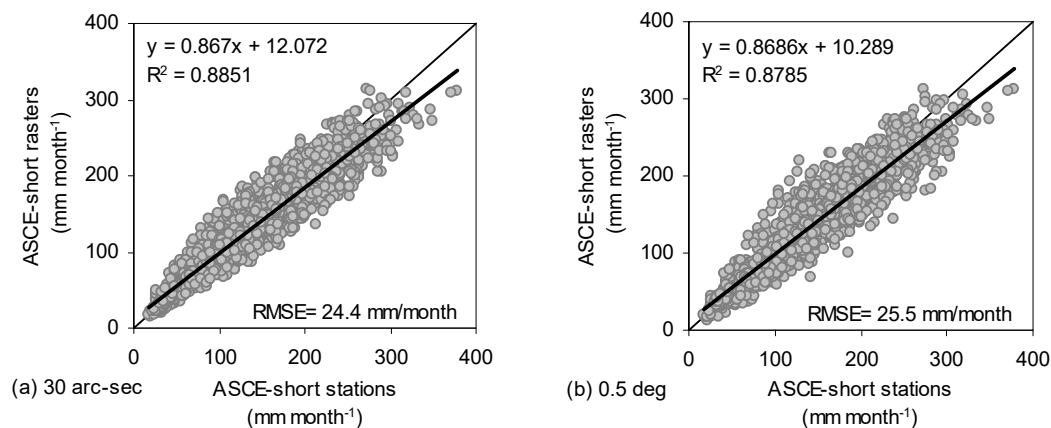


**Fig.R1** Comparison of  $ET_o$  ASCE-short values ( $\text{mm month}^{-1}$ ) between the 140 stations (both CA-USA and Australia stations) and (a) the produced rasters of 30 arc-sec resolution and (b) the produced rasters of 0.5 degree resolution.

The only reference about the finer resolutions is given in section 5. Data availability, where we added the following text “*Apart from the 0.5 degree resolution raster datasets, the database contains the same datasets at finer resolution (30 arc-sec, 2.5 arc-min, 5 arc-min and 10 arc-min). These finer datasets are provided in order to cover the observed resolution range in the initial climatic data (e.g. the temperature data of Hijmans et al. (2005) are provided at 30 arc-sec resolution). The finer resolutions were produced using bilinear interpolation on solar radiation, humidity and wind speed data of Sheffield et al. (2006). This interpolation method is not the most appropriate for such purposes. The data of finer resolutions can only be used as a tool to assess uncertainties associated to temperature variation effects within a 0.5 degree pixel or to estimate average values of the coefficients for larger territories in order to capture a better representation of the coastlines or islands that do not exist in 0.5 degree resolution (use of values from individual pixels is not recommended). A complete list of the datasets is provided in the Table S5.*”

**Comment R2.3:** *I have also doubts on the use of the coefficients calculated in this study to calculate  $ET_o$  using H-S and P-T equations. The authors obtain the calibration coefficients for the period 1950-2000 and assume stationary climate conditions. Nevertheless, under climate scenarios in which input climate variables change (I refer to wind speed, relative humidity and incoming solar radiation) under a non-stationary scenario, the obtained coefficients would not be useful to calculate  $ET_o$  based on scarce climate data. Different studies have showed recent changes in solar radiation (Wild et al., 2013), wind speed (McVicar et al., 2012b) and atmospheric humidity (Willet et al. 2014). Given that the main objective of this study is the re-calibration of the H-S and P-T equations, it would be necessary that authors provide not only the recalibrated coefficients but also a measure of the accuracy considering the errors in the interpolated variables used in P-M calculations.*

**Response:** We agree with the reviewer that climate change effects can significantly affect the prediction accuracy of the coefficients. This was the reason why we included data from 2000-2016 for all stations in the validation procedure (see periods of observations for each station in Table 1 of the manuscript). We also have to mention that more than 50% of stations in the total validation dataset have more data from years after 2000, while there are 4 stations with data only for the period ~2000-2016. Taking into account these specific features of the validation dataset, we cannot reject the hypothesis that the revised coefficients have a good explanatory power even for the years 2000-2016, since they improved significantly the  $ET_o$  predictions in comparison to the standard coefficients and gave better results from other models that use additional parameters (see new additional models in Table 2 and comparative results in Table 5 of the manuscript; the additional models were added after the request of Revier 1). We also thought to break the validation datasets into two periods (before and after 2000), since the produced  $ET_o$  rasters and the revised coefficients correspond to 1950-2000, but this idea could not be implemented for two reasons:

- The database of Australian stations provides freely available online only the mean monthly values of the parameters for the total periods of observations and not the complete records of monthly values for each specific year.
- The available data from CIMIS database for the stations of California-USA start after 1982 (Table 1 in the manuscript), and cover less than 36% of the total period 1950-2000, while they correspond to the late years of the specific period. It is well documented that climate differences were also observed even during the 1950-2000 (through comparisons between 1950-1975 and 1975-2000) in many parts of the world (Hang et al., 2000; Norrant and Douguédroit, 2006; Sheffield and Wood, 2008; You et al., 2011). Thus, we also did not divide the California-USA data into two periods in order to avoid any arguments that would probably occur based on the observation periods.

Since we followed the recommendation of the reviewer to remove the finer resolution results of 30 arc-sec (1 km) and present only the 0.5 degree results, we also performed an accuracy analysis for the internal parameters of ASCE- $ET_o$  between the values provided by the 0.5 degree rasters data (Hijmans et al. 2005; Sheffield et al. 2006) and the respective data of stations (Fig.R2 below). The temperature data of 30 arc-sec resolution were also converted to 0.5 deg for this analysis. Fig.R2a,b,c,d,e,f provides the respective comparisons for the mean monthly values of  $T_{max}$ ,  $T_{min}$ ,  $R_s$ ,  $R_n$ ,  $DE$  (vapour pressure deficit  $e_s-e_a$ ), and  $u_2$  between stations data and rasters of 0.5 degree resolution. The  $R_s$  values of both rasters and stations given in Fig.R2c are those after correcting the ones exceeding the clear sky solar radiation  $R_{so}$  (i.e. when  $R_s/R_{so}>1$ ,  $R_s=R_{so}$ ), as it is required before ASCE- $ET_o$  estimations (Allen et al., 1998; 2005). Additionally, the values of  $u_2$  given in Fig.R2f are those after adjusting the raster values of Sheffield et al. (2006) and Australia stations data from  $z=10$  m to 2 m height using the formula (Allen et al., 1998; 2005):

$$u_2 = u_z \frac{4.87}{\ln(67.8z - 5.42)} \quad (\text{Eq.R1})$$

The original wind data of Sheffield et al. (2006) and Australia stations are given for  $z=10$  m, while the data of California stations were already given at 2 m height.

The comparisons for the  $T_{max}$ ,  $T_{min}$ ,  $R_s$ ,  $R_n$ ,  $DE$  (vapour pressure deficit  $e_s-e_a$ ), and  $u_2$  between stations data and rasters of 0.5 degree resolution were added in the supplementary material (see Fig.S2a,b,c,d,e,f) and their reference in the text can be found in Page 10, lines 25-26.

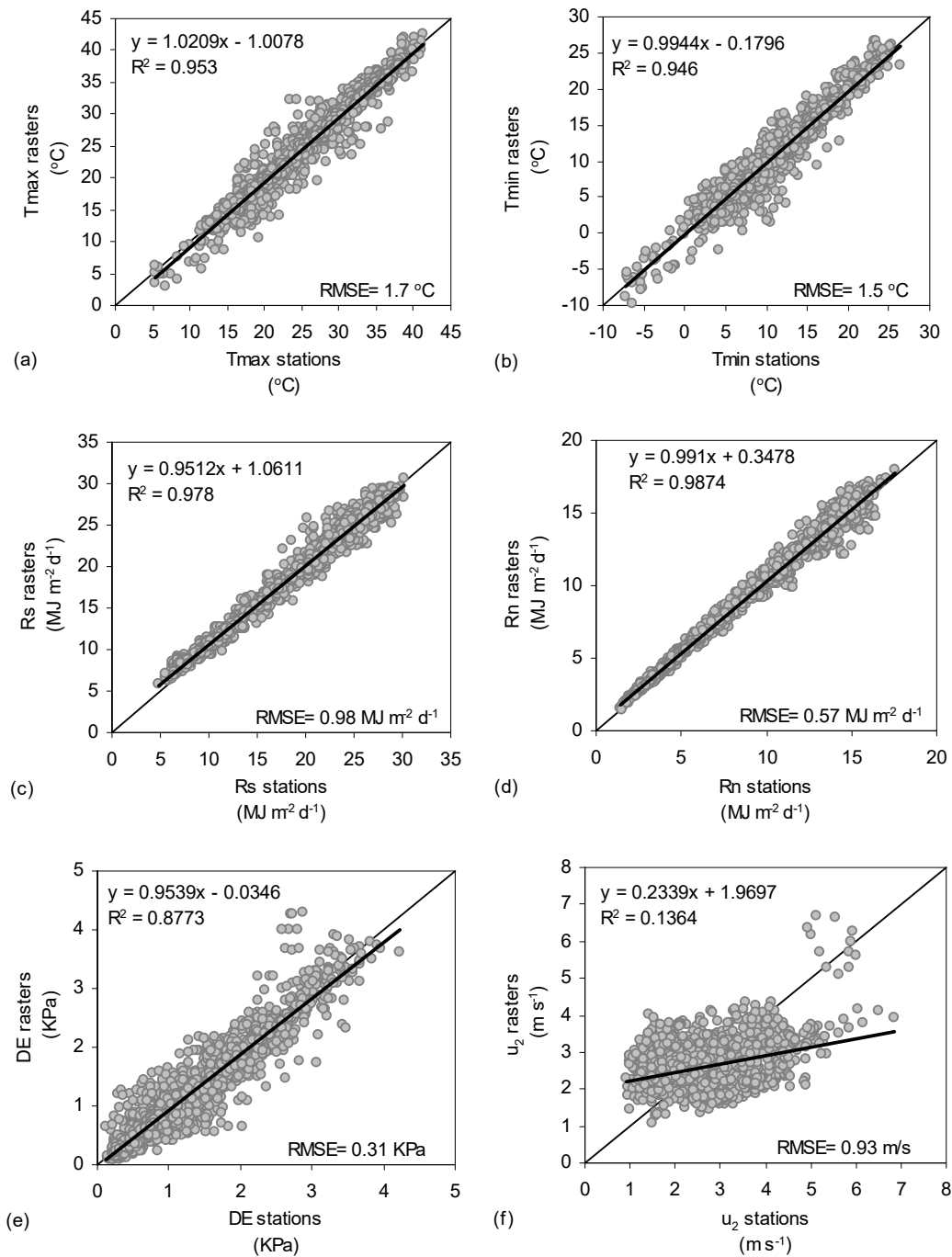


**Fig.R2** Comparison of mean monthly values between rasters data (0.5 degree resolution) and stations data for **(a)** the maximum monthly temperature  $T_{max}$ , **(b)** the minimum monthly temperature  $T_{min}$ , **(c)** the solar radiation  $R_s$ , **(d)** the net solar radiation  $R_n$ , **(e)** the vapour pressure deficit  $DE=e_s-e_a$ , and **(f)** the wind speed at 2 m height  $u_2$ .

For the cases of  $T_{max}$ ,  $T_{min}$ ,  $R_s$ ,  $R_n$  and  $DE$  (Fig.R2a,b,c,d,e), the comparisons between rasters and stations are satisfactory, if we consider that rasters provide values of 0.5 degree (~50 km) pixels of the period 1950-2000 while stations data cover also the period from 2000-2016. In the case of  $u_2$ , the correlation between rasters and stations data was not good. We examined with various ways the wind data in order to explain the possible sources of this problem. We derived some findings when comparing the mean monthly  $u_2$  values of all California-USA (Fig.R3a) and Australia (Fig.R3b) stations, separately. Fig.R3a shows that the total average raster values of mean monthly  $u_2$  from the pixel positions of CA-USA stations are higher than the respective measured  $u_2$  values, while in Fig.R3b

for Australia stations is observed the opposite trend. These differences are the main reason why the regression line in Fig.R2f is above the 45 degrees line for the values  $<2.5 \text{ m s}^{-1}$  (the majority of points belong to CA-USA stations) and below the 45 degrees line for the values  $>2.5 \text{ m s}^{-1}$  (the majority of points belong to Australia stations). This opposite trend between the two validation datasets was also the reason of the high RMSE in Fig.R2f. To avoid any possible misunderstanding that could arise from the merged California and Australia datasets, we also give the results of Fig.R1b separately for CA-USA and Australia stations in Fig.R4a,b, respectively. Despite the difference in  $u_2$  values between CA-USA stations and rasters (Figs.R3a), the regression line in Fig.R4a of  $ET_o$  presents a good slope and intercept probably because the wind differences are counterbalanced with differences in other parameters of  $ET_o$ . In the case of Australia stations (Fig.R4b), the higher observed  $u_2$  values from stations in comparison to rasters are probably the reason for the observed downward deviation of regression line from the 45° degrees line.

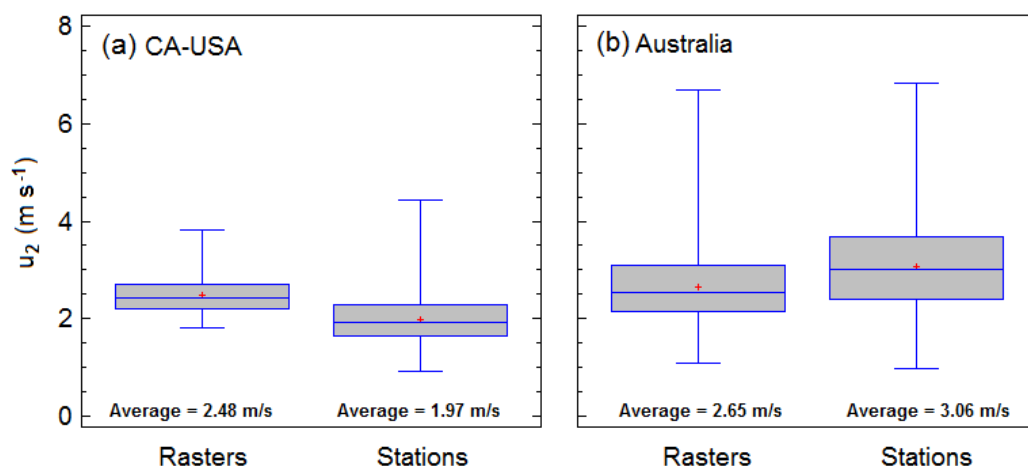


**Fig.R3** Comparison of mean monthly  $u_2$  values through Box-Whisker plots: (a) between 0.5 degree rasters (Sheffield et al., 2006) and California-USA stations, (b) between 0.5 degree rasters (Sheffield et al., 2006) and Australia stations.

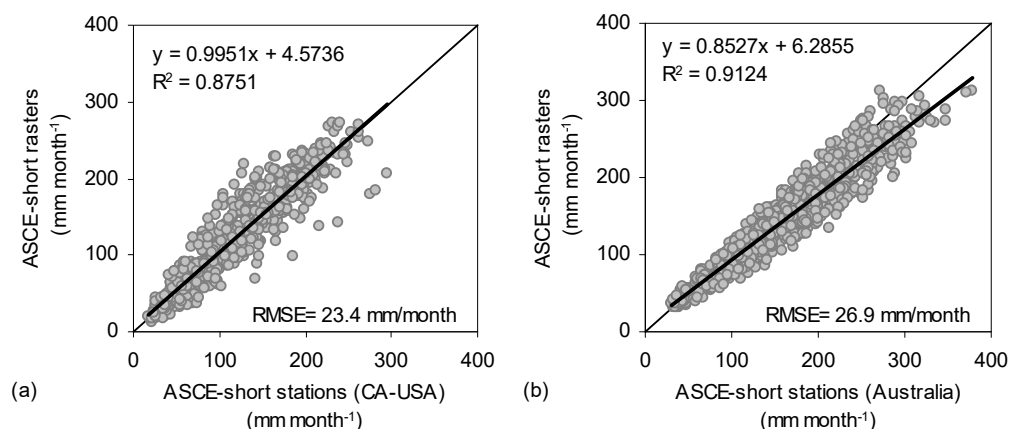


**Fig.R4** Comparison of  $ET_o$  ASCE-short values ( $\text{mm month}^{-1}$ ) between (a) the produced rasters of 0.5 degree and the 60 stations of CA-USA and (b) the produced rasters of 0.5 degree and the 80 stations of Australia.

Some justifications about the low correlation between wind data of rasters and stations (Fig.R2f) and the observed differences in Figs.R3a,b are the following:

- Part of this difference may be associated to climate change effects since the larger part of wind data from stations, especially for Australia stations, represent the period after 2000 while the rasters correspond to the period 1950-2000.

- The representativity of wind speed rasters of 1950-2000 produced by the model of Sheffield et al. (2006) may be low at 0.5 degree resolution due to the scarce existing wind data at global scale during the total period of simulation and especially for the years belonging to the first half of the total period.
- An additional factor responsible for the differences in Figs.3a,b may be the conversion of wind raster data of Sheffield et al. (2006) from  $z=10$  m to 2 m using Eq.R1. The degree of accuracy of this equation is unknown when is applied at global scale and for a pixel of 0.5 degree resolution, which may contain high topographical variability. The error, which may be introduced by the use of Eq.R1 is impossible to be assessed.
- In the case of CA-USA stations, the mean monthly  $u_2$  values (measured directly at 2 m height) were estimated after removing extremely high observed values, which were flagged by the CIMIS database as unreasonable extremes. Additionally, in some months of some stations,  $u_2$  values were missing. We also observed that many of these extreme and missing values were during months of extreme rainfall events. Many of these months were associated to extreme hurricane events, which are very common in California (at least 54 catastrophic events for the period 1950-2015, with extremely high wind speeds). For example, the Guillermo hurricane of 1997 led to wind speeds of  $\sim 70$  m s<sup>-1</sup> ([https://en.wikipedia.org/wiki/List\\_of\\_California\\_hurricanes](https://en.wikipedia.org/wiki/List_of_California_hurricanes)). We had already mentioned in the initial version of the manuscript that we removed flagged values from CA-USA data in order to make comparisons with the given  $ET_o$  values provided by the CIMIS database (Page 10, lines 13-21 and Fig.S1 in the supplementary material). On the other hand, we believe that in the climatic model of Sheffield et al. (2006), which is expanded also in the oceans, such events were included (the degree of inclusion is unknown) and this may be probably an additional reason of the larger pixel values observed in the wind rasters at the positions of CA-USA stations (Fig.R3a).
- In the case of Australian stations, the AGBM database (Australian Government – Bureau of Meteorology) provides 12 values of mean monthly wind speeds of the total observation periods for 9am and another 12 values for 3pm local time (the website mentions that wind speeds are generally measured at 10 m height). Thus, we estimated the average value of 9am and 3pm conditions in order to get the mean monthly wind speeds and then we used Eq.R1 to adjust them at 2 m height. Thus, it is unknown the degree of error by averaging the 9am and 3pm conditions in order to get the mean monthly wind speeds and also unknown the possible error by the use of Eq.R1 locally at the position of stations. This equation is usually not calibrated for meteorological stations with anemometers positioned above 2 m height.

Such uncertainties may also exist in the case of  $DE=e_s-e_a$  (Fig.R2e), since Sheffield et al. (2006) provides data of specific humidity that were directly converted to actual vapour pressure  $e_a$  using the equation of Peixoto and Oort (1996). This equation uses the additional parameter of atmospheric pressure as internal parameter. The atmospheric pressure in the case of rasters was estimated based on elevation data of 1 km resolution that were further converted to 0.5 degree resolution. The use of  $e_a$  data from 0.5 degree resolution pixels may also added additional error, especially when there is large topographic variability within the 0.5 degree pixel. On the other hand, the  $e_a$  of stations was estimated by relative humidity and temperature data.

Taking into account all the aforementioned observations, we would like to summarize our conclusions related to the specific comment:

- Apart from the wind speed data, it was found an adequate correspondence between the 0.5 degree raster data of  $T_{max}$ ,  $T_{min}$ ,  $R_s$ ,  $R_n$  and  $de$  of 1950-2000 with the respective values of stations, which are expanded until 2016.
- As regards the wind speed data, the discrepancy between rasters and stations can be justified:
  - a) either by possible wind differences before and after 2000,
  - b) or by the effect of Eq.R1, which is used to adjust the wind rasters and the wind data of Australia stations from 10 to 2 m height,

- c) or by uncertainties in the Sheffield et al. (2006) wind data due to the scarce existing wind data for calibrating their model at global scale during the period of 1950-2000 (especially for years before 1975),
- d) or by uncertainties introduced after eliminating extreme wind values in the data of CA-USA stations,
- e) or by uncertainties introduced after averaging the 9am and 3pm wind conditions in the data of Australia stations,
- f) or by combinations of all the aforementioned cases. Thus, uncertainties exist in both rasters and stations wind data, which can not be solved. These specific problems were included in the discussion section.

Despite the differences in the wind speed data between rasters and stations, the observed correlation between  $ET_o$  ASCE-short of 1950-2000 (0.5 degree resolution) and the respective values of California-USA and Australia stations (which are expanded until 2016) is adequate for a global scale application (Fig.R1b), if we consider a) that the  $ET_o$  values of rasters were obtained from large pixels (~50 km) and b) that uncertainties, especially in the wind datasets, exist not only in the raster datasets but also in the stations datasets. In order to prove that the re-adjusted coefficients of P-T and H-S methods are valuable, we included other models of reduced parameters from the literature in order to perform comparisons (see new additional models in Table 2 and comparative results in Table 5 of the manuscript). In order to provide information about the aforementioned uncertainties related to the data that may affect the validity of the revised coefficients, we added a new section in the Discussion with title “*Uncertainties in the data used for calibrating and validating the revised coefficients of P-T and H-S methods*”

Finally, we would like to stress that this study used the published data of Hijmans et al. (2005) and Sheffield et al. (2006) that have been used by too many other studies (7129 and 186 citations, respectively, source: SCOPUS, last accessed 12/6/2017). We believe that we used the best available global information for developing the rasters. Additionally, we clearly state that our products of reference evapotranspiration and revised coefficients correspond to 1950-2000 and thus we leave the choice to the readers/users for using them for more recent periods. Finally, we observed that Fick and Hijmans (2017) just published a new version of their database for the period before 2000 including solar radiation, humidity and wind speed at 1 km resolution. Thus, we believe that there may be not problems related to the fact that our raster products do not include information after 2000, or because the wind rasters showed discrepancies with observed data, which mainly cover periods after 2000.

**Comment R2.4:**

- Page 8. Really I do not find useful the annual coefficients in areas that show strong climate seasonality (as in the majority of world regions).
- In addition, there are not seasonal accuracy statistics, which can be much more relevant than annual ones.

**Response:** Before we proceed to any justifications about the use of annual coefficients, we would like to mention that the stations that we used in this study, present adequate seasonal variability, which can be visualized in the graphs of Fig.R5a,b,c,d. Figs.R5a,b show the box-whisker plots of mean monthly  $ET_o$  ASCE-short values for the California-USA and Australia stations, respectively, while Figs.R5c,d provide the respective frequency (number of stations) for classes that describe the maximum difference ( $\Delta_{max}$ ) between maximum and minimum values of mean monthly  $ET_o$  ASCE-short of the respective stations. Taking into account Fig.R5a,b,c,d, and especially R5c,d, we believe that the validation dataset includes stations of high seasonality. Based on Figs.R5c,d, more than 50% of the stations present  $\Delta_{max}$  of  $ET_o$ -short greater than 150 mm month<sup>-1</sup>.

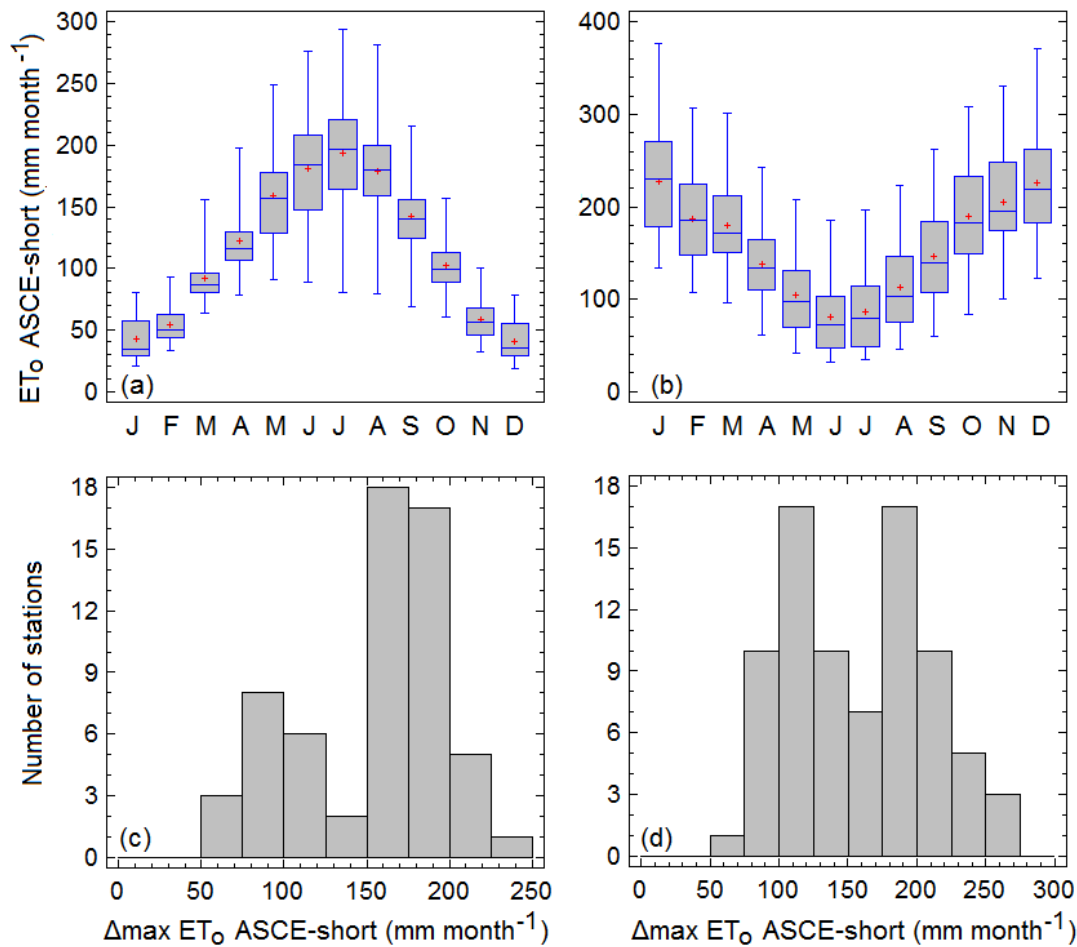


**Fig.R5** (a) Box-Whisker plot of mean monthly  $ET_0$  ASCE-short (mm month<sup>-1</sup>) for California-USA stations, (b) Box-Whisker plot of mean monthly  $ET_0$  ASCE-short (mm month<sup>-1</sup>) for Australia stations, (c) frequency (number of stations) for each class that describes the difference between maximum and minimum values of mean monthly  $ET_0$  ASCE-short for California-USA stations and (d) frequency (number of stations) for each class that describes the difference between maximum and minimum values of mean monthly  $ET_0$  ASCE-short for Australia stations.

We also have to stress that the revised coefficients of H-S and P-T methods are not just annual averages of the mean monthly coefficients but partial weighted averages (p.w.a.), which give more weight to the monthly coefficients of the months with higher  $ET_0$  during the year excluding the coefficients of colder months that present unreasonably high or low coefficients (see procedure of Eq.7 in the manuscript for estimating the weighted averages). Thus, based on our experience and after handling with the stations and the raster data, we believe that the p.w.a. annual coefficients are very useful in areas of strong seasonality. The detailed reasons for selecting the annual p.w.a. coefficients were incorporated in the new subsection of the Discussion with title: “Reasons for using annual p.w.a. coefficients instead of monthly or seasonal ones in the case of H-S and P-T methods”

It is also important to note that the derivation of annual coefficients is a pure optimization problem when stations data are used. For example, Cristea et al. (2013) derived coefficients of the P-T method for 106 stations that represent a range of climates across the contiguous USA. The coefficients were estimated by minimizing the sum of the squared residuals between the benchmark FAO-56 and P-T (optimization method) using data only for the period April-September. The obtained optimized values of the coefficients were interpolated in order to make a map of the  $a_{pt}$  coefficient (the map is not available for comparisons). In this study, the maps of the coefficients are produced based on raster data and not stations data, which means that optimization should be performed pixel by pixel (~62000 pixels globally for the 0.5 degree resolution excluding Antarctica). This procedure would require special

programming since readily available tool to perform this procedure does not exist in commercial or free GIS software packages. This is the main reason for using as an alternative method the Eqs.7 in GIS environment, since it can be calculated easily in raster calculators incorporated in the GIS packages while approximates to the optimized values because it gives more weight to the monthly coefficients of the warmer months. A solution could be the development of a tool for GIS purposes using rasters data that could be able to run using 24 rasters; 12 for the benchmark  $ET_o$  and another 12 for the P-T or H-S  $ET_o$  formula without the 1.26 and 0.0023 factors, respectively, in order to provide optimized annual values of their coefficients (for a global application filters to remove unreasonable values are also required).

Finally, we have to clarify that Figs.8-10 in the manuscript include results of mean monthly values of each month of each station and not one value per station. We mention this because in the second part of the comment the reviewer notes that “*there are not seasonal accuracy statistics, which can be much more relevant than annual ones*”. All the statistics that we provided in this study concern comparisons between observed and predicted mean monthly values by the models (160 stations  $\times$  12 mean monthly values = 1680 observations were tested for each parameter). We believe that the monthly comparison includes also the seasonal one. Seasonal separation would create a problem due to the different seasons between northern and southern hemisphere. Comparative statistics per season would also create a great expansion of the article in the results but also in the discussion section, which are already large after the addition of the additional models (request of the reviewer 1). Additionally, we would like to present the seasonal statistics in new studies where we will present further analysis related to optimization methods and other new models separately for California and Australia stations. In order to provide something relevant to seasonal variations to the reviewer, we prepared the Figs.R6 and R7, which will not be included in the manuscript. Fig.R6a and R6b give the average monthly  $ET_o$  based on the mean monthly estimations from California and Australia stations, respectively, using the ASCE-short method, the P-T(p.w.a.s.), the H-S(p.w.a.s.) and VAL3 model (best model according to Table 5a in the manuscript). Similarly, Fig.R7a and R7b give the average monthly  $R_s$  based on the mean monthly observations from California and Australia stations, respectively, and based on the  $R_s$  estimations using the radiation formula of H-S with revised coefficients.

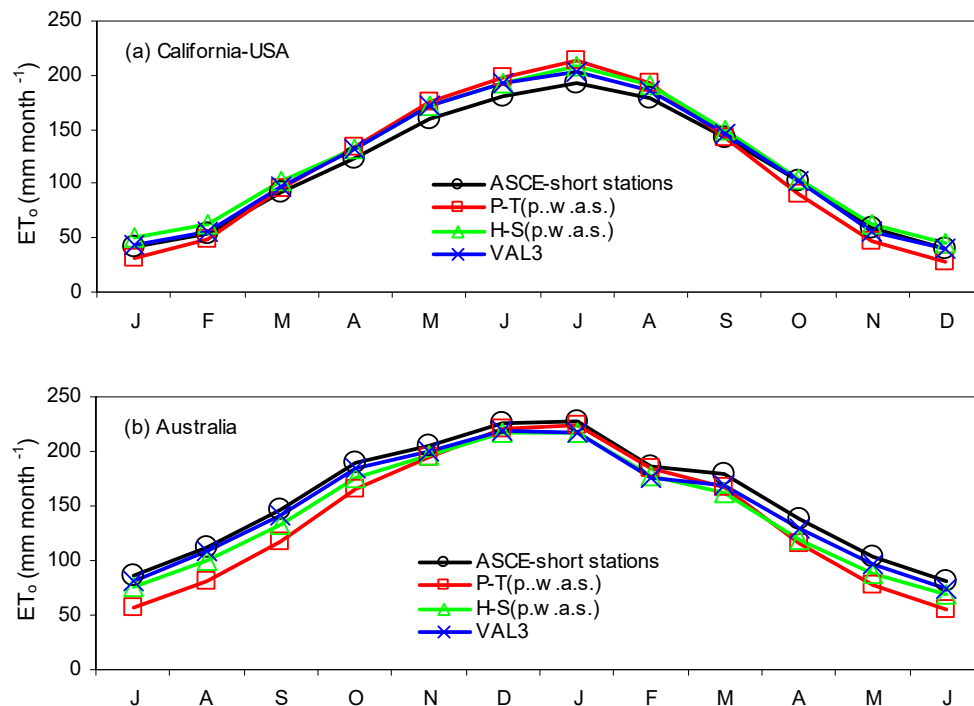


**Fig.R6** Monthly average  $ET_o$  based on mean monthly estimations using the ASCE-short method, the P-T(p.w.a.s.), the H-S(p.w.a.s.) and VAL3 model (best model according to Table 5a in the manuscript) for (a) the 60 stations of California and (b) the 80 stations of Australia (For Australia the graph starts from July).

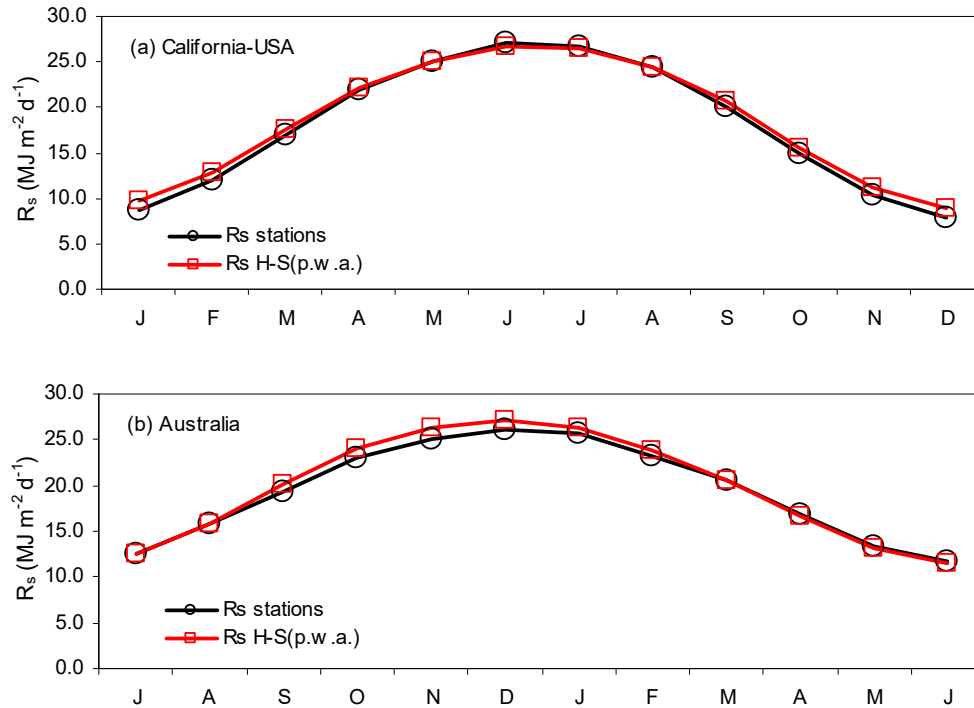


**Fig.R7** Monthly average  $R_s$  based on mean monthly observations and based on the radiation formula of H-S with revised coefficients for **(a)** the 60 stations of California and **(b)** the 80 stations of Australia (For Australia the graph starts from July).

Figs.R6,7 give a general indication about the seasonal variations in the  $ET_o$  and  $R_s$  estimations by the models separately for California and Australia datasets, while they also provide a general overview about the underestimation/overestimation of each model per month in comparison to the benchmark values (ASCE-short or observed  $R_s$ ). We believe that the general variation that was succeeded by the models is satisfactory in the context of a global application and any observed deviations are adequately justified by the uncertainties related to the data. The only thing that we have to address is the response of P-T(p.w.a.s.) model. The P-T(p.w.a.s.) was not as good as the H-S(p.w.a.s.) (the same thing was also observed between the standard H-S and P-T methods). The prevalence of H-S can be attributed to the fact that the majority of stations from Table 1 are located in territories with negative  $DMAD$  values (Fig.5a) giving a general advantage to H-S method for more robust estimations (this explanation is also mentioned in the manuscript, for more details see Page 20, lines 1-10). In the case of Australia the bad performance is evident during the cold months, but it presented better performance on the warmer months (DJF) in comparison to H-S(p.w.a.s.) and VAL3.

#### Other major corrections made in the text:

1. Some affiliations changed because some authors were transferred to other institutions or because one of the Institutions changed name.
2. The abstract reformed in order to be more descriptive.
3. Any analysis related to finer resolutions below 0.5 degrees was removed from the text following the comments of reviewer 2. For this reason, the 30 arc-sec resolution maps given in Figs.2,3,4,5,6,7 were substituted with the ones of 0.5 degree resolution with respective changes in the range of values in their legends. Any discussion about the comparison of different resolutions was also removed from the discussion section. Additionally, all the results and tables changed based on 0.5 degree resolution. Similar changes were also made in the supplementary material. The only

reference about the finer resolutions is given in section 5. Data availability, where we added the following text: “*Apart from the 0.5 degree resolution raster datasets, the database contains the same datasets at finer resolution (30 arc-sec, 2.5 arc-min, 5 arc-min and 10 arc-min). These finer datasets are provided in order to cover the observed resolution range in the initial climatic data (e.g. the temperature data of Hijmans et al. (2005) are provided at 30 arc-sec resolution). The finer resolutions were produced using bilinear interpolation on solar radiation, humidity and wind speed data of Sheffield et al. (2006). This interpolation method is not the most appropriate for such purposes. The data of finer resolutions can only be used as a tool to assess uncertainties associated to temperature variation effects within a 0.5 degree pixel or to estimate average values of the coefficients for larger territories in order to capture a better representation of the coastlines or islands that do not exist in 0.5 degree resolution (use of values from individual pixels is not recommended). A complete list of the datasets is provided in the Table S5.*”

4. The reviewer also commented that the manuscript is quite long (Comment R2.1). For this reason, we removed the accuracy analysis by splitting the stations based on their elevation, and we also removed the Taylor diagrams analysis since the criteria that we give in Table 5 are more than enough.
5. We added another 8 models of short reference crop evapotranspiration for comparative purposes after the request of Reviewer 1.
6. The Discussion section was completely reformed in order to create subsections (request of reviewer 1).
7. An error was found in the coordinates of Australian station Paynes Find station (A-69) of the validation dataset and the associated coefficients extracted from the specific coordinates. The position of the station was corrected in Fig.1 and any information related to the station was corrected. An additional arithmetic error was found and corrected in the  $ET_o$  ASCE estimations of Australian stations. We performed a detailed check for all stations data, all the calculations/equations used for rasters development, all the calculations/equations used for analyzing stations data.

## References

- Allen, R. G., Pereira, L. S., Raes, D., and Smith, M.: Crop Evapotranspiration: Guidelines for computing crop water requirements. Irrigation and Drainage Paper 56, Food and Agriculture Organization of the United Nations, Rome, 1998.
- Allen, R. G., Walter, I. A., Elliott, R., Howell, T., Itenfisu, D., and Jensen M.: The ASCE standardized reference evapotranspiration equation. Final Report (ASCE-EWRI). Pr. In: Allen RG, Walter IA, Elliott R, Howell T, Itenfisu D, Jensen M (Eds.) Environmental and Water Resources Institute, 2005. Task Committee on Standardization of Reference Evapotranspiration of the Environmental and Water Resources Institute, 2005.
- Fick, S. E., and Hijmans, R. J.: WorldClim 2: New 1-km spatial resolution climate surfaces for global land areas. International Journal of Climatology, Article in Press, 2017, DOI: 10.1002/joc.5086
- Hang, X., Vincent, L. A., Hogg, W. D., and Niitsoo, A.: Temperature and precipitation trends in Canada during the 20th century. Atmosphere - Ocean, 38 (3), 395-429, 2000.
- Hijmans, R. J., Cameron, S. E., Parra, J. L., Jones, P. G., and Jarvis, A.: Very high resolution interpolated climate surfaces for global land areas. Int. J. Climatol., 25, 1965-1978, 2005.
- McVicar, T. R., Roderick, M. L., Donohue, R. J., and Van Niel, T. G.: Less bluster ahead? ecohydrological implications of global trends of terrestrial near-surface wind speeds. Ecohydrology, 5, 381-388, 2012a.
- McVicar, T. R., Roderick, M. L., Donohue, R. J., Li, L. T., Van Niel, T. G., Thomas, A., Grieser, J., Jhajharia, D., Himri, Y., Mahowald, N. M., Mescherskaya, A. V., Kruger, A. C., Rehman, S., and Dinpashoh, Y.: Global review and synthesis of trends in observed terrestrial near-surface wind speeds: implications for evaporation. J. Hydrol., 416-417, 182-205, 2012b.
- Norrrant, C., and Douguédroit, A.: Monthly and daily precipitation trends in the Mediterranean (1950-2000). Theor. Appl. Climatol., 83, 89-106, 2006.

- Peixoto, J. P., and Oort, A. H.: The climatology of relative humidity in the atmosphere. *J. Climate*, 9, 3443-3463, 1996.
- Sheffield, J., Goteti, G., and Wood, E. F.: Development of a 50-yr high-resolution global dataset of meteorological forcings for land surface modeling. *J. Climate*, 19(13), 3088-3111, 2006.
- Sheffield, J., and Wood, E. F.: Global trends and variability in soil moisture and drought characteristics, 1950-2000, from observation-driven simulations of the terrestrial hydrologic cycle. *J. Climate*, 21, 432-458, 2008.
- Wild, M., Folini, D., Schär, C., Loeb, N., Dutton, E.G., and König-Langlo, G.: The global energy balance from a surface perspective, *Clim. Dyn.*, 40, 3107-3134, 2013.
- Willett, K. M., Dunn, R. J. H., Thorne, P. W., Bell, S., De Podesta, M., Parker, D. E., Jones, P. D., and Williams, C. N.: HadISDH land surface multi-variable humidity and temperature record for climate monitoring. *Clima. Past*, 10, 1983-2006, 2014.
- You, Q., Kang, S., Aguilar, E., Pepin, N., Flugel, W.-A., Yan, Y., Xu, Y., Zhang, Y., and Huang, J.: Changes in daily climate extremes in China and their connection to the large scale atmospheric circulation during 1961-2003. *Clim. Dyn.*, 36 (11-12), 2399-2417, 2011.
- Zomer, R. J., Trabucco, A., Bossio, D. A., van Straaten, O., and Verchot, L. V.: Climate change mitigation: A spatial analysis of global land suitability for clean development mechanism afforestation and reforestation. *Agr. Ecosyst. Environ.*, 126, 67-80, 2008.

# High resolution global grids of revised Priestley-Taylor and Hargreaves-Samani coefficients for assessing ASCE-standardized reference crop evapotranspiration and solar radiation

Vassilis G. Aschonitis<sup>1</sup>, Dimitris Papamichail<sup>2</sup>, Kleoniki Demertzi<sup>2</sup>, Nicolo Colombani<sup>1</sup>, Micol Mastrocicco<sup>3</sup>, Andrea Ghirardini<sup>1</sup>, Giuseppe Castaldelli<sup>1</sup>, Elisa-Anna Fano<sup>1</sup>

<sup>1</sup>Department of Life Sciences and Biotechnology, University of Ferrara, Ferrara, Italy

<sup>2</sup>Department of Hydraulics, Soil Science and Agricultural Engineering, Aristotle University of Thessaloniki, Thessaloniki, Greece

<sup>3</sup>Department of Environmental, Biological and Pharmaceutical Sciences and Technologies, University of Campania “Luigi Vanvitelli”, Caserta, Italy

Correspondence to: Vassilis G. Aschonitis (schvls@unife.it)

**Abstract.** The objective of the study is to provide global grids (0.5 degree) of revised annual coefficients for the Priestley-Taylor (P-T) and Hargreaves-Samani (H-S) evapotranspiration methods after calibration based on ASCE-standardized Penman-Monteith method (ASCE method includes two reference crops: short clipped grass and tall alfalfa). The analysis also includes the development of a global grid of revised annual coefficients for solar radiation ( $R_s$ ) estimations using the respective  $R_s$  formula of H-S. The analysis was based on global gridded climatic data of the period 1950-2000. The method for deriving annual coefficients of P-T and H-S methods was based on partial weighted averages (p.w.a.) of their mean monthly values. This method estimates the annual values considering the amplitude of the parameter under investigation ( $ET_o$  and  $R_s$ ) giving more weight to the monthly coefficients of the months with higher  $ET_o$  values (or  $R_s$  values for the case of H-S radiation formula). The method also eliminates the effect of unreasonably high or low monthly coefficients that may occur during periods where  $ET_o$  and  $R_s$  fall below a specific threshold. The new coefficients were validated based on data from 140 stations located in various climatic zones of USA and Australia with expanded observations up to 2016. The validation procedure for  $ET_o$  estimations of short reference crop showed that the P-T and H-S methods with the new revised coefficients outperformed the standard methods reducing the estimated  $RMSE$  in  $ET_o$  values by 40% and 25%, respectively. The estimations of  $R_s$  using the H-S formula with revised coefficients reduced the  $RMSE$  by 28% in comparison to the standard H-S formula. Finally, a raster database was built consisting of: (a) global maps for the mean monthly  $ET_o$  values estimated by ASCE-standardized method for both reference crops, (b) global maps for the revised annual coefficients of the P-T and H-S evapotranspiration methods for both reference crops and a global map for the revised annual coefficient of the H-S radiation formula, (c) global maps that indicate the optimum locations for using the standard P-T and H-S methods and their possible annual errors based on reference values. The database can support estimations of  $ET_o$  and solar radiation for locations where climatic data are limited while it can support studies, which require such estimations at larger scales (e.g. country, continent, world). The datasets produced in this study are archived in PANGAEA database

(<https://doi.pangaea.de/10.1594/PANGAEA.868808>) and in ESRN-database (<http://www.esrn-database.org> or <http://esrn-database.weebly.com>).

## 1 Introduction

The reference crop evapotranspiration  $ET_o$  is defined as the maximum value of water losses by evaporation and transpiration above a reference crop (e.g. grass), which can be achieved under no water restrictions. It is also one of the most important parameters for water balance estimations and irrigation planning of crops (Allen et al., 1998). Several methods have been proposed for  $ET_o$  estimations (Itenfisu et al., 2003; Allen et al., 2005; Wang and Dickinson, 2012; McMahon et al., 2013; Valipour, 2017; Valipour and Gholami Sefidkouhi, 2017; Valipour et al., 2017) with the most popular the FAO-56 Penman-Monteith (Allen et al., 1998), the Priestley-Taylor (Priestley and Taylor, 1972) and the Hargreaves-Samani (Hargreaves and Samani, 1982; 1985) methods. The FAO-56 has been updated to the ASCE-standardized method (Allen et al., 2005), which reflects the current state-of-the-art, providing  $ET_o$  estimations for two reference crops (a short and a tall reference crop, which correspond to clipped grass and alfalfa, respectively). The ASCE-standardized method has been proposed by the ASCE-EWRI Task Committee as the most precise method and requires a wide range of climatic parameters, which in many cases are not available. The problem of data availability can be confronted by other methods, such as the Priestley-Taylor and Hargreaves-Samani, which require less information for their determination. In fact, they are considered as the most precise among the simplified methods with reduced parameters (Xu and Singh, 2002; Sumner and Jacobs, 2005; Valipour, 2012; 2014).

The Priestley-Taylor (P-T) method requires net solar radiation and temperature data. The P-T formula includes an empirical factor known as advection coefficient  $a_{pt}$ , which is usually set equal to 1.26 (Priestley and Taylor, 1972) and generally ranges between 1.08 and 1.34 (Tateishi and Ahn, 1996; Xu et al., 2013). Other studies for various climatic conditions have shown that  $a_{pt}$  presents significant spatial and seasonal variability (Castellvi et al., 2001; Moges et al., 2003; Pereira, 2004; Tabari and Talaei, 2011; Aschonitis et al., 2015). Weiß and Menzel (2008) used the value 1.26 for wet and the value 1.75 for dry climatic conditions, as suggested by Maidment (1992). The value  $a_{pt}=1.26$  has been verified experimentally for bare irrigated soil (Eichinger et al., 1996). Theoretical simulations for the case of the reference crop in saturated soil have also verified the  $a_{pt}=1.26$  for the case of non or restricted advection effects (Lhomme, 1997; McMahon et al., 2013). Lower values of the advection coefficient have been reported by Singh and Irmak (2011) ( $a_{pt}=1.14$ ) for Nebraska (USA), by Abtew (1996) ( $a_{pt}=1.18$ ) for Florida (USA), by Kellner (2001) ( $a_{pt}=0.8$ ) for central Sweden, and by Xu and Singh (2002) ( $a_{pt}=0.9$ ) for Switzerland. Values of  $a_{pt}<1$  have been reported for forested steep areas (Shuttleworth and Calder, 1979; Giles et al. 1984; Flint and Childs, 1991). On the other hand, high values ranging between 1.82-2.14 have been reported for cold-dry lands of Iran (Tabari and Talaei, 2011). Aschonitis et al. (2015) analysed the monthly variation of  $a_{pt}$  for the Italian territories and observed through regression analysis that more than 90% of the spatial variability of the seasonal  $a_{pt}$  was explained by the spatial variability of vapour pressure deficit  $DE$  (positive correlation). The rate of  $a_{pt}$  variation per unit  $DE$

was found significantly different between seasons and it was negatively correlated to net solar radiation and/or temperature. The general trends of  $a_{pt}$  led to the conclusion that colder-drier conditions due to low net radiation and high vapour pressure deficit tend to increase its values.

The Hargreaves-Samani (H-S) method requires only temperature data, including four empirical factors (or three depending on the formula). A part of the equation empirically describes the incident solar radiation  $R_s$ . A basic problem of the Hargreaves-Samani method is that it tends to underestimate  $ET_o$  under high wind conditions ( $u_2 > 3 \text{ m s}^{-1}$ ) and to overestimate  $ET_o$  under conditions of high relative humidity (Allen et al., 1998). The last years, many scientists have performed analysis and re-calibration of the Hargreaves-Samani method for various climates (Trajkovic, 2007; Tabari, 2010; Tabari and Talaei, 2011; Azhar and Perera, 2011; Aschonitis et al., 2012; Mohawesh and Talazi, 2012; Rahimikhoob et al., 2012; Ravazzani et al., 2012; Bachour et al., 2013; Long et al., 2013; Mendicino and Senatore, 2013; Ngongondo et al., 2013; Berti et al., 2014; Heydari and Heydari, 2014), which indicates a global interest for simplified methods, mainly driven by the lack of data.

The analysis of  $ET_o$  at global scale is of special interest since it provides a general view about the spatiotemporal variation of this parameter, while (together with rainfall) provides significant information about the aridity of terrestrial systems. A basic limitation of global analysis is the lack of homogeneously distributed meteorological stations around the globe and especially in mountainous regions. The last years, climatic models, advanced interpolation and other methods have succeeded to generate datasets of various climatic parameters (Hijmans et al., 2005; Sheffield et al., 2006; Osborn and Jones, 2014; Brinckmann et al., 2016), facilitating the attempts to develop  $ET_o$  maps. Significant works of global  $ET_o$  estimations have been performed from various scientists. Mintz and Walker (1993) used the Thornthwaite (1948) method and provided isoline maps of  $ET_o$ . Tateishi and Ahn (1996) used the Priestley-Taylor method and provided  $ET_o$  maps at 0.5 degree resolution. Droogers and Allen (2002) used FAO-56 Penman-Monteith method, providing  $ET_o$  maps at 10 arc-min resolution and a modified Hargreaves-Samani method, which considers rainfall. Weiß and Menzel (2008) compared four different methods (Priestley-Taylor, Kimberly Penman, FAO-56 Penman-Monteith and Hargreaves-Samani) and provided  $ET_o$  maps at 0.5 degree resolution. Zomer et al. (2008) used Hargreaves-Samani method and provided the highest resolution (30 arc-sec) available for  $ET_o$  maps.

The objectives of the study are: a) to develop mean monthly maps of  $ET_o$  for the period 1950-2000 at global scale using the most precise ASCE-standardized method for both reference crops (short clipped grass and tall alfalfa); b) to develop global maps that provide the possible annual error in  $ET_o$  estimations using the standard P-T and H-S evapotranspiration methods in comparison to ASCE method for short reference crop and the possible annual error in solar radiation estimations using the temperature-based H-S radiation formula (this attempt will allow to identify the optimum locations for the application of the standard H-S and P-T evapotranspiration formulas based on their proximity to the results of ASCE for short reference crop); c) to develop global maps of re-adjusted annual coefficients for the H-S and P-T evapotranspiration methods for both short and tall reference crop based on a new method that estimates partial weighted averages of the monthly coefficients (the same procedure was also followed for the coefficients of the H-S radiation

formula); d) to validate the results of the re-adjusted P-T and H-S coefficients using data from meteorological stations from different locations with different climatic conditions; and e) to compare the predictive ability of the re-adjusted P-T and H-S coefficients for short reference crop evapotranspiration with the respective predictions obtained from other models that have low data requirements. The analysis and the produced datasets of this study were based on mean monthly climatic data of 0.5 degree resolution for the period 1950-2000. The final datasets of revised H-S and P-T coefficients will provide a global overview of the variation in their values and a common base for comparing the values of different regions since they are calibrated using common datasets and using the same technique. The produced global datasets of this study can support estimations of  $ET_o$  and solar radiation for locations where climatic data are limited while it can support studies, which require such estimations at larger scales (e.g. country, continent, world).

## 10 2 Data and methods

### 2.1 Global climatic data

The analysis presented in this study was based on global climatic data obtained from the following databases:

- The database of Hijmans et al. (2005) provides mean monthly values for the parameters of precipitation, maximum, minimum and mean temperature at 30 arc-sec spatial resolution. The data are provided as grids of mean monthly values of the period 1950-2000 (<http://www.worldclim.org/>). The database also includes a revised version of the GTOPO30 DEM based on SRTM DEM at 30 arc-sec spatial resolution, which was used for the estimation of atmospheric pressure. The DEM was also used as a base to calculate the distance from the coastlines in raster format at 30 arc-sec spatial resolution based on the Euclidean distance.
- The database of Sheffield et al. (2006) provides monthly values of parameters such as wind speed at the height of 10 m above the ground surface, solar radiation, specific humidity, precipitation and temperature for the period 1948-2006 at 0.5 degree spatial resolution. The data are available in the form of netcdf files of monthly values of each year for the period 1948-2006 (<http://hydrology.princeton.edu/data.pgf.php>).
- The database of Peel et al. (2007) provides the revised global Köppen-Geiger climate map. The data are provided in raster form with 0.1 degree spatial resolution. The climate map was developed using the GHCN version 2.0 dataset (Peterson and Vose, 1997), which includes precipitation data from 12396 stations and temperature data from 4844 stations data for the periods 1909-1991 and 1923-1993, respectively. The Köppen-Geiger map was used to obtain the climatic type of the meteorological stations used in the validation dataset.

In this study, the  $ET_o$  is estimated combining the databases of Hijmans et al. (2005) and Sheffield et al. (2006), as follows: a) mean monthly values of maximum, minimum, mean temperature and precipitation were obtained from Hijmans et al. (2005); while b) wind speed, specific humidity and incident solar radiation were obtained from Sheffield et al. (2006) database. The specific humidity was converted to actual vapour pressure using the equation given by Peixoto and Oort (1996). The final results and analysis presented in this study is based on the coarser 0.5 degree resolution.

All the calculations presented in the next sections were performed in ArcGIS 9.3 ESRI environment at WGS84 ellipsoid coordinate system. For area coverage calculations or for estimations of mean global values of various parameters, coordinate system conversions were performed from WGS84 to projected Cylindrical Equal Area system (Antarctica is not included in the maps, thus any % globe coverage calculations and derivation of mean global values of various parameters are referred to the rest terrestrial surface).

## 2.2 Methods

### 2.2.1 The ASCE standardized reference evapotranspiration method

The estimation of  $ET_o$  using the ASCE method is performed by the following equation (Allen et al. 2005):

$$ET_o = \frac{0.408\Delta(R_n - G) + \frac{\gamma u_2 (e_s - e_a) C_n}{(T_{\text{mean}} + 273.16)}}{\Delta + \gamma(1 + C_d u_2)} \quad (1)$$

where  $ET_o$  is the reference crop evapotranspiration ( $\text{mm d}^{-1}$ ),  $R_n$  is the net solar radiation at the crop surface ( $\text{MJ m}^{-2} \text{d}^{-1}$ ),  $u_2$  is the wind speed at 2 m height above the soil surface ( $\text{m s}^{-1}$ ),  $T_{\text{mean}}$  is the mean daily air temperature ( $^{\circ}\text{C}$ ),  $G$  is the soil heat flux density at the soil surface ( $\text{MJ m}^{-2} \text{d}^{-1}$ ),  $e_s$  is the saturation vapor pressure (kPa),  $e_a$  is the actual vapor pressure (kPa),  $\Delta$  is the slope of the saturation vapor pressure-temperature curve ( $\text{kPa } ^{\circ}\text{C}^{-1}$ ),  $\gamma$  is the psychrometric constant ( $\text{kPa } ^{\circ}\text{C}^{-1}$ ),  $C_n$  and  $C_d$  are constants, which vary according to the time step and the reference crop type and describe the bulk surface resistance and aerodynamic roughness. The short reference crop (ASCE-short) corresponds to clipped grass of 12 cm height and surface resistance of  $70 \text{ s m}^{-1}$  where the constants  $C_n$  and  $C_d$  have the values 900 and 0.34, respectively. The tall reference crop (ASCE-tall) corresponds to full cover alfalfa of 50 cm height and surface resistance of  $45 \text{ s m}^{-1}$ , where the constants  $C_n$  and  $C_d$  have the values 1600 and 0.38, respectively (Allen et al., 2005). The use of Eq.1 at daily or monthly step for short reference crop is equivalent to FAO-56 method (Allen et al., 1998).

### 2.2.2 The Priestley-Taylor method

The calculation of Priestley-Taylor (P-T) method is performed by the following equation (Priestley and Taylor, 1972):

$$ET_o = a_{pt} \frac{\Delta}{\lambda(\Delta + \gamma)} (R_n - G) \quad (2)$$

where  $ET_o$  is the potential evapotranspiration ( $\text{mm d}^{-1}$ ),  $R_n$  is the net solar radiation ( $\text{MJ m}^{-2} \text{d}^{-1}$ ),  $G$  is the soil heat flux density at the soil surface ( $\text{MJ m}^{-2} \text{d}^{-1}$ ),  $\Delta$  is the slope of the saturation vapor pressure-temperature curve ( $\text{kPa } ^{\circ}\text{C}^{-1}$ ),  $\gamma$  is the psychrometric constant ( $\text{kPa } ^{\circ}\text{C}^{-1}$ ),  $\lambda$  is the latent heat of vaporization ( $\text{MJ kg}^{-1}$ ) and  $a_{pt}$  is the P-T advection coefficient. The value of  $\lambda$  was considered equal to  $2.45 \text{ MJ kg}^{-1}$  (Allen et al., 1998) (this value is also constant in Eq.1 and appears as  $1/\lambda=0.408$ ). Eq.1 strictly refers to the reference crop evapotranspiration (i.e. short or tall crop), whereas Eq.2 has been used

for the calculation of evapotranspiration under non-limiting water conditions of short reference crop, bare soil or open water surface and for this reason is also called potential evapotranspiration, which is a more general term. Eq.2 is applied in this study as a reference crop evapotranspiration method and for this reason is compared with Eq.1 for short reference crop using the standard mean global value 1.26 for the factor  $a_{pt}$ .

### 5 2.2.3 The Hargreaves-Samani method

The Hargreaves-Samani (H-S) method (Hargreaves and Samani, 1982;1985) for  $ET_o$  includes an internal function, which estimates the incoming shortwave solar radiation  $R_s$  ( $\text{MJ m}^{-2} \text{day}^{-1}$ ), as follows:

$$R_s = K_{RS} \cdot R_a \cdot (TD)^{0.5} \quad (3)$$

where  $K_{RS}$  is the adjustment coefficient for the H-S radiation formula ( $^{\circ}\text{C}^{-0.5}$ ),  $R_a$  is the extraterrestrial radiation ( $\text{MJ m}^{-2} \text{day}^{-1}$ ) and  $TD$  is the temperature difference between maximum and minimum daily temperature ( $^{\circ}\text{C}$ ). According to Allen et al. (1998), the empirical  $K_{RS}$  coefficient differs for ‘interior’ or ‘coastal’ regions: a)  $K_{RS}=0.16$  for “interior” locations, where land mass dominates and air masses are not strongly influenced by a large water body and b)  $K_{RS}=0.19$  for “coastal” locations, situated on or adjacent to the coast of a large land mass and where air masses are influenced by a nearby water body. For general use of Eq.3, a mean global value of  $K_{RS}=0.17$  has been adopted in this study.  $R_a$  and  $R_s$  divided by  $\lambda$  change units from  $\text{MJ m}^{-2} \text{day}^{-1}$  to  $\text{mm day}^{-1}$  as it is required in the next equation of  $ET_o$ . The formula for estimating the  $ET_o$  by H-S method is given by the following equation (Hargreaves and Samani, 1982; 1985):

$$ET_o = 0.0135(T_{mean} + 17.8) \frac{R_s}{\lambda} = 0.0135(T_{mean} + 17.8) K_{RS} \cdot \frac{R_a}{\lambda} \cdot (TD)^{0.5} \quad (4a)$$

Considering Eq.4a, the  $K_{RS}$  and the exponent 0.5 are adjustment factors of radiation formula (Eq.3), while the 0.0135 and 17.8 are adjustment factors of the  $ET_o$  formula leading to a total amount of four empirical coefficients. Using the mean global value of  $K_{RS}=0.17$ , Eq.4a is simplified according to the following (Allen et al., 1998):

$$ET_o = c_{hs2} \cdot (T_{mean} + 17.8) \cdot \frac{R_a}{\lambda} \cdot (TD)^{0.5} = 0.0023(T_{mean} + 17.8) \cdot \frac{R_a}{\lambda} \cdot (TD)^{0.5} \quad (4b)$$

where in both Eqs.4a and 4b, the  $ET_o$  is the potential evapotranspiration ( $\text{mm d}^{-1}$ ),  $R_a$  is the extraterrestrial radiation ( $\text{MJ m}^{-2} \text{d}^{-1}$ ),  $\lambda$  is the latent heat of vaporization ( $\text{MJ kg}^{-1}$ ) and  $T_{mean}$  is the mean daily temperature ( $^{\circ}\text{C}$ ). The Eq.4b is applied in this study as a reference crop evapotranspiration method and for this reason is compared with Eq.1 for short reference crop. For the case of  $T_{mean} < -17.8$   $^{\circ}\text{C}$ , the term of  $(T_{mean}+17.8)$  was set to zero, which is necessary for a global application (Weiß and Menzel, 2008). In further steps of analysis, the coefficient 0.0135 (Eq.4a) is symbolized as  $c_{hs1}$  while the coefficient 0.0023 is symbolized as  $c_{hs2}$ , which is equal to  $c_{hs2} = c_{hs1} \cdot K_{RS}$ .

In order to reduce the errors of the aforementioned methods in the high latitudes and altitudes (polar and alpine environments) where negative temperatures exist, a filter was used in all methods to set mean monthly  $ET_o=0$  when mean monthly  $T_{max}$  is  $\leq 0$  (conditions of extreme frost).

## 2.2.4 Steps of analysis

*Step 1: Comparative analysis between the standard  $ET_o$  formulas of ASCE, P-T and H-S, and error analysis of H-S radiation formula*

The first step of the analysis includes the estimation of mean monthly and mean annual  $ET_o$  using the ASCE method (Eq.1) for the two reference crops (short and tall), the standard P-T method (Eq.2) with  $a_{pt}=1.26$  and the standard H-S method according to Eq.4b with  $c_{hs2}=0.0023$ . The difference between the  $ET_o$  methods will be captured using as a base the mean annual and the mean monthly  $ET_o$  values of ASCE-short.

In the case of mean annual  $ET_o$ , the analysis is based on the % of mean annual difference ( $MAD\%$ ) of each method M versus the mean annual  $ET_o$  of ASCE-short, which is given by:

$$MAD\%_{(M)} = 100 \left[ \frac{YET_{o(M)} - YET_{os}}{YET_{os}} \right] \quad (5)$$

where  $YET_{os}$  is the mean annual  $ET_o$  of ASCE-short method,  $YET_{o(M)}$  is the mean annual  $ET_o$  of M method (as M is used ASCE-tall either the standard P-T or the standard H-S). The  $MAD\%$  for ASCE-tall was estimated in order to assess the effects of reference crop type at different climatic environments on the annual estimations of  $ET_o$ . The  $MAD\%$  of P-T and H-S methods was used to investigate the strength of the two standard methods to approximate the annual  $ET_o$  of ASCE-short. Positive values of  $MAD\%$  indicate overestimation of the mean annual  $ET_o$  values using the M method in comparison to ASCE-short method while negative values indicate underestimation, respectively. Furthermore, the difference between the absolute  $MAD\%$  values ( $DMAD$ ) of the standard P-T (with  $a_{pt}=1.26$ ) and H-S (with  $c_{hs2}=0.0023$ ) methods was estimated in order to assess which of the two methods is more appropriate to be used locally, based on its proximity to ASCE-short method. The  $DMAD$  is estimated as follows:

$$DMAD = |MAD\%_{(H-S)}| - |MAD\%_{(P-T)}| \quad (6)$$

where positive  $DMAD$  values indicate better performance of standard P-T while negative values indicate better performance of standard H-S method in a region. Regions that showed  $DMAD$  values between -1 and +1 were considered transitional zones where both methods showed approximately the same proximity to the annual ASCE-short estimations.

In the case of mean monthly  $ET_o$ , the coefficient of determination  $R^2$  and the root mean square difference  $RMSD$  (equivalent to  $RMSE$ ) (Droogers and Allen, 2002) were used to compare the mean monthly values of ASCE-tall, standard P-T ( $a_{pt}=1.26$ ) and standard H-S ( $c_{hs2}=0.0023$ ) methods with the respective values of the ASCE-short method.

The procedures of  $MAD\%$ ,  $R^2$  and  $RMSD$  were also used to analyse the mean annual and mean monthly estimations of  $R_s$  by the standard solar radiation formula of H-S (Eq.3 with  $K_{RS}=0.17$ ) versus the given  $R_s$  values of Sheffield et al. (2006).

30

*Step 2: Readjustment of annual P-T and H-S coefficients for both reference crops*

For the case of P-T, the readjustment of the mean monthly  $a_{pt}$  coefficient was performed directly for each location by solving for  $a_{pt}$  after equating Eq.1 with Eq.2 of each month. A filter was used in order to set  $a_{pt}$  equal to 0 when Eq.1 or/and

Eq.2 without  $a_{pt}$  were equal to 0. In this case, the  $a_{pt}$  changes its physical meaning in order to indicate that mean monthly  $ET_o$  approximates to 0. Doing the above procedures for both short and tall reference crop, twelve images of mean monthly readjusted  $a_{pt}$  coefficients were produced for each reference crop.

For the case of H-S method, the readjustment of the coefficients was performed in two stages. In the first stage, the readjustment was performed in the radiation formula (Eq.3) only for the  $K_{RS}$  coefficient while the exponent 0.5 (square root) of the  $DT$  remained the same. The mean monthly  $K_{RS}$  was estimated using the values of solar radiation  $R_s$  given by Sheffield et al. (2006). In the second stage, the readjustment was performed in the evapotranspiration formula (Eq.4b) for the coefficient of  $c_{hs2}$  using as a base the ASCE method for both reference crops, while the coefficients of 17.8 and 0.5 remained the same. In this way the readjusted values of  $c_{hs2}$  and  $K_{RS}$  would also provide readjusted values of the  $c_{hs1}$  since  $c_{hs1} = c_{hs2}/K_{RS}$ . A similar filter to set  $c_{hs2}=0$  as in the case of  $a_{pt}$  was used, when Eq.1 or/and Eq.4b without  $c_{hs2}$  were equal to 0. Following the above procedures, twelve images of mean monthly readjusted  $c_{hs2}$  coefficients for each reference crop (short and tall) and twelve  $K_{RS}$  images were produced.

The new mean monthly  $a_{pt}$ ,  $c_{hs2}$  and  $K_{RS}$  coefficients were used to build respective mean annual coefficients. The robustness of mean annual coefficients are strongly related to their ability to capture better the values of the dependent variable (i.e.  $ET_o$  and  $R_s$ ), especially in the months that present larger values. For this reason, weighted annual averages of mean monthly  $a_{pt}$ ,  $c_{hs2}$  and  $K_{RS}$  coefficients were estimated. Under cold conditions, the monthly coefficients may present unrealistic values that significantly affect the weighted averages. In order to solve this problem, threshold values for the mean monthly dependent variables (i.e.  $ET_o$  and  $R_s$ ) were set before their inclusion in the weighted average estimations. Preliminary analysis for the readjustment of  $a_{pt}$  and  $c_{hs2}$  coefficients (based on the values of ASCE-short) showed that when the mean monthly  $ET_o$  values of ASCE-short, H-S and P-T were below  $45 \text{ mm month}^{-1}$  ( $\sim 1.5 \text{ mm d}^{-1}$ ), then unrealistic mean monthly values of  $a_{pt}$  and  $c_{hs2}$  coefficients appeared. As unrealistic values were considered those that were at least one order of magnitude larger or smaller from the standard values of  $a_{pt}=1.26$  and  $c_{hs2}=0.0023$ . Taking into account the above, the following procedure was performed in order to obtain partial weighted annual averages (after excluding months with  $ET_o \leq 45 \text{ mm month}^{-1}$ ) of mean monthly  $a_{pt}$  and  $c_{hs2}$  coefficients for short reference crop based on ASCE-short method:

$$\text{when } ET_{os\ i} > 45 \text{ mm month}^{-1} \text{ then } Fr_i=1 \text{ else } =0 \quad (7a)$$

and

$$\text{when } ET_{oi\ (M)} > 45 \text{ mm month}^{-1} \text{ then } Fm_i=1 \text{ else } =0 \quad (7b)$$

$$ET_{os\ adj.\ i} = ET_{os\ i} \cdot Fr_i \cdot Fm_i \quad (7c)$$

$$YET_{os\ adj.} = \sum_{i=1}^{12} (ET_{os\ adj.\ i}) \quad (7d)$$

$$C = \sum_{i=1}^{12} \left( \frac{ET_{os\ adj.i}}{YET_{os\ adj.}} \cdot C_i \right) \quad (7e)$$

where  $ET_{os\ i}$  is the mean monthly value of  $ET_o$  (mm month<sup>-1</sup>) obtained from the ASCE-short method,  $ET_{oi\ (M)}$  is the mean monthly value of  $ET_o$  (mm month<sup>-1</sup>) obtained from the M method (M is either P-T or H-S),  $Fr_i$  is the filter function of reference method with values 0 or 1,  $Fm_i$  is the filter function of M method with values 0 or 1,  $ET_{os\ adj. i}$  is the adjusted mean monthly value of  $ET_o$  from ASCE-short method, which becomes 0 when  $Fr_i$  or  $Fm_i$  is 0,  $YET_{os\ adj.}$  is the sum of the monthly adjusted  $ET_{os\ adj. i}$  values,  $C_i$  is the mean monthly coefficient of M method (i.e.  $a_{pt}$  or  $c_{hs2}$ ) calibrated based on ASCE-short method (results from the previous step of analysis),  $C$  is the partial weighted average (p.w.a.) of the mean monthly coefficients of M method (i.e.  $a_{pt}$  or  $c_{hs2}$ ) for short reference crop and  $i$  is month.

For estimating the p.w.a. of mean monthly  $a_{pt}$  and  $c_{hs2}$  for tall reference crop, the same procedure of Eqs.7 was followed using the mean monthly values of  $ET_o$  from ASCE-tall to estimate the  $Fr_i$  values in Eq.7a, while the adjusted values of  $ET_o$  ASCE-tall were also used in Eqs.7c,d,e. For  $C_i$  values in Eq.7e, the estimated mean monthly values of  $a_{pt}$  or  $c_{hs2}$  based on ASCE-tall method were used. Even though the mean monthly values of ASCE-tall are generally higher from ASCE-short, the threshold of 45 mm month<sup>-1</sup> in Eqs.7a,b remained the same since it was observed that the difference between ASCE-short and ASCE-tall is very small when  $ET_{os\ i}$  falls below ~50 mm month<sup>-1</sup>.

A similar procedure (using the set of Eqs.7) was also followed to obtain the p.w.a. of mean monthly  $K_{RS}$  of H-S method for  $R_s$  estimations. The  $Fr_i$  values in Eq.7a were estimated using as reference the mean monthly  $R_s$  values of Sheffield et al. (2006), which were also used after adjustment in Eqs.7c,d,e. The  $Fm_i$  values in Eq.7b were estimated using the respective  $R_s$  values of the standard H-S with  $K_{RS}=0.17$ . For  $C_i$  values in Eq.7e, the mean monthly values of  $K_{RS}$  calibrated based on  $R_s$  values of Sheffield et al. (2006) were used. The threshold used for adjusting  $R_s$  values in Eqs.7a,b was set equal to 3.61 MJ m<sup>-2</sup> d<sup>-1</sup> (~110 MJ m<sup>2</sup> month<sup>-1</sup>), which is equivalent to 45 mm month<sup>-1</sup> (conversion of mm month<sup>-1</sup> to MJ m<sup>-2</sup> month<sup>-1</sup> was performed after multiplying with  $\lambda=2.45$  MJ kg<sup>-1</sup>). The threshold for  $R_s$  adjustment was tested before its use and it was found that works satisfactorily excluding unrealistic monthly values of  $K_{RS}$ . As unrealistic values were considered those values that were at least one order of magnitude larger or smaller from the standard value of  $K_{RS}=0.17$ .

### 25 *Step 3: Use of stations for the validation of the p.w.a. coefficients of P-T and H-S methods and comparisons with other models of reduced parameters*

Stations from two databases (California Irrigation Management System - CIMIS database, <http://www.cimis.water.ca.gov>, and Australian Government – Bureau of Meteorology AGBM database, <http://www.bom.gov.au/>), were used in this study in order to validate the p.w.a. coefficients of P-T and H-S methods. The first database includes stations from California-USA and it was selected for the following reasons: a) it has been used as a basis for the development of Hargreaves-Samani method (Hargreaves and Samani, 1985; Hargreaves and Allen, 2002) and CIMIS method (Snyder and Pruitt, 1985, Snyder and Pruitt, 1992) and b) provides a dense and descriptive network of

stations for a specific region that combines coastal, plain, mountain and desert environments (Table 1, Fig.1a). The second database includes stations from Australia and it was selected because the stations network covers a large territory with large variety of climate classes (Table 1, Fig.1b) but also because the Priestley-Taylor method has been calibrated for locations of eastern Australia (Priestley and Taylor, 1972). The selection of stations from AGBM database was performed in such way in order to cover all the possible existing Köppen climatic types and elevation ranges of Australian continent (Table 1). In total, 140 stations were used, 60 stations were selected from CIMIS and 80 stations from the AGBM that have at least 15 years of observations (some stations, that do not follow this rule, were selected due to their special climate Köppen class or the high elevation of their location). Observations from years after 2000 up to 2016 were included (when they were available) in the stations data, in order to show that the new revised coefficients are applicable for recent periods.

[FIGURE 1]

[TABLE 1]

In the case of CIMIS stations, the monthly data for all climatic parameters were obtained, including  $ET_o$  estimations using the CIMIS method (Snyder and Pruitt, 1985, Snyder and Pruitt, 1992), but they required quality control before their use. Quality control signs are provided by the database for all climatic data, indicating extreme values, while possible errors are flagged but they are not automatically excluded. For this reason, the user should consider the signs in order to prepare a robust dataset. For this study, proper control was performed and very extreme or erroneous monthly values were excluded. Excluded values were less than 1‰ of the total values of all stations and all parameters. The final clean dataset was subjected to a secondary but indirect quality control through the comparison between the estimated mean monthly values of  $ET_o$  of ASCE-short method (Eq.1) using the clean climatic data of all USA-CA stations versus the respective mean monthly  $ET_o$  values given by CIMIS database (linear regression result between mean monthly values for  $n$  obs.=12×60=720:  $y=0.994x-1.07$  with  $R^2=0.98$ ) (see Fig.S1 in the supplementary material). Data cleaning was not followed in the case of Australia stations, since the AGBM database provides the mean monthly values of the climatic parameters for the total periods of observation and not for individual years. The general statistics of the mean monthly observed values of climatic parameters obtained from the 140 stations of California-USA and Australia are given in Table S1 of the supplementary material. A comparison of  $T_{max}$ ,  $T_{min}$ ,  $R_s$ ,  $R_n$ ,  $DE$  (vapour pressure deficit) and  $u_2$  parameters between the rasters (0.5 degree) and the stations data are provided in Figs.S2a,b,c,d,e,f of the Supplementary material.

The validation procedure was performed using the data of the stations in Table 1 by comparing the mean monthly values of  $ET_o$  derived by the P-T (Eq.2) and H-S (Eq.4b,c) methods with the standard  $a_{pt}$  and  $c_{hs2}$  coefficients and with the re-adjusted ones versus the ASCE method for short reference crop (Eq.1). The same procedure was also performed for the new  $a_{pt}$  and  $c_{hs2}$  coefficients for the tall reference crop and for the re-adjusted coefficient  $K_{RS}$  in the radiation formula of H-S (Eq.3). For the case of ASCE method for short reference crop, additional models of reduced parameters were used from the literature in order to perform comparisons with the standard and re-adjusted P-T and H-S models. The selection of these models was made in such way in order to satisfy the following criteria/characteristics:

- The selected models have been calibrated either using global data or a representative amount of data from California or

Australia. Models that have been tested for California and Australia and showed good performance were also included.

- The selected models showed better performance when tested using the validation datasets of California and Australia stations in comparison to other tested models but also a good performance to other regions based on studies from the literature. It has to be mentioned that an extremely large amount of models were examined taking into account the modified H-S and P-T models obtained from works that have been already mentioned in the introduction and the large lists of models presented in the works of Valipour (2015a,b; 2017) and Valipour et al. (2017). Strict modifications of P-T and H-S models with fixed coefficients calibrated for local conditions were not used because they cannot adapt their coefficients to the large climatic variability of the validation dataset.
- The majority of the selected models require additional parameters in comparison to P-T and H-S models. This criterion was used in order to compare the strength of the re-adjusted P-T and H-S coefficients versus such models.

Based on the aforementioned criteria, the following eight models were selected for comparisons with the standard and re-adjusted H-S and P-T models (Table 2):

- Two modified models of H-S by Droogers and Allen (2002), where the second one uses precipitation as additional parameter. The models were calibrated using global data.
- Three models of reduced parameters given by Valiantzas (2013a,b; 2014), which were calibrated using 535 stations from Europe, Asia, Africa. The first model uses temperature and radiation data, while the other two use temperature, radiation, and humidity data. The models have been tested for California (Valiantzas, 2013c) and Australia conditions (Ahooghalandari et al., 2017).
- Two models of reduced parameters by Ahooghalandari et al. (2016) calibrated/validated using stations from various locations of Australia. The models use temperature and relative humidity data.
- The Copais model of Alexandris et al. (2006) that uses temperature, radiation and humidity data. The model was calibrated/validated using data from Greece, California and Oregon-USA while it has shown a very good response to many other regions of the world including Australia (Ahooghalandari et al., 2017).

## [TABLE 2]

The following statistical criteria were used in the validation procedure: coefficient of determination  $R^2$ , modified coefficient of determination  $bR^2$  based on  $y=bx$  (Krause et al., 2005), mean absolute error  $MAE$ , root mean square error  $RMSE$ , percent bias  $PBIAS\%$ , Nash-Sutcliffe efficiency  $NSE$  (Nash and Sutcliffe, 1970), index of agreement  $d$  (Willmott, 1981) and Kling-Gupta efficiency (Gupta et al., 2009). The criteria were calculated using the package {HydroGOF} in R language (Zambrano-Bigiarini, 2015, see the package manual for formulas).

### 3. Results

#### 3.1 Comparative analysis between the standard $ET_o$ formulas of ASCE, P-T and H-S and error analysis of H-S radiation formula

The global maps of mean monthly  $ET_o$  at 0.5 degree resolution for the period 1950-2000 using a) the methods of ASCE (Eq.1) for both reference crops (ASCE-short and ASCE-tall), b) the standard P-T method (Eq.2) for  $a_{pt}=1.26$  and c) the standard H-S method (Eq.4b) for  $c_{hs2}=0.0023$ , were developed. The respective mean annual  $ET_o$  maps are given in Fig.2a,b,c,d, respectively. Similarly, the mean annual  $R_s$  values provided by Sheffield et al. (2006) and the respective  $R_s$  values estimated by the standard H-S radiation formula (Eq.3 with  $K_{RS}=0.17$ ) are given in Fig.3a,b, respectively.

[FIGURE 2]

[FIGURE 3]

The  $MAD\%$  (Eq.5) maps of ASCE-tall, standard P-T and standard H-S methods versus ASCE-short are given in Fig.4a,b,c, respectively, while in Fig.4d is also given the  $MAD\%$  of the standard solar radiation formula of H-S versus the  $R_s$  values given by Sheffield et al. (2006). The percentage globe coverage (excluding Antarctica) for different classes of  $MAD\%$  and the  $R^2$  and  $RMSD$  based on respective comparisons of the mean monthly values of  $ET_o$  and  $R_s$  methods are given in Table 3.

[FIGURE 4]

[TABLE 3]

The case of  $MAD\%$  between the  $ET_o$  methods of ASCE-tall and ASCE-short (Fig.4a and Table 3) indicates that there is a 25.2% of map coverage in the  $MAD\%$  class of  $\pm 10\%$  where the effects of reference crop type are significantly minimized (Table 3). These territories include the regions of tropical rainforests in Latin America, central Africa and Indonesia, regions of large mountain formations-ranges of high elevation and regions of taigas and tundras of North America and Asia (Fig.4a). The low values of vapor pressure deficit is the main characteristic of these regions. On the contrary, the largest differences between the two reference crops appear in arid and semi-arid environments due to the high values of vapor pressure deficit. The high correlation  $R^2=0.98$  (Table 3) between the mean monthly  $ET_o$  values of ASCE-tall and ASCE-short suggests that it is feasible to develop reliable regional monthly coefficients or regression models, which can convert the  $ET_o$  estimations from short to tall reference crop especially when the  $ET_o$  of short reference crop is estimated with a method of reduced parameters (e.g. P-T or H-S) (a paradigm has been presented by Aschonitis et al., 2012).

Even though  $MAD\%$ ,  $R^2$  and  $RMSD$  for the standard P-T and H-S methods (Fig.4b and c, Table 3) indicate a better performance of the second one to approximate the ASCE-short in a global scale, both methods seem to be equally valuable because their proximity to ASCE-short is maximized at relatively different climatic regions. This is indicated by the difference between the absolute  $MAD\%$  values ( $DMAD$ ) (Eq.6) of the P-T and H-S methods (Fig.5a). The interpretation of Fig.5a was performed using as a base the major Climatic Groups (CGs) of the Köppen-Geiger climate map obtained by Peel et al. (2007) (Fig.5b). The spatial extent of the major CGs of the Köppen-Geiger climate classification (without Antarctica)

and the percentage prevalence of P-T versus H-S in the CGs based on the *DMAD* values are given in Table 4. According to Table 4 and Figs.5a,b, the H-S method prevails in regions of B group (arid and semi-arid) and E group (polar/alpine/tundras), while the P-T method prevails in the regions of A group (tropical/megathermal), C group (temperate/mesothermal climates) and D group (continental/microthermal). Even though the P-T method seems to be more powerful in more climatic zones, in reality the H-S method prevails in the 49.3% of the regions while P-T in the 46.6% (the remaining proportion of 4.1% mainly corresponds to inner Greenland and very high mountain areas with annual  $ET_o=0$  or to regions where both methods gave equal results). The prevalence of standard H-S method to drier environments and the respective prevalence of standard P-T method in more humid environments can be explained by the fact that the standard coefficient of H-S was calibrated for California conditions (semi-arid/arid environments) (Hargreaves and Samani, 1985) while the standard coefficient of P-T was calibrated taking into account more humid environments (Priestley and Taylor, 1972).

[FIGURE 5]

[TABLE 4]

The spatial variation of *MAD*% for the case of  $R_s$  estimations using the standard solar radiation formula of H-S for  $K_{RS}=0.17$  (Eq.3) versus the mean annual  $R_s$  values of Sheffield et al. (2006) is given in Fig.4d. It is indicative that 55.3% of the territories are included in the *MAD*% range  $\pm 10\%$ , while the 95.2% is included in the range between  $\pm 25\%$  (Table 3). Significant deviations of  $R_s$  estimations using the standard H-S method appear mostly in the region of Greenland (Fig.4d). The values of  $R^2$  και *RMSD* (Table 3) indicate a good performance of the method in the case of monthly estimations. The overall results indicate that the use of the standard value  $K_{RS}=0.17$  can provide satisfactory indirect estimations of  $R_s$  for the most part of the world only by the use of temperature data.

### 3.2 Partial weighted averages of mean monthly $a_{pt}$ , $c_{hs2}$ and $K_{RS}$

The p.w.a. of mean monthly  $a_{pt}$  and  $c_{hs2}$  for short (p.w.a.s.) and tall (p.w.a.t.) reference crop were derived from the application of Eqs.7 and they are given in Figs.6, while the respective p.w.a. of mean monthly  $K_{RS}$  values are given in Fig.7. The global means of p.w.a. of  $a_{pt}$  and  $c_{hs2}$  for short reference crop (presented below each map of Fig.6a,c), and the global mean of p.w.a. of  $K_{RS}$  values for  $R_s$  (presented below Fig.7) approximate to the standard values of  $a_{pt}=1.26$ ,  $c_{hs2}=0.0023$  and  $K_{RS}=0.17$ , respectively.

[FIGURE 6]

[FIGURE 7]

As regards the spatial variation of  $a_{pt}$  for short reference crop (Fig.6a), the higher values were observed in extremely arid and desert environments exceeding the value of 1.8 (due to extremely high vapour pressure deficit), while the extremely cold and extremely humid environments presented values  $<1.0$ . Interesting cases are the alpine-tundra and extreme humid tropical environments, which presented similar values between  $\sim 0.8-1.0$ , due to the low values of vapour pressure deficit. Values of  $a_{pt}$  below 0.8 were observed in sub-polar areas. The spatial variation of  $a_{pt}$  for tall reference crop (Fig.6b) follows

similar patterns with  $a_{pt}$  of short reference crop but with increased values, which can be described by the following relationship  $a_{pt(p.w.a.t.)}=1.73 \cdot a_{pt(p.w.a.s.)} - 0.58$ ,  $R^2=0.996$ ,  $p<0.0001$ . This relationship is valid for  $a_{pt(p.w.a.s.)}>0.8$  for preserving  $a_{pt(p.w.a.t.)} \geq a_{pt(p.w.a.s.)}$ .

As regards the spatial variation of  $c_{hs2}$  for short reference crop (Fig.6c), the higher values were observed in extremely arid and desert environments exceeding 0.0026 (due to extremely high vapour pressure deficit), while the extremely cold and extremely humid environments presented values  $<0.0018$ . Similarities appear again in the case of alpine-tundra and extreme humid tropical environments, which presented values between  $\sim 0.0014$ - $0.0018$ , due to the low values of vapour pressure deficit. Values of  $c_{hs2}$  below 0.0014 were observed in sub-polar areas. The spatial variation of  $c_{hs2}$  for tall reference crop (Fig.6d) follows similar patterns with  $c_{hs2}$  of short reference crop but with increased values, which can be described by the following relationship  $c_{hs2(p.w.a.t.)}=1.793 \cdot c_{hs2(p.w.a.s.)} - 0.00114$ ,  $R^2=0.967$ ,  $p<0.0001$ . This relationship is valid for  $c_{hs2(p.w.a.s.)}>0.0014$  for preserving  $c_{hs2(p.w.a.t.)} \geq c_{hs2(p.w.a.s.)}$ .

In the case of  $K_{RS}$  (Fig.7), extreme deviations from the value of 0.17 were observed in Greenland with values above 0.21 and in south-east China with values below 0.13 (regions of Chongqing, Guizhou, Hunan, Jiangxi, Guangxi). The spatial variation of  $K_{RS}$  does not follow a specific pattern in relation to climate zones, while in many cases, it was observed an increasing trend of its values closer to the coastlines (Fig.7). Additional observations about the effect of distance from the coastline  $Dc$  on  $K_{RS}$  are given in the discussion section.

### 3.3 Validation of the re-adjusted $a_{pt}$ , $c_{hs2}$ and $K_{RS}$ coefficients

The validation of the re-adjusted  $a_{pt}$ ,  $c_{hs2}$  coefficients for  $ET_o$  estimations (for both reference crops) and the  $K_{RS}$  coefficient for  $R_s$  was performed taking into account the mean monthly values of the climatic parameters of all stations from Table 1. The re-adjusted coefficients for each station obtained from the 0.5 degree resolution maps are given in Table S2 of the Supplementary material while the comparison between  $ET_o$  estimations (for both reference crops) between rasters and stations is provided in Figs.S2g,h, respectively. The comparison of different methods is described in the next paragraphs, while the overall results of the statistical criteria for all the examined cases are given in Table 5.

#### [TABLE 5]

Table 5a and Fig.8 show the  $ET_o$  ( $\text{mm month}^{-1}$ ) comparisons between the ASCE-short values versus the values of the P-T and H-S methods with the standard and the re-adjusted (p.w.a.s.) coefficients and versus the values of the additional models given in Table 2. From the results of Fig.8 together with the results of the statistical criteria (Table 5a), the following observations were derived:

- The P-T(p.w.a.s.) and H-S(p.w.a.s.) models (Fig.8b,d) outperformed to all the statistical criteria (Table 5a) in comparison to the respective standard P-T(1.26) and H-S(0.0023) models (Fig.8a,c) reducing the  $RMSE$  values at 40 and 25%, respectively.

- The comparison of statistical criteria between H-S(0.0023), H-S(p.w.a.s.), DRAL1 and DRAL2, which follow the general formula of H-S method and are based on calibrations with global data, showed the following order of accuracy H-S(p.w.a.s.)>DRAL1> DRAL2>H-S(0.0023).
- The standard P-T(1.26) showed the worst results to all criteria (Table 4a), while the use of P-T(p.w.a.s.) succeeded to improve the predictions giving better results from H-S(0.0023), DRLA2, VAL1 and AKJ2 models.
- The H-S(p.w.a.s.) provided better results from DRAL1, DRAL2, VAL1, AKJ1, AKJ2 where the latter four require data for more climatic parameters.
- The order of accuracy of the models was the following: VAL3>VAL2>Copais>H-S(p.w.a.s.)>AKJ1>P-T(p.w.a.s.)>DRAL1> DRAL2>H-S(0.0023)>AKJ2>VAL1>P-T(1.26) (the order was based on absolute comparisons of the accuracy rankings for each criterion, see Table S3 in Supplementary material). The *RMSE* difference between H-S(p.w.a.s.) and the best VAL3 model was 6.8 mm month<sup>-1</sup> (or 0.23 mm d<sup>-1</sup>), while the respective difference between P-T(p.w.a.s.) and VAL3 was 13.5 mm month<sup>-1</sup> (or 0.45 mm d<sup>-1</sup>). These differences are satisfactory, especially for the case of H-S(p.w.a.s.), which uses less climatic data from VAL3. Of course, these differences are even smaller when compared to VAL2 and Copais, which also use more climatic parameters. Justifications for the less satisfactory performance of P-T(p.w.a.s.) are given in the Discussion section.

**[FIGURE 8]**

Table 5b and Fig.9a,b show the  $ET_o$  (mm month<sup>-1</sup>) comparisons between the ASCE-tall values versus the values of P-T and H-S method using the readjusted  $a_{pt}$  and  $c_{hs2}$  coefficients for tall reference crop (p.w.a.t.), respectively. Since there are not currently other methods of reduced parameters calibrated based on ASCE  $ET_o$  for tall reference crop, the comparison is restricted between the two methods. The results of Fig.9a,b together with the results of the statistical criteria (Table 5b) indicate a better performance of the H-S (with  $c_{hs2}$ =p.w.a.t.). The higher errors observed in H-S(p.w.a.t.) and P-T(p.w.a.t) in comparison to the respective errors of H-S(p.w.a.s.) and P-T(p.w.a.s) for short reference crop is justified by the fact that ASCE-tall is significantly higher from ASCE-short, especially in the drier environments (ASCE-tall was found ~28% higher from ASCE-short at global scale based on the mean values given in Fig.2a,b, and ~38% higher based on the comparison of the total mean values estimated by the California-USA and Australia stations data).

**[FIGURE 9]**

Table 5c and Fig.10a,b show the comparisons between the  $R_s$  (MJ m<sup>-2</sup> d<sup>-1</sup>) of stations data versus the respective values of standard radiation formula of H-S (Eq.3) with  $K_{RS}$ = 0.17 and with  $K_{RS}$ = p.w.a, respectively. The results of Fig.10a,b together with the results of the statistical criteria (Table 5c) indicate a better performance of the H-S  $R_s$  with  $K_{RS}$ = p.w.a. even though the performance of the standard H-S  $R_s$  is also satisfactory.

**[FIGURE 10]**

#### 4. Discussion

##### *Uncertainties in the data used for calibrating and validating the revised coefficients of P-T and H-S methods*

The re-calibrated coefficients of the H-S and P-T methods were estimated using raster datasets that cover the period 1950-2000 assuming stationary climate conditions, while the validation datasets of California-USA and Australia stations are expanded up to 2016. Recent studies have shown changes/anomalies after 2000 in temperature (Hansen et al., 2010; Sun et al., 2017), solar radiation (Wild et al., 2013), wind speed (McVicar et al., 2012a,b) and atmospheric humidity (Willet et al., 2014) and such changes could affect the validity of the revised coefficients. The comparisons of  $T_{max}$ ,  $T_{min}$ ,  $R_s$ ,  $R_n$ ,  $DE$  (vapour pressure deficit), and  $u_2$  values between the rasters data and the stations data, showed a very good correspondence for the case of  $T_{max}$ ,  $T_{min}$ ,  $R_s$ ,  $R_n$  (Fig.S2a,b,c,d) and a relatively good correspondence for the case of  $DE$  (Fig.S2e). In the case of  $u_2$ , a discrepancy was observed between the rasters and stations data (Fig.S2f). The separate examination of  $u_2$  for the CA-USA and Australia stations (Fig.S3), showed that the total average of mean monthly  $u_2$  values of CA-USA stations was lower from the rasters data of Sheffield et al. (2006) (data extracted from the stations' positions) while the opposite trend was found for  $u_2$  values of Australia stations. This discrepancy between the  $u_2$  values of rasters and stations can be justified by:

- 15 • Possible changes in wind speeds after 2000, since the majority of wind speed data in the stations datasets correspond to periods after 2000.
- Uncertainties in the Sheffield et al. (2006) wind data due to the scarce existing wind data for calibrating their model at global scale during the period of 1950-2000 and especially during the years belonging to the first half of the simulation period.
- 20 • The effect of the equation  $u_2=4.87u_z/\ln(67.8z-5.42)$  (Allen et al., 1998; 2005), which was used to adjust the wind rasters of Sheffield et al. (2006) and the wind data of Australia stations from  $z=10$  to 2 m height. The degree of accuracy of the aforementioned equation to convert wind data at 2 m is unknown. This equation is usually not calibrated for meteorological stations with anemometers positioned above 2 m height, while the uncertainty is even larger when is applied at global scale and for a pixel of 0.5 degree resolution, which may contain high topographic variability.
- 25 • The bias that may have been introduced after cleaning extreme wind values in the data of CA-USA stations, which may be associated to hurricane events. The region of California is strongly affected by hurricanes and the higher wind speeds in the rasters of Sheffield et al. (2006) data may partly occurred because they have included such events in their climatic simulations.
- The bias that may have been introduced by the wind data of Australia stations. The AGBM database (Australian Government – Bureau of Meteorology) provides 12 values of mean monthly wind speeds of the total observation periods for 9am and another 12 values for 3pm local time. In order to get the mean monthly wind speeds of the stations, the average value of 9 am and 3 pm conditions was used for each month.
- 30

- Combinations of all the aforementioned cases.

Uncertainties may also exist in the case of  $DE=e_s-e_a$  (Fig.S2e), since Sheffield et al. (2006) provides data of specific humidity that were directly converted to actual vapour pressure  $e_a$  using the equation of Peixoto and Oort (1996), which uses the additional parameter of atmospheric pressure as internal parameter. The atmospheric pressure in the case of rasters was estimated based on elevation data of 1 km resolution (30 arc-sec), which were further converted to 0.5 degree resolution. The use of  $e_a$  data from 0.5 degree resolution pixels may also added additional error, especially when there is large topographic variability within the 0.5 degree pixel. On the other hand, the  $e_a$  of stations was estimated by relative humidity and temperature data.

Thus, uncertainties exist in both rasters and stations data. In future studies, further improvements in the revised coefficients can be made by using global raster data, which incorporate the conditions after 2000, and by solving many of the aforementioned problems related to both stations data and raster data produced by climatic models.

#### *Reasons for using annual p.w.a. coefficients instead of monthly or seasonal ones in the case of H-S and P-T methods*

The analysis presented in this study passed through various stages before the selection of the annual p.w.a. form of the coefficients (Eqs.7). Some steps in the preliminary analysis were to analyse: (a) the different forms of averages (e.g. mean, mode, median, geometric mean, harmonic mean etc) for deriving annual coefficients, and (b) the strength of the derived mean monthly and seasonal coefficients versus the annual p.w.a. coefficients and versus the coefficients of the standard methods,.

As regards the use of weighted annual average (w.a.) of the mean monthly coefficients instead of other forms of averages (e.g. mean, mode, median, geometric mean - g.m., harmonic mean – h.m.), preliminary analysis was performed using data extracted by the climatic rasters from many positions of the world. During this analysis, trials to derive annual coefficients were made using an optimization algorithm separately for each position. The results showed that the optimized annual values were always closer to the monthly coefficients of the warmer months since the optimization algorithms try to reduce the total error, which is mainly dominated by the months that show larger  $ET_o$  values (or  $R_s$  for the case of  $K_{RS}$  calibration). The optimized values were also compared to the different types of annual averages (e.g. mean, mode, median, g.m., h.m., w.m.), which were estimated after excluding values of monthly coefficients associated to months with  $ET_o$  and  $R_s$  values  $<45 \text{ mm month}^{-1}$  (for  $R_s$  the equivalent is  $3.61 \text{ MJ m}^{-2} \text{ d}^{-1}$ ) The w.a. outperformed in all cases because it is the only form that considers the amplitude of the parameter under investigation ( $ET_o$  and  $R_s$ ) (Eq.7), giving more weight to the monthly coefficients that are related to the warmer months. This attribute of w.a. is extremely significant since it is the only type that considers the seasonal observed differences in monthly  $ET_o$  (for  $a_{pt}$  and  $c_{hs2}$ ) and  $R_s$  (for  $K_{RS}$ ) minimizing the possible errors during warmer months.

The case of mean monthly coefficients was also examined (results not shown). The results showed that the assessment of annual  $ET_o$  and seasonal  $ET_o$  during the warm season using the mean monthly coefficients outperforms in comparison to the standard methods, but their predictive strength was not as good as p.w.a. coefficients especially during

cold season. Similar findings were observed when different time intervals for calculating seasonal averages of the coefficients were used (e.g. 3-months averages or 6-months averages). The basic observed problem with monthly/seasonal coefficients associated to the global scale application of this study was that many parts of the world presented unreasonably high or low monthly/seasonal values of the coefficients (at least one order of magnitude larger or smaller from the standard values) during cold seasons. This problem occurred because P-T and H-S evapotranspiration models do not include the effect of humidity and wind, which becomes greater when temperature is low (in very low temperatures even the ASCE results can be questioned). Such values may lead to significant errors in monthly/seasonal  $ET_o$  estimations during cold periods when there are deviations of climatic conditions (seasonal shifts/disturbances or climate changes in general) from those used for calibrating the coefficients. These were the reasons for using the threshold of  $45 \text{ mm month}^{-1}$  to exclude such values from p.w.a. of the coefficients. Thus, the p.w.a. annual values were chosen as the best solution for a global application because they counterbalance the errors that could be introduced by intra-annual/intra-seasonal climatic variability or other errors such as those described in the previous section of the Discussion (errors associated to the data).

It is also important to note that the derivation of annual coefficients is a pure optimization problem when stations data are used. For example, Cristea et al. (2013) derived coefficients of the P-T method for 106 stations that represent a range of climates across the contiguous USA. The coefficients were estimated for each station by minimizing the sum of the squared residuals between the benchmark FAO-56 and P-T using data only for the period April-September. The obtained optimized values of the coefficients were interpolated in order to make a map of the  $a_{pt}$  coefficient. In this study, the maps of the coefficients were produced based on raster data and not stations data, which means that optimization should be performed pixel by pixel (~62000 pixels globally for the 0.5 degree resolution excluding Antarctica). This procedure would require special programming since readily available tool to perform this procedure does not exist in commercial or free GIS software packages. This is the main reason for using as an alternative method the Eqs.7 in GIS environment, since it can be calculated easily in raster calculators incorporated in the GIS packages. A solution could be the development of a tool for GIS purposes using rasters data that could be able to run using 24 rasters; 12 for the benchmark  $ET_o$  and another 12 for the P-T or H-S  $ET_o$  formula without the 1.26 and 0.0023 factors, respectively, in order to provide optimized annual values of their coefficients (for a global application filters to remove unreasonable values are also required).

#### *Observations derived by the application of H-S radiation formula*

Special attention was also given in the case of  $K_{RS}$  coefficient for estimating  $R_s$ . Although there were indications that the spatial variation of p.w.a.  $a_{pt}$  and  $c_{hs2}$  coefficients at global scale may be linked to general climatic characteristics (Fig.5), the respective variation of p.w.a.  $K_{RS}$  coefficient could not clearly be linked with a specific climatic or topographic characteristic. The only observed dependence, which showed some relevance to the spatial variation of  $K_{RS}$ , was a relatively negative correlation with the distance from the coastline  $D_c$ . This observed dependence can be only used as a general observation and not as a basis for applying in general the empirical rule of Allen et al. (1998) ( $K_{RS}=0.16$  for “interior” and  $K_{RS}=0.19$  for “coastal” locations). The large uncertainty in the aforementioned rule was also indicated by Samani (2000)

and it is verified by the analysis presented in Fig.S4a of the supplementary material. Fig.S4a shows a relatively negative correlation between  $K_{RS}$  and  $Dc$  (for  $Dc < 500$  km) but also shows an extremely high variability of  $K_{RS}$  close to the coastlines where  $K_{RS}$  values are not necessarily higher in comparison to the values observed in the interior regions. The observed lower variability of  $K_{RS}$  at interior regions is probably related to the fact that coastlines are more affected by oceanic-climatic phenomena, which anyway present high spatial variability at global scale. The raster data of  $K_{RS}$  (Fig.7) can be used as indicator to control the validity of the rule but also to control the validity of the given values 0.16-0.19 for a specific region. Samani (2000) also observed that the monthly  $K_{RS}$  values may be influenced by the difference between monthly maximum and minimum temperature  $TD$ . This effect was also investigated through correlation between the mean monthly  $K_{RS}$  coefficients and the mean monthly  $TD$  values of the stations data (Fig.S4b, in supplementary material). The results showed that the hypothesis related to the effect of  $TD$  on  $K_{RS}$  may be stronger locally in comparison to the effect of  $Dc$ , but again the variation of  $K_{RS}$  is extremely large in the  $TD$  range between 8-15 °C (Fig.S4b), not allowing secure conclusions for a global scale application. The result of Fig.S4b is based only on the stations of Table 1, and for this reason the variation in a global scale is expected much larger.

#### 15 *Recommendations for reducing the uncertainties when the re-adjusted coefficients of P-T and H-S models are used*

The uncertainties, which may be introduced by climate disturbances/changes or other uncertainties related to the data used for calibrating the coefficients, can be reduced taking into account some of the following observations and recommendations.

A separate analysis using only the stations of California showed that a regional mean value of the coefficients derived by p.w.a. values may present even better performance because it probably counterbalances other uncertainties associated to the spatial climatic variability within a specific region. A factor for such uncertainties may be rainfall, which may not show significant seasonal deviations or deviations from the expected annual values for a large region but may show different spatial patterns every year within the region affecting the accuracy of the coefficients. The aforementioned observation was verified by the application of H-S method for  $ET_o$  of short reference crop for the stations of California when the average value of  $c_{hs2}=0.0024$  obtained from the respective p.w.a.s values of the stations (Table S.2) was used (this value also approximates the standard value of 0.0023). The average value of sixty p.w.a.s. coefficients of the CA-USA stations gave better results from the individual coefficients (Fig.S5 and Table S4, in supplementary material). The aforementioned observations suggest that a robust territorial segmentation based on general topographic characteristics (e.g. elevation, slope, latitude and longitude, distance from the coastline etc) and general climatic characteristics (e.g. Köppen class, general precipitation and temperature patterns) can provide a proper zonation of large territories for deriving very robust mean values of  $a_{pt}$ ,  $c_{hs2}$  and  $K_{RS}$  coefficients using the respective p.w.a. values of each zone. Robust zonations based on grids of mean monthly precipitation and temperature using the data of Hijmans et al. (2005), or the mean monthly  $ET_o$  rasters provided by this study can easily be performed using cluster analysis in GIS environment (Demertzi et al., 2014; Aschonitis et al., 2016a,b).

The comparison between P-T and H-S evapotranspiration methods with re-adjusted coefficients but also their comparison with the other models of Table 2 also provided significant information. From the comparison between P-T and H-S with re-adjusted coefficients, it was observed that H-S provided better results in both short and tall reference crop. The prevalence of H-S can be attributed to the fact that more than ~80% of stations from Table 1 are located in territories with negative *DMAD* values (Fig.5a) giving a general advantage to H-S method for more robust estimations. This observation can justify the better performance of the standard H-S (with  $c_{hs2}=0.0023$ ) in comparison to the standard P-T (with  $a_{pt}=1.26$ ) for short reference crop (Table 5a) and indirectly validates the *DMAD* map. Considering these observations, it is recommended to take into account both the *MAD* (Fig.4,b,c) and *DMAD* (Fig.5a) maps before selecting one of the two methods either using the standard or the p.w.a. coefficients. From the comparisons with the other models of Table 2, it was observed that three models, which use temperature, radiation and humidity data (i.e. VAL3, VAL2, Copais, and especially VAL3), provided better estimations. These models have shown very good performance using data from other case studies (Pan et al., 2011; Shiri et al., 2014; Kisi, 2014; Gao et al., 2015; Valipour, 2015a,2015c; Djaman et al., 2015, 2016, 2017; Ahooghalandari et al., 2017), and their use is recommended instead of the P-T and H-S with re-adjusted coefficients, when the only missing climatic parameter is wind speed.

A very interesting observation was also made about the tall reference crop based on the results of *MAD*% map (Fig.4a). In the *MAD*% class of  $\pm 10\%$  of Fig.4a were observed some small negative values, which correspond to the ~2% of map coverage. These values indicate slightly larger annual values of ASCE-short in comparison to ASCE-tall. This result was observed in regions of extremely small vapour pressure deficit (areas of very high elevation, either of very cold, or extremely humid conditions scattered around the world) and it is a peculiarity of Eq.1 and probably an artefact. This result occurred because the second term of the nominator in Eq.1 (which includes the vapour pressure deficit term and the  $C_n$  coefficient) approximates to 0 when  $e_s - e_a$  becomes extremely small, while the denominator of Eq.1 is always larger in ASCE-tall in comparison to ASCE-short due to the difference in  $C_d$  value (0.34 for short and 0.38 for tall reference crop). A recommendation for partly solving this problem for tall reference crop applications is to use the revised coefficients of P-T and H-S methods derived for short reference crop in the places where the annual value of ASCE-tall is lower from ASCE-short. This recommendation is based on the fact that annual ASCE-tall is expected to be always larger from the respective value of ASCE-short. This peculiarity was not corrected in the ASCE-tall maps and the respective  $a_{pt}$  and  $c_{hs2}$  coefficients for tall reference crop in order to show the absolute estimations of the ASCE-tall and the respective coefficients. Taking into account the *MAD* map (Fig.4a), the users can find the location of these pixels.

## 5. Data availability

The produced datasets of this study have been archived in PANGAEA database (<https://doi.pangaea.de/10.1594/PANGAEA.868808>) and in ESRN-database, which is currently supported by the University of Ferrara (Italy), Aristotle university of Thessaloniki (Greece) and University of Campania “Luigi Vanvitelli” (Italy) (<http://www.esrn-database.org/gis-data.html> or <http://esrn-database.weebly.com/gis-data.html>). Apart from the 0.5 degree

resolution raster datasets, the database contains the same datasets at finer resolution (30 arc-sec, 2.5 arc-min, 5 arc-min and 10 arc-min). These finer datasets are provided in order to cover the observed resolution range in the initial climatic data (e.g. the temperature data of Hijmans et al. (2005) are provided at 30 arc-sec resolution). The finer resolutions were produced using bilinear interpolation on solar radiation, humidity and wind speed data of Sheffield et al. (2006). This interpolation method is not the most appropriate for such purposes. The data of finer resolutions can only be used as a tool to assess uncertainties associated to temperature variation effects within a 0.5 degree pixel or to estimate average values of the coefficients for larger territories in order to capture a better representation of the coastlines or islands that do not exist in 0.5 degree resolution (use of values from individual pixels is not recommended). A complete list of the datasets is provided in the Table S5.

10

## 6. Conclusions

The study provided global grids of revised annual coefficients for the Priestley-Taylor (P-T) and Hargreaves-Samani (H-S) methods for estimating  $ET_o$  for both short and tall reference crop. The coefficients were calibrated using respective grids of  $ET_o$  estimated with the ASCE-standardized method. Respective grids of annual coefficients were also derived for the radiation formula of H-S. The calibration procedures were based on global gridded climatic data of the period 1950-2000. The method for deriving annual coefficients of P-T and H-S methods was based on partial weighted averages (p.w.a.) of the respective mean monthly coefficients. This method estimates the annual values considering the amplitude of the parameter under investigation ( $ET_o$  and  $R_s$ ) giving more weight to the monthly coefficients of the months with higher  $ET_o$  values (or  $R_s$  values for the case of H-S radiation formula). The method also eliminates the effect of unreasonable monthly coefficients that may occur during periods when  $ET_o$  and  $R_s$  fall below a specific threshold. The new coefficients were validated based on data from 140 stations located at various climatic zones of USA and Australia with expanded observations up to 2016. Additional tests were also performed for the case of short reference crop evapotranspiration using additional models with low requirements for climatic data. The validation procedure for  $ET_o$  estimations of short reference crop showed that the P-T and H-S methods with revised coefficients outperformed the standard methods reducing the estimated  $RMSE$  in  $ET_o$  values by 40% and 25%, respectively. The estimations of  $R_s$  using the H-S formula with revised coefficients reduced the  $RMSE$  by 28% in comparison to the standard formula. The comparisons with other models of short reference crop, showed that the P-T and H-S methods with revised coefficients can compete models of additional climatic parameters. In the case where only wind speed is missing from available data, the use of VAL2, VAL3 and Copais methods (temperature, radiation and humidity data requirements) is recommended. Finally, a raster database of 0.5 degree resolution was built consisting of: (a) global maps for the mean monthly  $ET_o$  values estimated by ASCE-standardized method for both reference crops, (b) global maps for the revised annual coefficients of the P-T and H-S evapotranspiration methods for both reference crops and a global map for the revised annual coefficients of the H-S radiation formula, (c) global maps that indicate the optimum locations for using the standard P-T and H-S methods and their possible annual errors based on reference values ( $MAD\%$  and  $DMAD$

maps). The online free availability of the database can support estimations of  $ET_o$  and solar radiation for locations where climatic data are limited while it can support studies, which require such estimations at larger scales (e.g. country, continent, world).

The methods used in this study, their respective results and the observed uncertainties can be used as a base for future works focusing on: (a) the validation of the coefficients for other parts of the world, especially using climatic data obtained after 2000, and the comparison with other models of low data requirements (b) the recalibration of the coefficients using data from climatic models that include observations from more recent years and analysis of climate change effects on the coefficients, (c) the use of the available climatic datasets obtained from climatic models in order to calibrate models of the coefficients for various locations and not fixed values such as the ones given in this study, (d) analysis of alternative methods for deriving annual coefficients that approximate optimized values or incorporation of optimization algorithms in GIS environment for capturing the optimum solution per pixel, (e) the confrontation of uncertainties related to the data used for calibration and validation (e.g. low representativity of interpolated climatic parameters due to the lack of data in many parts of the world, errors associated to commonly used equations; such as the one used for adjusting wind data at 2 m height; uncertainties associated to the observed data etc).

15

**Supplementary material.** Supplementary information related to the article is given in the following [supplementary file \(to be added by the journal\)](#).

**Acknowledgements.** This study was performed in the context of two Post-Doctoral research studies by Dr.Vassilis Aschonitis financed by Ferrara University (Italy) and Aristotle University of Thessaloniki (Greece).

20

## References

- Abtew, W.: Evapotranspiration measurements and methoding for three wetland systems in South Florida. J. Am. Water Resour. Assoc. 32, 465-473, 1996.
- Ahooghalandari, M., Khiadani, M., and Jahromi, M. E.: Developing Equations for Estimating Reference Evapotranspiration in Australia. Water Resour. Manage., 30, 3815-3828, 2016.
- Ahooghalandari, M., Khiadani, M., and Jahromi, M. E.: Calibration of Valiantzas' reference evapotranspiration equations for the Pilbara region, Western Australia. Theor.Appl. Climatol., 128, 845-856, 2017.
- Allen, R. G., Pereira, L. S., Raes, D., and Smith, M.: Crop Evapotranspiration: Guidelines for computing crop water requirements. Irrigation and Drainage Paper 56, Food and Agriculture Organization of the United Nations, Rome, 1998.
- Allen, R. G., Walter, I. A., Elliott, R., Howell, T., Itenfisu, D., and Jensen M.: The ASCE standardized reference evapotranspiration equation. Final Report (ASCE-EWRI). Pr. In: Allen RG, Walter IA, Elliott R, Howell T, Itenfisu D, Jensen M (Eds.) Environmental and Water Resources Institute, 2005. Task Committee on Standardization of Reference

Evapotranspiration of the Environmental and Water Resources Institute, 2005.

- Alexandris, S., Kerkides, P., and Liakatas, A.: Daily reference evapotranspiration estimates by the “Copais” approach. *Agr. Water Manage.*, 82, 371-386, 2006.
- Aschonitis, V. G., Antonopoulos, V. Z., and Papamichail, D. M.: Evaluation of pan coefficient equations in a semi-arid Mediterranean environment using the ASCE standardized Penman-Monteith method. *Agr. Sci.*, 3, 58-65, 2012.
- Aschonitis, V., Demertzi, K., Papamichail, D., Colombani, N., and Mastrocicco, M.: Revisiting the Priestley-Taylor method for the assessment of reference crop evapotranspiration in Italy. *Ital. J. Agrometeorol.*, 20, 5-18, 2015.
- Aschonitis, V., Miliareisis, G., Demertzi, K., and Papamichail, D.: Terrain segmentation of Greece using the spatial and seasonal variation of reference crop evapotranspiration. *Adv. Meteorol.*, art. no. 3092671, 2016a.
- 10 Aschonitis, V. G., Awe, G.O., Abegunrin, T. P., Demertzi, K. A., Papamichail, D. M., and Castaldelli, G.: Geographic segmentation, spatial dependencies, and evaluation of the relative position of rain-gauges based on gridded data of mean monthly precipitation: application in Nigeria. *Hydrol. Res.*, nh2016095, 2016b, (in press) DOI: 10.2166/nh.2016.095
- Azhar, A. H., and Perera, B. J. C.: Evaluation of reference evapotranspiration estimation methods under Southeast Australian conditions. *J. Irrig. Drain Eng.*, 137, 268-279, 2011.
- 15 Bachour, R., Walker, W. R., Torres-Rua, A. F., and McKee, M.: Assessment of reference evapotranspiration by the hargreaves method in the Bekaa Valley, Lebanon. *J. Irrig. Drain. Eng. ASCE*, 139 (11), 933-938, 2013.
- Berti, A., Tardivo, G., Chiaudani, A., Rech, F., and Borin, M.: Assessing reference evapotranspiration by the Hargreaves method in north-eastern Italy. *Agr. Water Manage.*, 140, 20-25, 2014.
- Brinckmann, S., Krähenmann, S., and Bissolli, P.: High-resolution daily gridded data sets of air temperature and wind speed  
20 for Europe, *Earth Syst. Sci. Data*, 8, 491-516, 2016.
- Castellvi, F., Stockle, C. O., Perez, P. J., and Ibanez, M.: Comparison of methods for applying the Priestley-Taylor equation at a regional scale. *Hydrol. Process.*, 15, 1609-1620, 2001.
- Cristea, N. C., Kampf, S. K., and Burges, S. J.: Revised coefficients for Priestley-Taylor and Makkink-Hansen equations for estimating daily reference evapotranspiration. *J. Hydrol. Eng.*, 18, 1289-1300, 2013.
- 25 Demertzi, K., Papamichail, D., Aschonitis, V., and Miliareisis, G.: Spatial and seasonal patterns of precipitation in Greece: The terrain segmentation approach. *Global Nest J.*, 16, 988-997, 2014.
- Djaman, K., Balde, A. B., Sow, A., Muller, B., Irmak, S., N'Diaye, M. K., Manneh, B., Moukoumbi, Y. D., Futakuchi, K., Saito, K.: Evaluation of sixteen reference evapotranspiration methods under sahelian conditions in the Senegal River Valley. *J. Hydrol. Reg. Stud.*, 3, 139-159, 2015.
- 30 Djaman, K., Irmak, S., Kabenge, I., and Futakuchi, K.: Evaluation of FAO-56 penman-monteith model with limited data and the valiantzas models for estimating grass-reference evapotranspiration in Sahelian conditions. *Journal of Irrigation and Drainage Engineering*, 142 (11), art. no. 04016044, 2016.
- Djaman, K., Irmak, S., and Futakuchi, K.: Daily reference evapotranspiration estimation under limited data in eastern Africa. *J. Irrig. Drain Eng.*, 143 (4), art. no. 06016015, 2017.

- Droogers, P., and Allen, R. G.: Estimating reference evapotranspiration under inaccurate data conditions. *Irrig. Drain. Syst.*, 16, 33-45, 2002.
- Eichinger, W. E., Parlange, M. B., and Strickler, H.: On the concept of equilibrium evaporation and the value of the Priestley-Taylor coefficient. *Water Resour. Res.*, 32, 161-164, 1996.
- 5 Flint, A. L., and Childs, S. W.: Use of the Priestley-Taylor evaporation equation for soil water limited conditions in a small forest clearcut. *Agric. Forest Meteorol.*, 56, 247-260, 1991.
- Gao, X., Peng, S., Xu, J., Yang, S., and Wang, W.: Proper methods and its calibration for estimating reference evapotranspiration using limited climatic data in Southwestern China. *Arch. Agron. Soil Sci.*, 61, 415-426, 2015.
- Giles, D. G., Black, T. A., and Spittlehouse, D. L.: Determination of growing season soil water deficits on a forested slope  
10 using water balance analysis. *Can. J. For. Res.* 15, 107-114, 1984.
- Gupta, H. V., Kling, H., Yilmaz, K. K., and Martinez, G. F.: Decomposition of the mean squared error and NSE performance criteria: Implications for improving hydrological modelling. *J. Hydrol.*, 377, 80-91, 2009.
- Hansen, J., Ruedy, R., Sato, M., and Lo K.: Global surface temperature change, *Rev. Geophys.*, 48, RG4004, 2010.
- Hargreaves, G. H., and Samani, Z. A.: Estimating potential evapotranspiration. *J. Irrig. Drain Eng. ASCE*, 108, 223-230,  
15 1982.
- Hargreaves, G. H., and Samani, Z. A.: Reference crop evapotranspiration from ambient air temperature. *American Society of Agricultural Engineers*, 12 pp, 1985. <http://libcatalog.cimmyt.org/download/reprints/97977.pdf>
- Hargreaves, G. H., and Allen, R. G.: History and evaluation of hargreaves evapotranspiration equation. *J. Irrig. Drain Eng. ASCE*, 129, 53-63, 2002.
- 20 Heydari, M. M., and Heydari, M.: Calibration of Hargreaves-Samani equation for estimating reference evapotranspiration in semiarid and arid regions. *Arch. Agron. Soil Sci.*, 60, 695-713, 2014.
- Hijmans, R. J., Cameron, S. E., Parra, J. L., Jones, P. G., and Jarvis, A.: Very high resolution interpolated climate surfaces for global land areas. *Int. J. Climatol.*, 25, 1965-1978, 2005.
- Itenfisu, D., Elliott, R.L., Allen, R. G., and Walter, I. A.: Comparison of reference evapotranspiration calculations as part of  
25 the ASCE standardization effort. *J. Irrig. Drain Eng. ASCE*, 129, 440-448, 2003.
- Kellner, E.: Surface energy fluxes and control of evapotranspiration from a Swedish Sphagnum mire. *Agr. Forest Meteorol.*, 110, 101-123, 2001.
- Kisi, O.: Comparison of different empirical methods for estimating daily reference evapotranspiration in mediterranean climate. *J. Irrig. Drain Eng.*, 140, art. no. 04013002, 2014.
- 30 Krause, P., Boyle, D. P., and Bäse, F.: Comparison of different efficiency criteria for hydrological model assessment. *Adv. Geosci.*, 5, 89-97, 2005.
- Lhomme, J. -P.: A theoretical basis for the Priestley-Taylor coefficient. *Bound.-Lay. Meteorol.*, 82, 179-191, 1997.
- Long, H., Shuai, X., Lei, Q., and Zhang, R.: Spatiotemporal distribution of calibration coefficients of hargreaves equation for estimating potential evapotranspiration in Mainland China. *J. Irrig. Drain Eng. ASCE*, 139, 293-299, 2013.

- Maidment, D. R.: Handbook of hydrology. McGraw-Hill, New York, 1992.
- McMahon, T. A., Peel, M. C., Lowe, L., Srikanthan, R., and McVicar, T. R.: Estimating actual, potential, reference crop and pan evaporation using standard meteorological data: a pragmatic synthesis. *Hydrol. Earth Syst. Sci.*, 17, 1331-1363, 2013.
- 5 McVicar, T. R., Roderick, M. L., Donohue, R. J., and Van Niel, T. G.: Less bluster ahead? ecohydrological implications of global trends of terrestrial near-surface wind speeds. *Ecohydrology*, 5, 381-388, 2012a.
- McVicar, T. R., Roderick, M. L., Donohue, R. J., Li, L. T., Van Niel, T. G., Thomas, A., Grieser, J., Jhajharia, D., Himri, Y., Mahowald, N. M., Mescherskaya, A. V., Kruger, A. C., Rehman, S., and Dinpashoh, Y.: Global review and synthesis of trends in observed terrestrial near-surface wind speeds: implications for evaporation. *J. Hydrol.*, 416-417, 182-205, 10 2012b.
- Mendicino, G., and Senatore, A.: Regionalization of the hargreaves coefficient for the assessment of distributed reference evapotranspiration in Southern Italy. *J. Irrig. Drain. Eng. ASCE*, 139, 349-362, 2013.
- Mintz, Y., and Walker, G. K.: Global fields of soil moisture and land surface evapotranspiration derived from observed precipitation and surface air temperature. *J. Appl. Meteor.*, 32, 1305-1334, 1993.
- 15 Moges, S. A., Katambara, Z., and Bashir, K.: Decision support system for estimation of potential evapotranspiration in Pangani Basin. *Phys. Chem. Earth* 28, 927-934, 2003.
- Mohawesh, O. E., and Talazi, S. A.: Comparison of Hargreaves and FAO56 equations for estimating monthly evapotranspiration for semi-arid and arid environments. *Arch. Agron. Soil Sci.*, 58, 321-334, 2012.
- Nash, J. E., and Sutcliffe, J. V.: River flow forecasting through conceptual models, Part I - A discussion of principles. *J. Hydrol.*, 10, 282-290, 1970.
- 20 Ngongondo, C., Xu, C. -Y., Tallaksen, L. M., and Alemaw, B.: Evaluation of the FAO Penman-monteith, Priestley-Taylor and Hargreaves models for estimating reference evapotranspiration in southern Malawi. *Hydrol. Res.*, 44, 706-722, 2013.
- Osborn, T. J. and Jones, P. D.: The CRUTEM4 land-surface air temperature data set: construction, previous versions and dissemination via Google Earth, *Earth Syst. Sci. Data*, 6, 61-68, 2014.
- 25 Pan, Y., Gong, H.-L., Li, X.-J., Zhu, L., and Zhang, J.: Application of Valiantzas approach to estimating reference evapotranspiration in China. *Shuikexue Jinzhan/Adv. Water Sci.*, 22 (1), 30-37, 2011.
- Peel, M. C., Finlayson, B. L., and McMahon, T. A.: Updated world map of the Köppen-Geiger climate classification. *Hydrol. Earth Syst. Sci.*, 11, 1633-1644, 2007.
- Peixoto, J. P., and Oort, A. H.: The climatology of relative humidity in the atmosphere. *J. Climate*, 9, 3443-3463, 1996.
- 30 Pereira, A. R.: The Priestley-Taylor parameter and the decoupling factor for estimating reference evapotranspiration. *Agr. Forest Meteorol.*, 125, 305-313, 2004.
- Peterson, T. C., and Vose, R. S.: An overview of the global historical climatology network temperature database. *B. Am. Meteorol. Soc.*, 78, 2837-2849, 1997.
- Priestley, C. H. B., and Taylor, R. J.: On the assessment of surface heat flux and evaporation using large-scale parameters.

- Mon. Weather Rev., 100, 81-92, 1972.
- Rahimikhoob, A., Behbahani, M. R., and Fakheri, J.: An evaluation of four reference evapotranspiration models in a subtropical climate. *Water Resour. Manage.*, 26, 2867-2881, 2012.
- Ravazzani, G., Corbari, C., Morella, S., Gianol, P., and Mancini, M.: Modified Hargreaves-Samani equation for the assessment of reference evapotranspiration in alpine river basins. *J. Irrig. Drain. Eng. ASCE*, 138, 592-599, 2012.
- 5 Samani, Z.: Estimating solar radiation and evapotranspiration using minimum climatological data. *J. Irrig. Drain. Eng. ASCE*, 126, 265-267, 2000.
- Sheffield, J., Goteti, G., and Wood, E. F.: Development of a 50-yr high-resolution global dataset of meteorological forcings for land surface modeling. *J. Climate*, 19, 3088-3111, 2006.
- 10 Shiri, J., Nazemi, A.H., Sadraddini, A.A., Landeras, G., Kisi, O., Fakheri Fard, A., and Marti, P.: Comparison of heuristic and empirical approaches for estimating reference evapotranspiration from limited inputs in Iran. *Comput. Electron. Agr.*, 108, 230-241, 2014.
- Shuttleworth, W. J., and Calder, I. R.: Has the Priestley-Taylor equation any relevance to forest evaporation? *J. Appl. Meteorol.*, 18, 639-646., 1979.
- 15 Singh, R. K., and Irmak, A.: Treatment of anchor pixels in the METRIC model for improved estimation of sensible and latent heat fluxes. *Hydrol. Sci. J.* 56, 895-906, 2011.
- Snyder, R. L., and Pruitt. W. O.: Estimating reference evapotranspiration with hourly data. VII-1-VII-3. R. Snyder, D. W. Henderson, W. O., Pruitt, and A. Dong (eds), *Calif. Irrig. Mgmt. Systems*, Final Rep., Univ. Calif., Davis, 1985.
- Snyder, R. L., and Pruitt. W. O.: Evapotranspiration data management in California. Presented at the Amer. Soc. of Civil Engr. Water Forum '92', Aug. 2-6, 1992, Baltimore, MD, 1992.
- 20 Sumner, D. M., and Jacobs, J. M.: Utility of Penman–Monteith, Priestley–Taylor, reference evapotranspiration, and pan evaporation methods to estimate pasture evapotranspiration. *J. Hydrol.*, 308, 81-104, 2005.
- Sun, X., Ren, G., Xu, W., Li, Q., and Ren, Y.: Global land-surface air temperature change based on the new CMA GLSAT data set. *Sci. Bull.*, 62, 236-238, 2017.
- 25 Tabari, H.: Evaluation of reference crop evapotranspiration equations in various climates. *Water Resour. Manage.*, 24, 2311-2337, 2010.
- Tabari, H., and Talaei, P. H.: Local calibration of the Hargreaves and Priestley–Taylor equations for estimating reference evapotranspiration in arid and cold climates of Iran based on the Penman–Monteith model. *J. Hydrol. Eng.*, 16, 837-845, 2011.
- 30 Tateishi, R., and Ahn, C. H.: Mapping evapotranspiration and water balance for global land surfaces. *ISPRS J. Photogramm.*, 51, 209-215, 1996.
- Thornthwaite, C. W.: An approach toward a rational classification of climate.. *Geogr. Rev.*, 38, 55-94, 1948.
- Trajkovic, S.: Hargreaves versus Penman–Monteith under humid condition. *J. Irrig. Drain. Eng.*, 133, 38-42, 2007.

- Valiantzas, J. D.: Simple ETo forms of Penman's equation without wind and/or humidity data. I: Theoretical development. *J. Irrig. Drain Eng.*, 139, 1-8, 2013a.
- Valiantzas, J. D.: Simplified reference evapotranspiration formula using an empirical impact factor for penman's aerodynamic term. *J. Hydrol. Eng.*, 18, 108-114, 2013b.
- 5 Valiantzas, J. D.: Simple ETo forms of Penman's equation without wind and/or humidity data. II: Comparisons with reduced set-FAO and other methodologies. *J. Irrig. Drain. Eng.*, 139, 9-19, 2013c.
- Valiantzas, J. D.: Closure to "Simple ETo forms of Penman's equation without wind and/or humidity data. I: Theoretical development" by John D. Valiantzas. *J. Irrig. Drain Eng.*, 140, art. no. 07014017, 2014.
- Valipour, M.: Ability of Box-Jenkins models to estimate of reference potential evapotranspiration (A Case Study: Mehrabad synoptic station, Tehran, Iran). *IOSR J. Agr. Vet. Sci.*, 1, 1-11, 2012.
- 10 Valipour, M.: Application of new mass transfer formulae for computation of evapotranspiration. *J. Appl. Water Eng. Res.*, 2, 33-46, 2014.
- Valipour, M.: Investigation of Valiantzas' evapotranspiration equation in Iran. *Theor. Appl. Clim.*, 121, 267-278, 2015a.
- Valipour, M.: Evaluation of radiation methods to study potential evapotranspiration of 31 provinces. *Meteorol. Atmos. Phys.*, 127, 289-303, 2015b.
- 15 Valipour, M.: Importance of solar radiation, temperature, relative humidity, and wind speed for calculation of reference evapotranspiration. *Arch. Agron. Soil Sci.*, 61, 239-255, 2015c.
- Valipour, M.: Analysis of potential evapotranspiration using limited weather data. *Appl. Water Sci.*, 7, 187-197, 2017.
- Valipour, M., Gholami Sefidkouhi, M. A.: Temporal analysis of reference evapotranspiration to detect variation factors. *Int. J. Global Warm.*, (in press), 2017 doi: 10.1504/IJGW.2018.10002058
- 20 Valipour, M., Gholami Sefidkouhi, M. A., and Raeni-Sarjaz, M.: Selecting the best model to estimate potential evapotranspiration with respect to climate change and magnitudes of extreme events. *Agr. Water Manage.*, 180, 50-60, 2017.
- Wang, K., and Dickinson, R. E.: A review of global terrestrial evapotranspiration: Observation, modeling, climatology, and climatic variability. *Rev. Geophys.*, 50, RG2005, 2012.
- 25 Weiß, M., and Menzel, L.: A global comparison of four potential evapotranspiration equations and their relevance to stream flow modelling in semi-arid environments. *Adv. Geosci.*, 18, 15-23, 2008.
- Wild, M., Folini, D., Schär, C., Loeb, N., Dutton, E.G., and König-Langlo, G.: The global energy balance from a surface perspective. *Clim. Dyn.*, 40, 3107-3134, 2013.
- 30 Willett, K. M., Dunn, R. J. H., Thorne, P. W., Bell, S., De Podesta, M., Parker, D. E., Jones, P. D., and Williams, C. N.: HadISDH land surface multi-variable humidity and temperature record for climate monitoring. *Clima. Past*, 10, 1983-2006, 2014.
- Willmot, C. J.: On the validation of models. *Phys. Geogr.*, 2, 184-194, 1981.
- Xu, C. -Y., and Singh V. P.: Cross comparison of empirical equations for calculating potential evapotranspiration with data

from Switzerland. *Water Resour. Manage.*, 16, 197-219, 2002.

Xu, J., Peng, S., Ding, J., Wei, Q., and Yu, Y.: Evaluation and calibration of simple methods for daily reference evapotranspiration estimation in humid East China. *Arch. Agron. Soil Sci.*, 59, 845-858, 2013.

Zambrano-Bigiarini, M.: Hydrogof: Goodness-of-fit functions for comparison of simulated and observed hydrological time series. R package, version 0.3-8, 2015. <https://cran.r-project.org/web/packages/hydroGOF/hydroGOF.pdf>

Zomer, R. J., Trabucco, A., Bossio, D. A., van Straaten, O., and Verchot, L. V.: Climate change mitigation: A spatial analysis of global land suitability for clean development mechanism afforestation and reforestation. *Agr. Ecosyst. Environ.*, 126, 67-80, 2008.

10

15

20

25

30

35

40

45

TABLES

5 **Table 1.** Meteorological stations from USA-California (CIMIS database) and Australia (AGBM database).

No.	Code	Station	Country	Elevation (m)	Lat (Dec.deg.)	Long (Dec.Deg.)	Period	Köppen Class*
CA-1	006	Davis	USA-CA	18	38.54	-121.78	Sep 1982 - Aug 2016	Csa
CA-2	002	FivePoints	USA-CA	87	36.34	-120.11	Jun 1982 - Aug 2016	BWk
CA-3	005	Shafter	USA-CA	110	35.53	-119.28	Jun 1982 - Aug 2016	BSk
CA-4	007	Firebaugh/Telles	USA-CA	56	36.85	-120.59	Sep 1982 - Aug 2016	BWk
CA-5	012	Durham	USA-CA	40	39.61	-121.82	Oct 1982 - Aug 2016	Csa
CA-6	008	Gerber	USA-CA	76	40.04	-122.17	Sep 1982 - Aug 2014	Csa
CA-7	015	Stratford	USA-CA	59	36.16	-119.85	Nov 1982 - Aug 2016	BSk
CA-8	019	Castroville	USA-CA	3	36.77	-121.77	Nov 1982 - Aug 2016	Csb
CA-9	021	Kettleman	USA-CA	104	35.87	-119.89	Nov 1982 - Aug 2016	BWk
CA-10	027	Zamora	USA-CA	15	38.81	-121.91	Dec 1982 - May 2006	Csa
CA-11	030	Nicolaus	USA-CA	10	38.87	-121.55	Jan 1983 - Dec 2011	Csa
CA-12	032	Colusa	USA-CA	17	39.23	-122.02	Jan 1983 - Aug 2016	Csa
CA-13	033	Visalia	USA-CA	107	36.30	-119.22	Jan 1983 - Feb 2007	BSk
CA-14	035	Bishop	USA-CA	1271	37.36	-118.41	Feb 1983 - Aug 2016	BSk
CA-15	039	Parlier	USA-CA	103	36.60	-119.50	May 1983 - Aug 2016	BSk
CA-16	041	Calipatria/Mulberry	USA-CA	-34	33.04	-115.42	Jul 1983 - Aug 2016	BWh
CA-17	043	McArthur	USA-CA	1009	41.06	-121.46	Dec 1983 - Aug 2016	Csb
CA-18	044	U.C.Riverside	USA-CA	311	33.96	-117.34	Jun 1985 - Aug 2016	BSk
CA-19	047	Brentwood	USA-CA	14	37.93	-121.66	Nov 1985 - Aug 2016	Csb
CA-20	049	Oceanside	USA-CA	15	33.26	-117.32	Mar 1986 - Oct 2003	BSk
CA-21	054	Blackwells Corner	USA-CA	215	35.65	-119.96	Oct 1986 - Aug 2016	BWk
CA-22	056	Los Banos	USA-CA	29	37.10	-120.75	Jun 1988 - Aug 2016	BSk
CA-23	061	Orland	USA-CA	60	39.69	-122.15	May 1987 - May 2010	Csa
CA-24	062	Temecula	USA-CA	433	33.49	-117.23	Nov 1986 - Aug 2016	BSk
CA-25	064	Santa Ynez	USA-CA	149	34.58	-120.08	Nov 1986 - Aug 2016	Csb
CA-26	068	Seeley	USA-CA	12	32.76	-115.73	May 1987 - Aug 2016	BWh
CA-27	070	Manteca	USA-CA	10	37.83	-121.22	Nov 1987 - Aug 2016	BSk
CA-28	071	Modesto	USA-CA	11	37.65	-121.19	Jul 1987 - Aug 2016	BSk
CA-29	077	Oakville	USA-CA	58	38.43	-122.41	Jan 1989 - Aug 2016	Csb
CA-30	075	Irvine	USA-CA	125	33.69	-117.72	Oct 1987 - Aug 2016	BSk
CA-31	078	Pomona	USA-CA	223	34.06	-117.81	Mar 1989 - Aug 2016	Csa
CA-32	080	Fresno State	USA-CA	103	36.82	-119.74	Oct 1988 - Aug 2016	BSk
CA-33	083	Santa Rosa	USA-CA	24	38.40	-122.80	Jan 1990 - Aug 2016	Csb
CA-34	084	Browns Valley	USA-CA	287	39.25	-121.32	Apr 1989 - Aug 2016	Csa
CA-35	085	Hopland F.S.	USA-CA	354	39.01	-123.08	Sep 1989 - Apr 2016	Csa
CA-36	086	Lindcove	USA-CA	146	36.36	-119.06	May 1989 - Aug 2016	Csa
CA-37	087	Meloland	USA-CA	-15	32.81	-115.45	Dec 1989 - Aug 2016	BWh
CA-38	088	Cuyama	USA-CA	698	34.94	-119.67	May 1989 - Aug 2016	BSk
CA-39	091	Tulelake F.S.	USA-CA	1230	41.96	-121.47	Mar 1989 - Aug 2016	Dsb

CA-40	092	Kesterson	USA-CA	23	37.23	-120.88	Oct 1989 - Aug 2016	BSk
CA-41	094	Goletta foothills	USA-CA	195	34.47	-119.87	Jul 1989 - Jul 2016	Csb
CA-42	099	Santa Monica	USA-CA	104	34.04	-118.48	Dec 1992 - Aug 2016	Csb
CA-43	103	Windsor	USA-CA	26	38.53	-122.83	Dec 1990 - Aug 2016	Csb
CA-44	104	De Laveaga	USA-CA	91	37.00	-122.00	Sep 1990 - Aug 2016	Csb
CA-45	105	Westlands	USA-CA	58	36.63	-120.38	Apr 1992 - Aug 2016	BWk
CA-46	106	Sanel Valley	USA-CA	160	38.98	-123.09	Feb 1991 - Aug 2016	Csa
CA-47	57	Buntingville	USA-CA	1221	40.29	-120.43	June 1986 - Sep 2016	Dsb
CA-48	90	Alturas	USA-CA	1343	41.44	-120.48	Apr 1989 - Sep 2016	Dsb
CA-49	151	Ripley	USA-CA	77	33.53	-114.63	Dec 1998 - Sep 2016	BWh
CA-50	183	Owens Lake North	USA-CA	1123	36.49	-117.92	Dec 2002 - Sep 2016	BWk
CA-51	147	Otay Lake	USA-CA	177	32.63	-116.94	Apr 1999 - Sep 2016	Csb
CA-52	175	Palo Verde II	USA-CA	70	33.38	-114.72	Jan 2001 - Sep 2016	BWh
CA-53	135	Blynthe NE	USA-CA	84	33.66	-114.56	Jan 1997 - Sep 2016	BWh
CA-54	155	Bryte	USA-CA	12	38.60	-121.54	Dec 1998 - Sep 2016	Csa
CA-55	159	Monrovia	USA-CA	181	34.15	-117.99	Oct 1999 - Sep 2016	Csa
CA-56	161	Patterson	USA-CA	56	37.44	-121.14	Aug 1999 - Sep 2016	BSk
CA-57	174	Long Beach	USA-CA	5	33.80	-118.09	Sep 2000 - Sep 2016	Csb
CA-58	173	Torrey Pines	USA-CA	102	32.90	-117.25	Nov 2000 - Sep 2016	Csa
CA-59	150	Miramar	USA-CA	136	32.89	-117.14	Apr 1999 - Sep 2016	Csa
CA-60	153	Escondido SPV	USA-CA	119	33.08	-116.98	Feb 1999 - Sep 2016	Csb
A-1	32040	Townsville Aero	Australia	4	-19.25	146.77	(1940/1996-2016)#	Aw
A-2	33307	Woolshed	Australia	556	-19.42	146.54	(1990/2003-2016)	Aw
A-3	2056	Kununurra Aero	Australia	44	-15.78	128.71	(1971/1990-2016)	BSh
A-4	35264	Emerald	Australia	189	-23.57	148.18	(1990/1998-2016)	BSh
A-5	24024	Loxton R.C.	Australia	30	-34.44	140.6	(1984/1998-2016)	BSk
A-6	74037	Yanco AG.I.	Australia	164	-34.62	146.43	(1957/1999-2016)	BSk
A-7	74258	Deniliquin Airp.AWS	Australia	94	-35.56	144.95	(1990/2003-2016)	BSk
A-8	75041	Griffith Airp.AWS	Australia	134	-34.25	146.07	(1958/1990-2016)	BSk
A-9	76031	Mildura Airp.	Australia	50	-34.24	142.09	(1946/1993-2016)	BSk
A-10	24048	Renmark Apt.1	Australia	32	-34.2	140.68	(1990/2003-2016)	BWk
A-11	40082	University of QLD G.	Australia	89	-27.54	152.34	(1897/1990-2016)	Cfa
A-12	40922	Kingaroy Airp.	Australia	434	-26.57	151.84	(1990/2003-2016)	Cfa
A-13	41359	Oakey Aero	Australia	406	-27.4	151.74	(1970/1996-2016)	Cfa
A-14	41522	Dalby Airp.	Australia	344	-27.16	151.26	(1990/2006-2016)	Cfa
A-15	41525	Warwick	Australia	475	-28.21	152.1	(1990/2000-2016)	Cfa
A-16	41529	Toowoomba Airp.	Australia	641	-27.54	151.91	(1990/1997-2016)	Cfa
A-17	80091	Kyabram	Australia	105	-36.34	145.06	(1964/1990-2016)	Cfa
A-18	81049	Tatura I.S.A.	Australia	114	-36.44	145.27	(1942/1990-2016)	Cfa
A-19	81124	Yarrowonga	Australia	129	-36.03	146.03	(1990/2003-2016)	Cfa
A-20	81125	Shepparton Airp.	Australia	114	-36.43	145.39	(1990/1996-2016)	Cfa
A-21	41175	Applethorpe	Australia	872	-28.62	151.95	(1966/2006-2016)	Cfb
A-22	81123	Bendigo Airp.	Australia	208	-36.74	144.33	(1990/2004-2016)	Cfb
A-23	85072	East Sale Airp.	Australia	5	-38.12	147.13	(1943/1996-2016)	Cfb
A-24	85279	Bairnsdale Airp.	Australia	49	-37.88	147.57	(1942/2003-2016)	Cfb

A-25	85280	Morwell L.V.Airp.	Australia	56	-38.21	146.47	(1984/1999-2016)	Cfb
A-26	85296	Mount Moornapa	Australia	480	-37.75	147.14	(1990/2003-2016)	Cfb
A-27	90035	Colac	Australia	261	-38.23	143.79	(1990/2003-2016)	Cfb
A-28	9538	Dwellingup	Australia	267	-32.71	116.06	(1934/1990-2016)	Csb
A-29	9617	Bridgetown	Australia	179	-33.95	116.13	(1990/2003-2016)	Csb
A-30	23373	Nuriootpa Pirsa	Australia	275	-34.48	139.01	(1990/1996-2016)	Csb
A-31	26021	Mount Gambier Aero	Australia	63	-37.75	140.77	(1942/1994-2016)	Csb
A-32	26091	Coonawarra	Australia	57	-37.29	140.83	(1985/1990-2016)	Csb
A-33	66062	Sydney (Obs.Hill)	Australia	39	-33.86	151.21	(1858/1990-2016)	Cfb
A-34	33002	Ayr DPI Res.St.	Australia	17	-19.62	147.38	(1951/1994-2016)	Cwa
A-35	7176	Newman Aero	Australia	524	-23.42	119.8	(1971/2003-2016)	BWh
A-36	13017	Giles	Australia	598	-25.03	128.3	(1956/1990-2016)	BWh
A-37	11052	Forrest	Australia	159	-30.85	128.11	(1990/2003-2016)	BWh
A-38	11003	Eucla	Australia	93	-31.68	128.9	(1876/1995-2016)	BSk
A-39	12071	Salmon Gums	Australia	249	-32.99	121.62	(1932/2003-2016)	BSk
A-40	7045	Meekatharra Airp.	Australia	517	-26.61	118.54	(1944/1992-2016)	BWh
A-41	1025	Doongan	Australia	385	-15.38	126.31	(1988/1990-2016)	Aw
A-42	2012	Halls Creek Airp.	Australia	422	-18.23	127.66	(1944/1996-2016)	BSh
A-43	13015	Carnegie	Australia	448	-25.8	122.98	(1942/1990-2016)	BWh
A-44	3080	Curtin Aero	Australia	78	-17.58	123.83	(1990/2003-2016)	BSh
A-45	6022	Gascoyne Junction	Australia	144	-25.05	115.21	(1907/1990-2016)	BWh
A-46	9789	Esperance	Australia	25	-33.83	121.89	(1969/1990-2016)	Csb
A-47	91223	Marrawah	Australia	107	-40.91	144.71	(1971/1990-2016)	Cfb
A-48	18106	Nullarbor	Australia	64	-31.45	130.9	(1888/2006-2016)	BWk
A-49	16090	Cooper Pedy Airp.	Australia	225	-29.03	134.72	(1990/2004-2016)	BWh
A-50	16085	Marla Police St.	Australia	323	-27.3	133.62	(1985/1990-2016)	BWh
A-51	13011	Warburton Airfield	Australia	459	-26.13	126.58	(1940/2003-2016)	BWh
A-52	15528	Yuendumu	Australia	667	-22.26	131.8	(1952/1990-2016)	BWh
A-53	15666	Rabbit Flat	Australia	340	-20.18	130.01	(1990/1996-2016)	BWh
A-54	14829	Lajamanu Airp.	Australia	316	-18.33	130.64	(1952/1990-2016)	BSh
A-55	15135	Tennant Creek Airp.	Australia	376	-19.64	134.18	(1969/1992-2016)	BSh
A-56	37010	Camooweal Township	Australia	231	-19.92	138.12	(1891/2003-2016)	BWh
A-57	14707	Wollogorang	Australia	60	-17.21	137.95	(1967/1990-2016)	Aw
A-58	14938	Mango Farm	Australia	15	-13.74	130.68	(1980/1990-2016)	Aw
A-59	69134	Batemans Bay	Australia	11	-35.72	150.19	(1985/1991-2016)	Cfb
A-60	14198	Jabiru Airp.	Australia	27	-12.66	132.89	(1971/1990-2016)	Aw
A-61	28008	Lockhart River Airp.	Australia	19	-12.79	143.3	(1956/2001-2016)	Am
A-62	34084	Charters Towers Airp.	Australia	290	-20.05	146.27	(1990/1992-2016)	BSh
A-63	29038	Kowanyama Airp.	Australia	10	-15.48	141.75	(1912/1999-2016)	Aw
A-64	32078	Ingham Composite	Australia	12	-18.65	146.18	(1968/1990-2016)	Am
A-65	40854	Logan City W.T.P.	Australia	14	-27.68	153.19	(1990/1992-2016)	Cfa
A-66	8095	Mullewa	Australia	268	-28.54	115.51	(1896/1990-2016)	BSh
A-67	8251	Kalbarri	Australia	6	-27.71	114.17	(1970/1990-2016)	BSh
A-68	8225	Eneabba	Australia	100	-29.82	115.27	(1964/1990-2016)	Csa
A-69	7139	Paynes Find	Australia	339	-29.27	117.68	(1919/1990-2016)	BWh

A-70	10007	Bencubbin	Australia	359	-30.81	117.86	(1912/1990-2016)	BSh
A-71	10092	Merredin	Australia	315	-31.48	118.28	(1903/1990-2016)	Bsk
A-72	12038	Kalgoorlie-Boulder Airp.	Australia	365	-30.78	121.45	(1939/1994-2016)	BSh
A-73	16098	Tarcoola Aero	Australia	123	-30.71	134.58	(1990/1999-2016)	BWh
A-74	18195	Minnipa Pirs	Australia	165	-32.84	135.15	(1990/2003-2016)	Bsk
A-75	46126	Tibooburra Airp.	Australia	176	-29.44	142.06	(1990/2003-2016)	BWh
A-76	48245	Boorke Airp. AWS	Australia	107	-30.04	145.95	(1990/2002-2016)	BSh
A-77	55325	Tamworth Airp. AWS	Australia	395	-31.07	150.84	(1990/2006-2016)	Cfa
A-78	38026	Birdsville Airp.	Australia	47	-25.9	139.35	(1990/2001-2016)	BWh
A-79	30161	Richmond Airp.	Australia	206	-20.7	143.12	(1990/2003-2016)	BSh
A-80	33013	Collinsville Airp.	Australia	196	-20.55	147.85	(1939/1990-2016)	BSh

\*Köppen classification obtained from Peel et al. (2007).

# In the case of Australian stations, the periods of observations vary between different climatic parameters. e.g. for the case (1939/1990-2016), the two dates separated with “/” show the starting date of the oldest and newest record of parameters used in calculations, respectively, while 2016 is the ending date of the records.

5

10

15

20

25

30

35

**Table 2.** Additional models of reduced parameters obtained from the international literature, which provide equivalent results to  $ET_o$  for short reference crop,

Reference	Abbreviation	Formula	Climate data requirements*
Droogers and Allen (2002)	DRAL1 (Eq.8)	$ET_o = 0.00102R_a (T_{mean} + 16.8) \cdot (TD)^{0.5}$	$T_{max}, T_{min}$
Droogers and Allen (2002)	DRAL2 (Eq.9)	$ET_o = 0.0005304R_a (T_{mean} + 17.0) \cdot (TD - 0.0123P)^{0.76}$	$T_{max}, T_{min}, P$
Alexandris et al. (2006)	Copais (Eq.10)	$ET_o = 0.057 + 0.227C_2 + 0.643C_1 + 0.0124C_1C_2$ $C_1 = 0.6416 - 0.00784RH + 0.372R_s - 0.00264R_sRH$ $C_2 = -0.0033 + 0.00812T_{mean} + 0.101R_s + 0.00584R_sT_{mean}$	$T_{mean}, R_s, RH$
Valiantzas (2013a, 2014)	VAL1 (Eq.11)	$ET_o = 0.0393R_s\sqrt{T_{mean} + 9.5} - 0.19R_s^{0.6}\varphi^{0.15}$ $+ 0.0061(T_{mean} + 20)(1.12T_{mean} - T_{min} - 2)^{0.7}$	$T_{mean}, T_{min}, R_s$
Valiantzas (2013a; 2014)	VAL2 (Eq.12)	$ET_o = 0.0393R_s\sqrt{T_{mean} + 9.5} - 0.19R_s^{0.6}\varphi^{0.15}$ $+ 0.078(T_{mean} + 20)\left(1 - \frac{RH}{100}\right)$	$T_{mean}, R_s, RH$
Valiantzas (2013b)	VAL3 (Eq.13)	$ET_o = 0.0393R_s\sqrt{T_{mean} + 9.5} - 2.4\left(\frac{R_s}{R_a}\right)^2$ $+ Cu(T_{mean} + 20)\left(1 - \frac{RH}{100}\right)$	$T_{mean}, R_s, RH$ ( $Cu=0.054$ for $RH>65\%$ and $Cu=0.083$ for $RH\leq 65\%$ )
Ahooghalandari et al. (2016)	AKJ1 (Eq.14)	$ET_o = 0.252 \cdot 0.408R_a + 0.221T_{mean}\left(1 - \frac{RH}{100}\right)$	$T_{mean}, RH$
Ahooghalandari et al. (2016)	AKJ2 (Eq.15)	$ET_o = 0.29 \cdot 0.408R_a + 0.15T_{max}\left(1 - \frac{RH}{100}\right)$	$T_{max}, RH$

\*  $T_{mean, max, min}$ : Mean, maximum and minimum temperature ( $^{\circ}C$ ),  $TD$ : difference between maximum and minimum temperature ( $^{\circ}C$ ),  $R_s$ : incident solar radiation ( $MJ\ m^{-2}\ d^{-1}$ ),  $R_a$ : extraterrestrial solar radiation ( $MJ\ m^{-2}\ d^{-1}$ ),  $RH$ : relative humidity (%),  $\varphi$ : absolute value of latitude (rads),  $P$ : precipitation ( $mm\ month^{-1}$ )

**Table 3.** The % coverage\* of *MAD*% classes based on mean annual values (according to Figs. 4),  $R^2$  and *RMSD* based on comparisons of the mean monthly values of  $ET_o$  and  $R_s$  methods (comparisons based on 0.5 degree resolution maps).

<i>MAD</i> % range	† $ET_o$ (ASCE-tall) for $C_n=1600$ , $C_d=0.38$ (Eq.1)	† $ET_o$ (P-T) for $a_{pt}=1.26$ (Eq.2)	† $ET_o$ (H-S) for $c_{hs2} = 0.0023$ (Eq.4b)	‡ $R_s$ (H-S) for $K_{RS}=0.17$ (Eq.3)
≤ -50%	0.0%*	0.8%	0.0%	1.0%
-50 up to -25%	0.0%	14.8%	5.2%	2.2%
-25 up to -10%	0.0%	10.8%	15.4%	7.1%
-10 up to 10%	25.2%	21.3%	24.8%	55.3%
10 up to 25%	40.9%	22.5%	19.6%	32.8%
25 up to 50%	33.6%	21.9%	29.2%	1.6%
> 50%	0.3%	7.9%	5.8%	0.0%
$R^2$	0.98	0.77	0.89	0.92
<i>RMSD</i>	39.6§	36.0§	24.5§	2.4#

\*The % coverage was estimated after conversion from WGS84 ellipsoid to projected Cylindrical Equal Area coordinate system without considering Antarctica.

5 † *MAD*% of the three  $ET_o$  methods is estimated versus ASCE-short.

‡ *MAD*% of the standard solar radiation method of H-S is estimated versus the  $R_s$  data of Sheffield et al. (2006).

§ The unit of *RMSD* for  $ET_o$  is  $\text{mm month}^{-1}$ .

# The unit of *RMSD* for  $R_s$  is  $\text{MJ m}^{-2} \text{d}^{-1}$ .

10

**Table 4.** Spatial extent of the major climatic groups CGs from Köppen-Geiger climate map (Peel et al., 2007), % prevalence of P-T versus H-S within each CG based on the *DMAD* values.

Climatic group (CG) of Köppen-Geiger	% extent of CGs* based on Peel et al. (2007) map	P-T versus H-S prevalence % inside a CG#		
		H-S ( $DMAD \leq -1$ )	Trans. Zone $-1 < DMAD < 1$ †	P-T ( $DMAD \geq 1$ )
A - tropical/megathermal	20.66%	32.0%	3.6%	64.4%
B - arid/semi-arid	32.90%	86.4%	1.3%	12.3%
C - temperate/mesothermal	14.58%	32.8%	3.2%	64.1%
D - continental/microthermal	27.00%	26.9%	2.1%	71.0%
E - polar/alpine (without Antarctica)	4.86%	71.1%	16.3%‡	12.5%

15 \*The % coverage was estimated after conversion from WGS84 ellipsoid to projected Cylindrical Equal Area coordinate system without considering Antarctica.

# % coverage of *DMAD* values were estimated after pixel resampling using the resolution of Köppen map.

† *DMAD* range were both methods present similar proximity to ASCE-short method (transitional zone).

20 ‡ Big part of this percentage corresponds to regions with annual  $ET_o$  equal to 0 (e.g. inner Greenland). Such cases are included in the trans. zone of Fig.5a.

25

**Table 5.** Statistical criteria from the comparisons **(a)** between  $ET_o$  values from ASCE-short and the methods used for estimating short reference crop evapotranspiration (i.e. P-T with standard and re-adjusted coefficients, H-S with standard and re-adjusted coefficients and all equations given in Table 2), **(b)** between  $ET_o$  values from ASCE-tall and P-T, H-S methods with re-adjusted coefficients for tall reference crop, **(c)**  $R_s$  values from stations and  $R_s$  obtained from the H-S radiation formula with standard and re-adjusted coefficients.

Case	Criterion	MAE	RMSE	NRMSE%	PBIAS%	R <sup>2</sup>	bR <sup>2</sup>	NSE	d	KGE
	Optimum value	0	0	0	0	1	1	1	1	1
a	P-T (Eq.2) with $a_{pt}=1.26$	36.92	48.87	90.9	33.3	0.763	0.591	0.173	0.849	0.539
	P-T (Eq.2) with $a_{pt}=p.w.a.s.$	22.71	29.43	40.3	7.5	0.856	0.832	0.837	0.956	0.883
	H-S (Eq.4b) with $c_{hs2}=0.0023$	21.19	30.36	53.2	10.8	0.858	0.772	0.717	0.941	0.746
	H-S (Eq.4b) with $c_{hs2}=p.w.a.s.$	17.13	22.72	34.4	2.5	0.895	0.878	0.881	0.971	0.921
	DRAL1 (Eq.8)	19.53	27.05	44.5	4.8	0.859	0.818	0.802	0.955	0.833
	DRAL2 (Eq.9)	22.92	30.28	45.0	3.2	0.818	0.808	0.798	0.949	0.894
	Copais (Eq.10)	14.49	20.70	34.3	7.3	0.940	0.870	0.882	0.974	0.829
	VAL1 (Eq.11)	21.36	31.87	59.8	15.1	0.888	0.763	0.642	0.932	0.657
	VAL2 (Eq.12)	12.13	17.96	29.3	4.2	0.948	0.900	0.914	0.981	0.859
	VAL3 (Eq.13)	11.45	15.94	24.1	1.4	0.949	0.934	0.942	0.986	0.940
	AKJ1 (Eq.14)	21.17	24.24	42.0	-10.6	0.955	0.887	0.824	0.964	0.771
AKJ2 (Eq.15)	30.36	33.69	59.5	-16.3	0.938	0.820	0.645	0.931	0.718	
b	P-T (Eq.2) with $a_{pt}=p.w.a.t.$	40.43	52.38	50.6	8.4	0.770	0.754	0.743	0.930	0.845
	H-S (Eq.4b) with $c_{hs2}=p.w.a.t.$	31.87	42.34	45.2	3.7	0.823	0.806	0.795	0.950	0.885
c	H-S $R_s$ (Eq.3) with $K_{RS}=0.17$	1.64	1.99	29.6	-4.5	0.930	0.885	0.912	0.977	0.932
	H-S $R_s$ (Eq.3) with $K_{RS}=p.w.a.$	1.05	1.43	22.3	-0.8	0.952	0.944	0.950	0.988	0.972

10

15

20

25

FIGURES

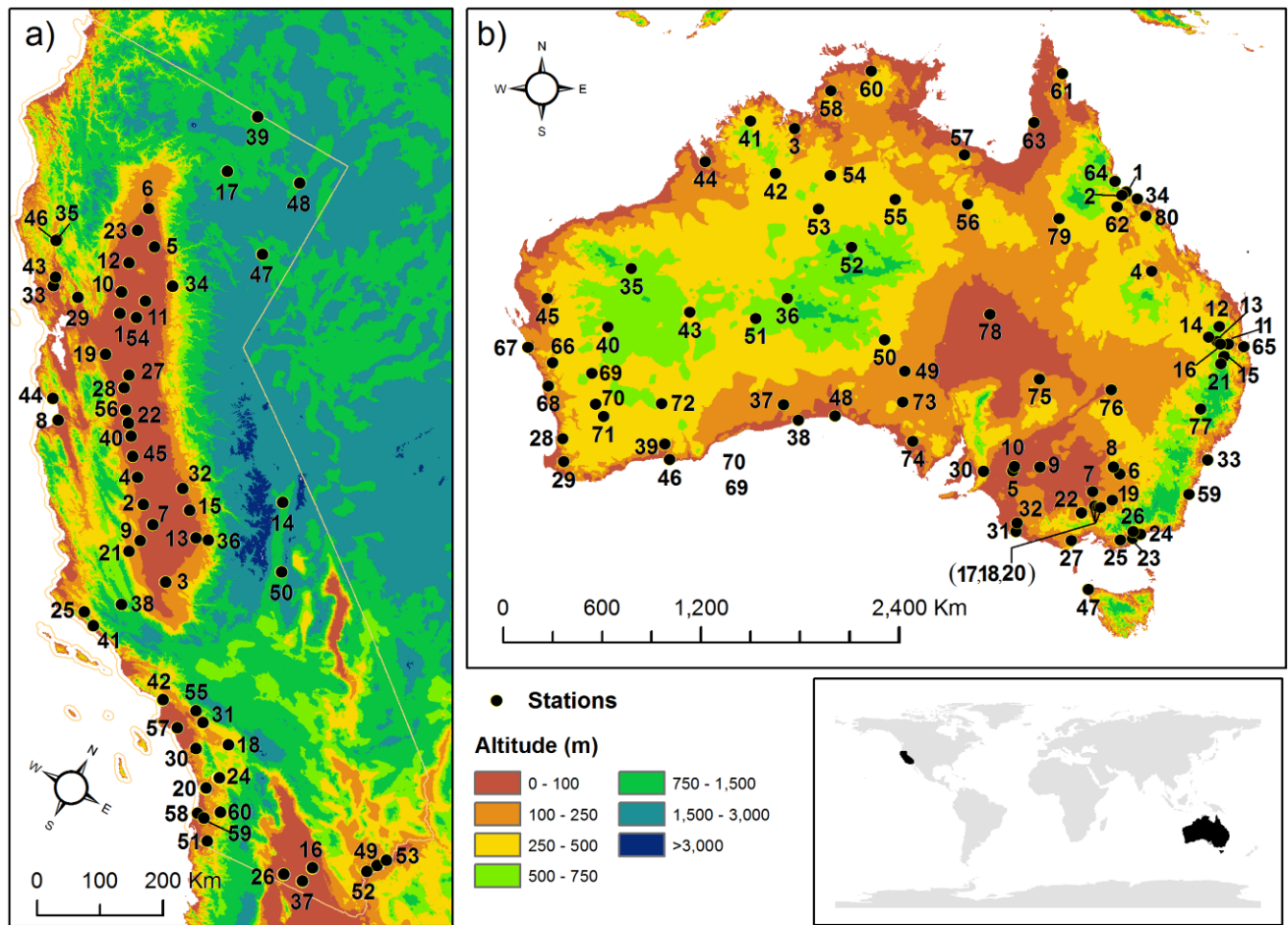


**Figure 1.** Position of stations (a) from California-USA obtained by CIMIS database and (b) from Australia obtained by AGBM database (the numbers indicate the No. of stations from Table 1 without the abbreviations CA- and A-).

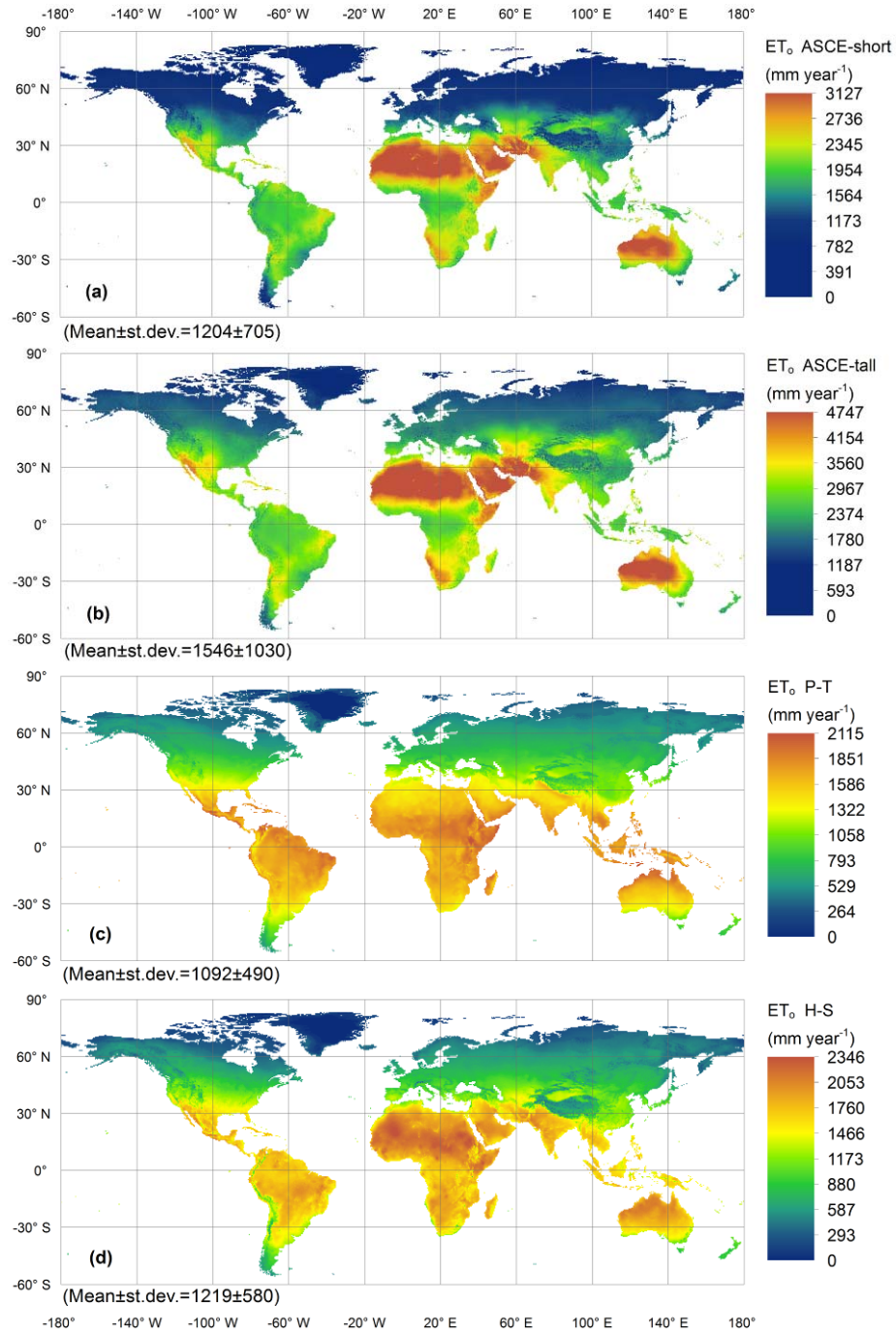


**Figure 2.** Mean annual values (mm year<sup>-1</sup>) of  $ET_o$  for the period 1950-2000 using (a) the ASCE-short method, (b) the ASCE-tall method, (c) the standard P-T method for  $a_{pt}=1.26$  and (d) the standard H-S method for  $c_{hs2}=0.0023$  (0.5 degree resolution maps, mean ± st.dev. are estimated after conversion from WGS84 to Cylindrical Equal Area coordinate system).

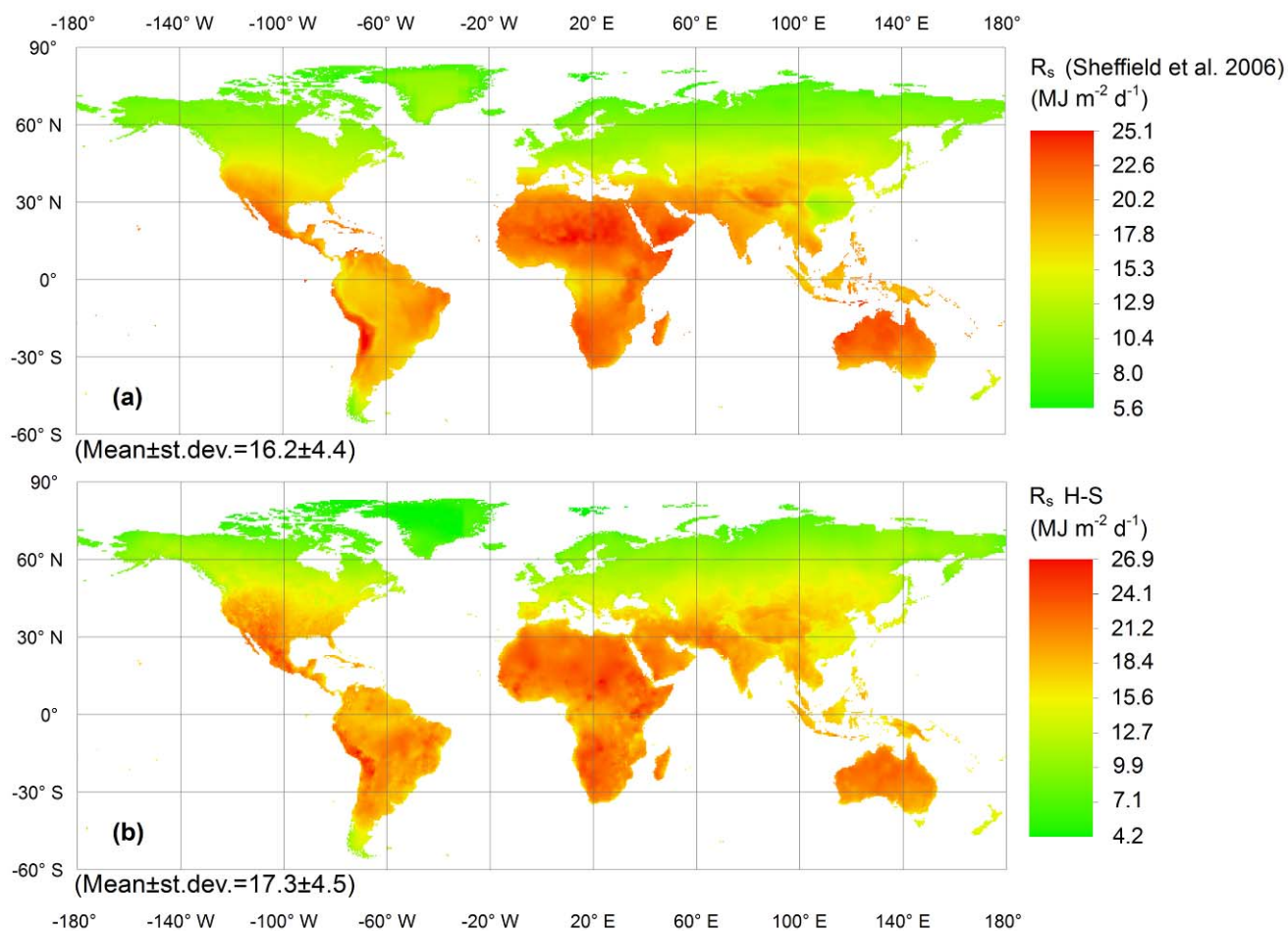


**Figure 3.** Mean annual values of  $R_s$  ( $\text{MJ m}^{-2} \text{d}^{-1}$ ) for the period 1950-2000 (a) from the database of Sheffield et al. (2006) and (b) estimated using the standard H-S radiation formula for  $K_{RS}=0.17$  (Eq.3) (0.5 degree resolution maps, mean±st.dev.

5 are estimated after conversion from WGS84 to Cylindrical Equal Area coordinate system).

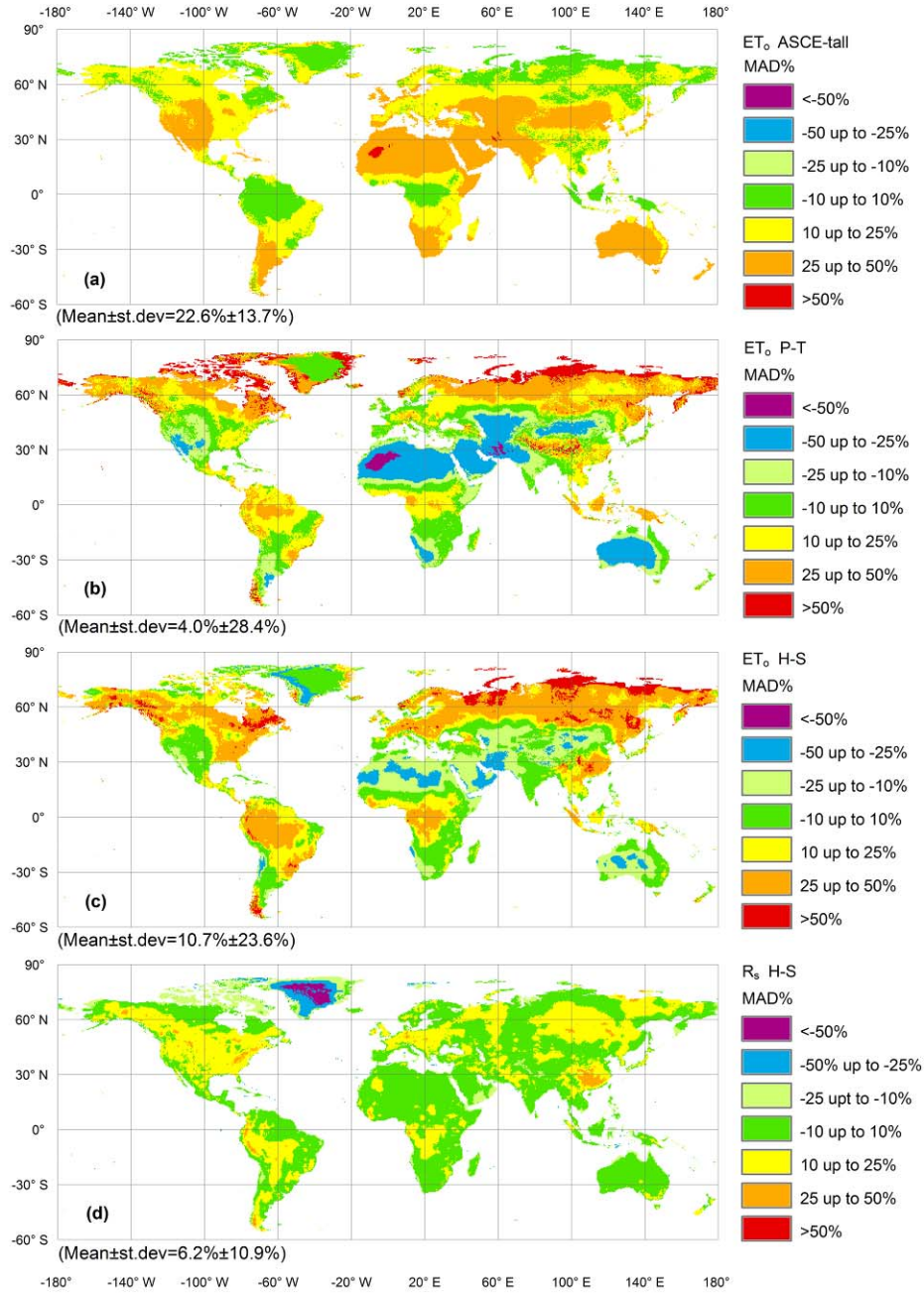


**Figure 4.** Mean annual difference % ( $MAD\%$ ) of  $ET_o$  between the ASCE-short and **(a)** the ASCE-tall method, **(b)** the standard P-T method for  $a_{pt}=1.26$ , **(c)** the standard H-S method for  $c_{hs2} = 0.0023$ , and **(d)**  $MAD\%$  between  $R_s$  values of Sheffield et al. (2006) and the standard solar radiation formula of H-S for  $K_{RS}=0.17$  (0.5 degree resolution maps, 5 mean ± st.dev. are estimated after conversion from WGS84 to Cylindrical Equal Area coordinate system).

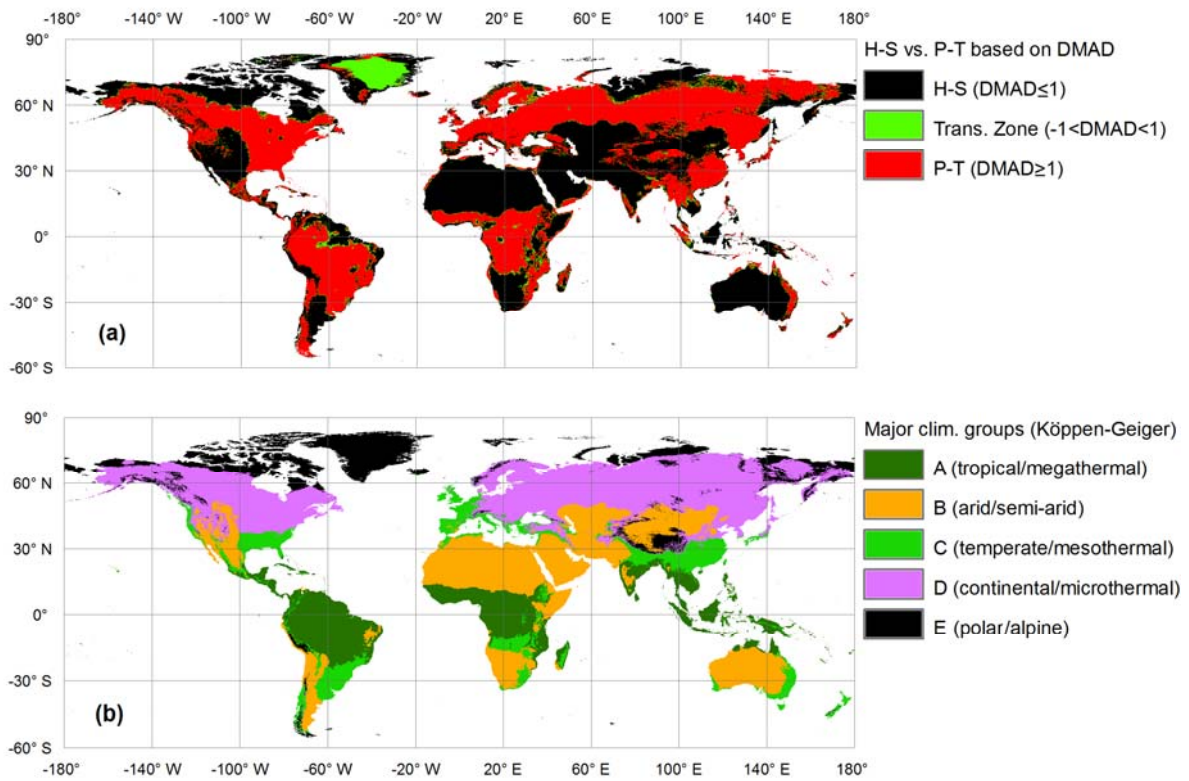


**Figure 5.** (a) P-T versus H-S prevalence according to their proximity to ASCE-short method expressed by the *DMAD* values (0.5 degree resolution map) and (b) Spatial extent of the major climatic groups of the Köppen-Geiger climate classification according to Peel et al. (2007).

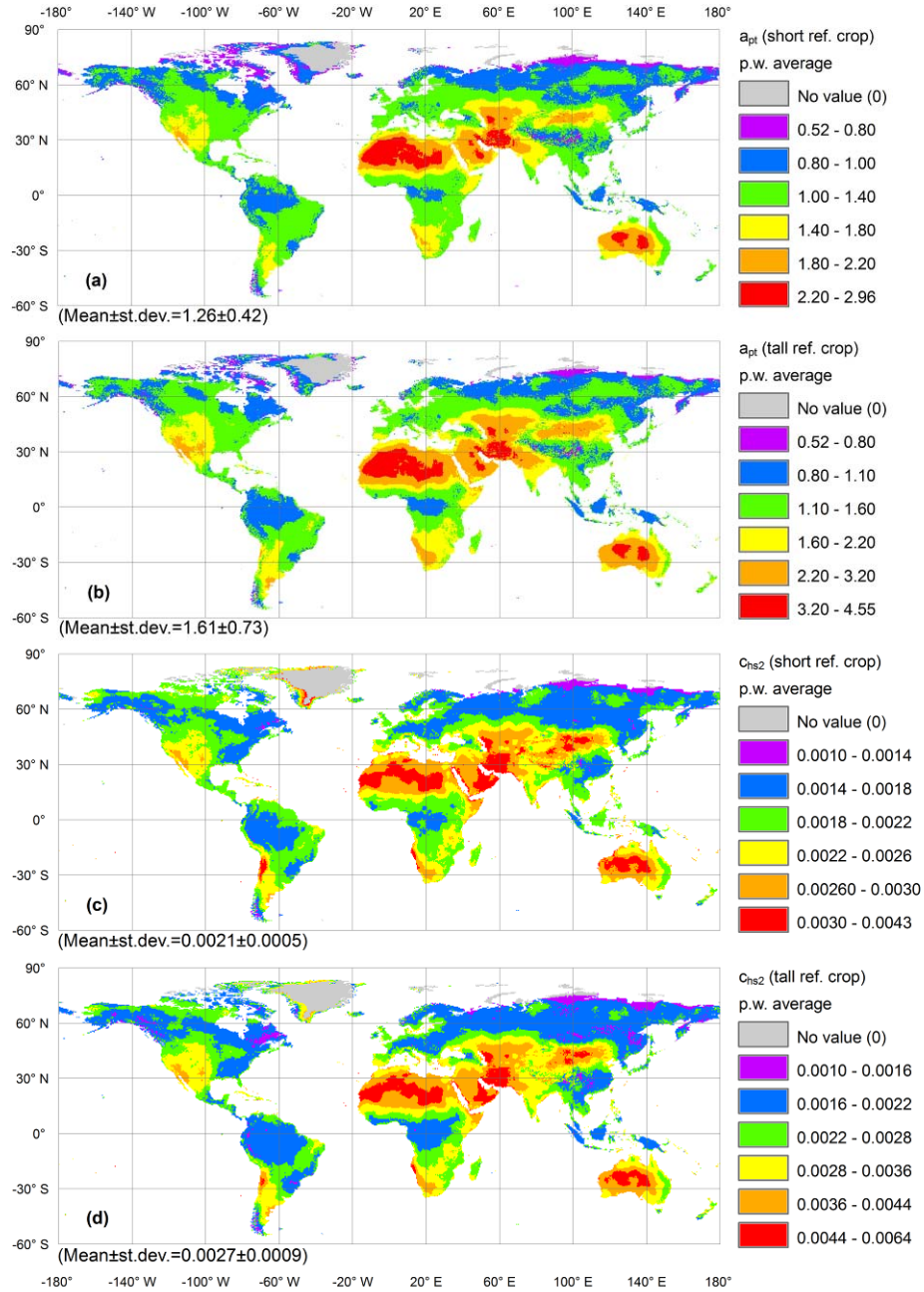
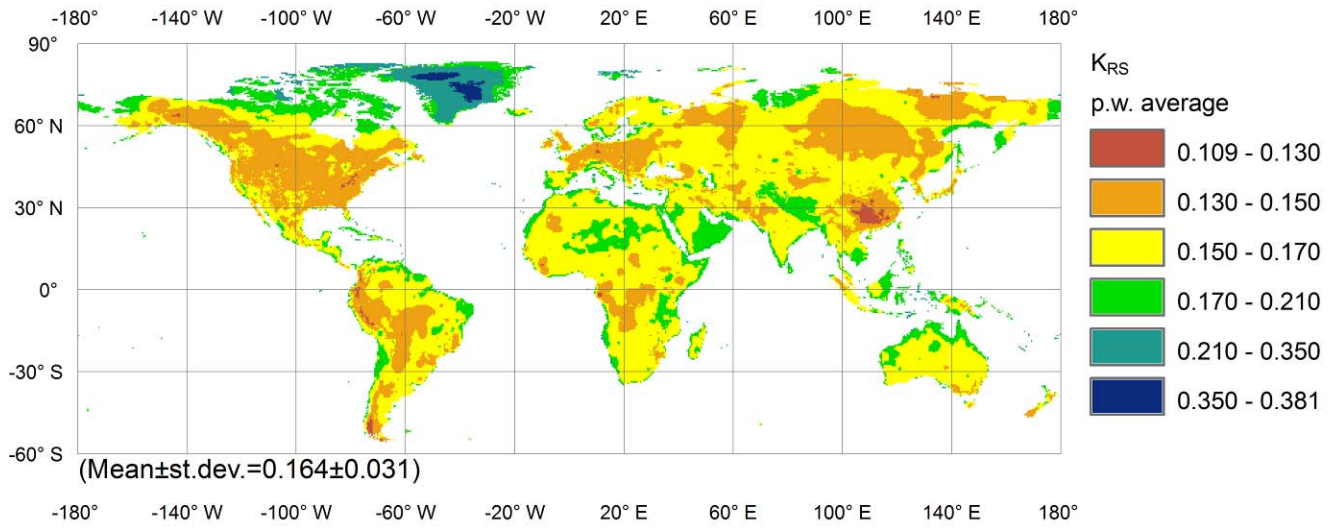


**Figure 6.** Partial weighted averages of mean monthly (a)  $a_{pt}$  for short reference crop, (b)  $a_{pt}$  for tall reference crop, (c)  $c_{hs2}$  for short reference crop and (d)  $c_{hs2}$  for tall reference crop (0.5 degree resolution maps, mean ± st.dev. are estimated after conversion from WGS84 to Cylindrical Equal Area coordinate system excluding pixels of 0 value).

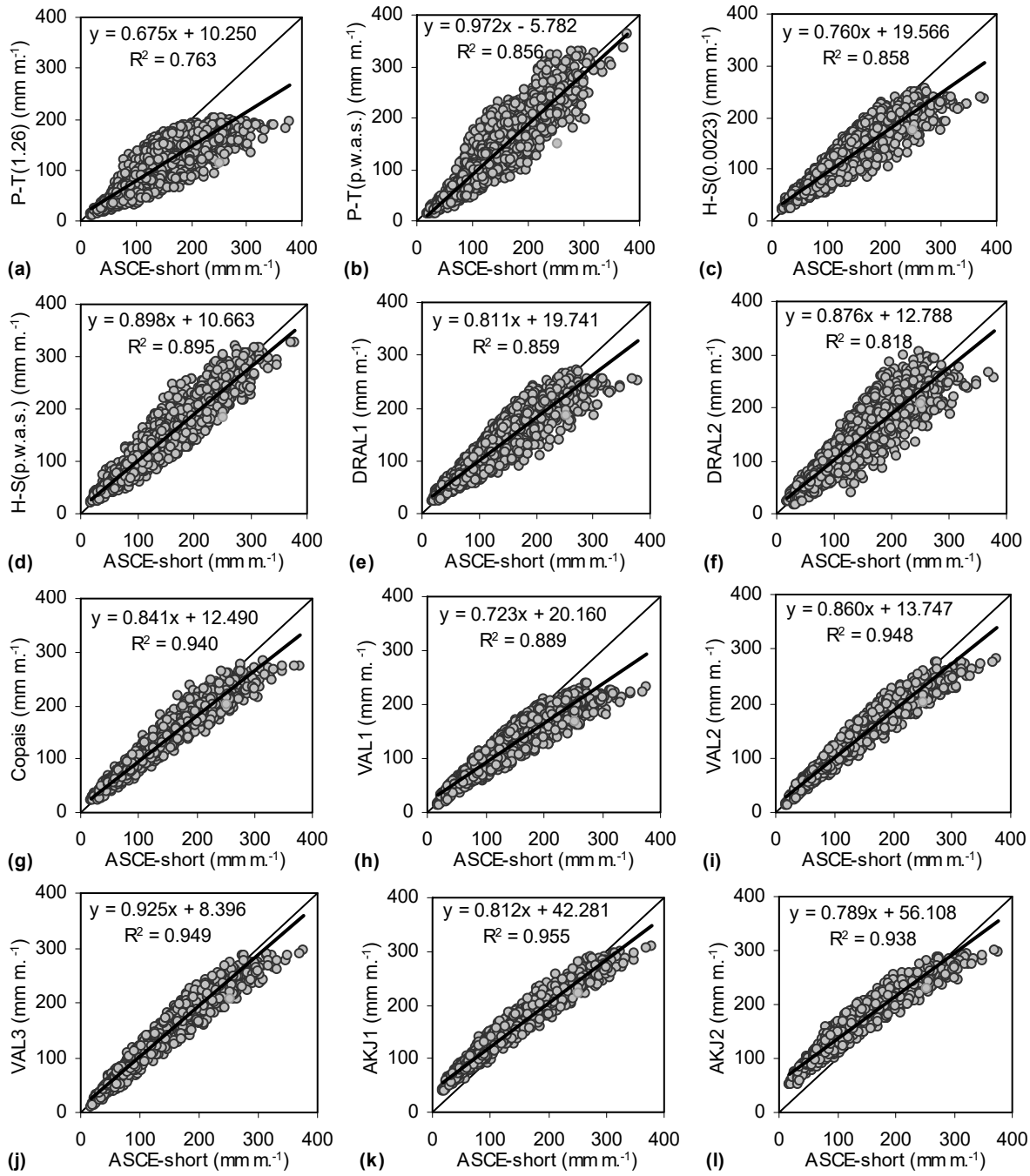


5 **Figure 7.** Partial weighted averages of mean monthly  $K_{RS}$  (0.5 degree resolution maps, mean±st.dev. are estimated after conversion from WGS84 to Cylindrical Equal Area coordinate system).

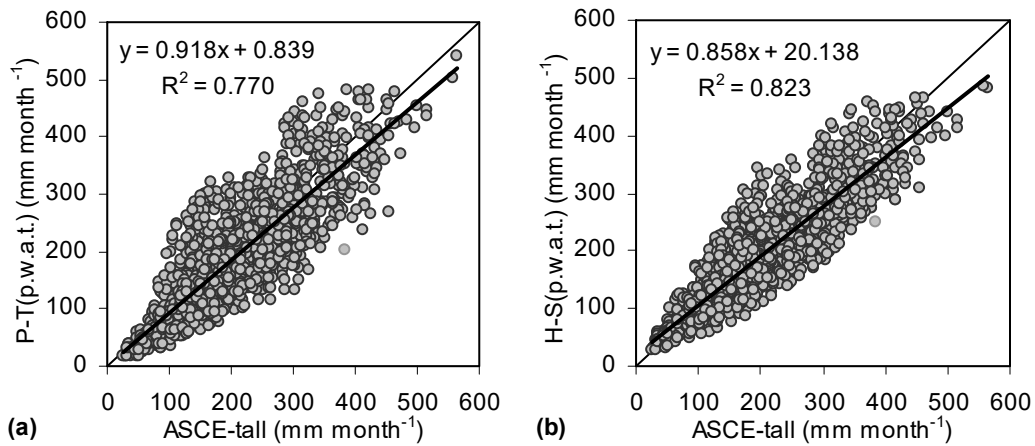
10

15

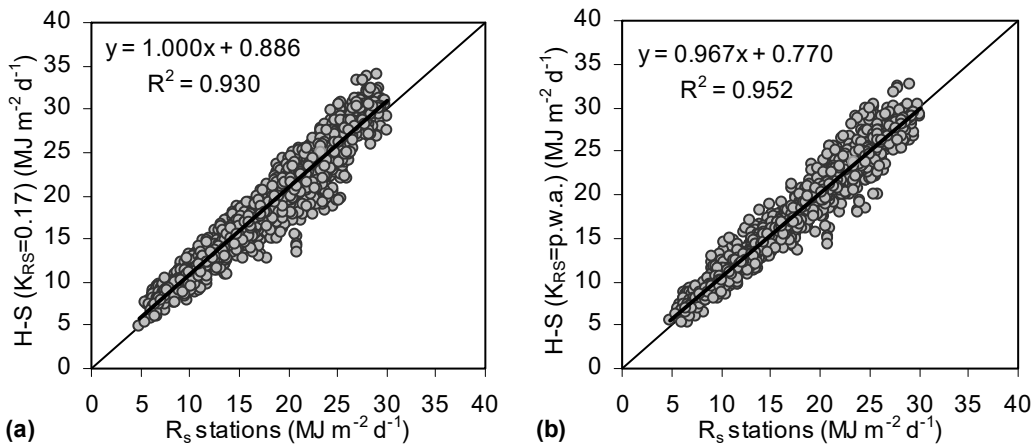
20



5 **Figure 8.** Comparative 1:1 plots between the results of  $ET_o$  ASCE-short ( $\text{mm month}^{-1}$ ) versus (a) the standard P-T method with  $a_{pt}=1.26$ , (b) the P-T method with  $a_{pt}=p.w.a.s.$  (0.5 degree resolution), (c) the standard H-S method with  $c_{hs2}=0.0023$ . (d) the H-S method with  $c_{hs2}=p.w.a.s.$  (0.5 degree resolution), (e) DRAL1 (Eq.8), (f) DRAL2 (Eq.9), (g) Copais (Eq.10), (h) VAL1 (Eq.11), (i) VAL2 (Eq.12), (j) VAL3 (Eq.13), (k) AKJ1 (Eq.14), (l) AKJ2 (Eq.15).



5 **Figure 9.** Comparative 1:1 plots between the results of  $ET_o$  ASCE-tall (mm month<sup>-1</sup>) versus (a) the P-T method with  $a_{pt}$ =p.w.a.t. (0.5 degree resolution), (b) the H-S method with  $c_{hs2}$ =p.w.a.t. (0.5 degree resolution).



10 **Figure 10.** Comparative 1:1 plots between the  $R_s$  (MJ m<sup>-2</sup> d<sup>-1</sup>) values of CA-USA and Australia stations versus the results of H-S radiation formula (Eq.3) (a) with  $K_{RS} = 0.17$ , (b) with  $K_{RS}$ =p.w.a. (0.5 degree resolution).

## Supplementary Material

**Indirect verification of the data cleaning that was performed in the derived data from CIMIS database.**

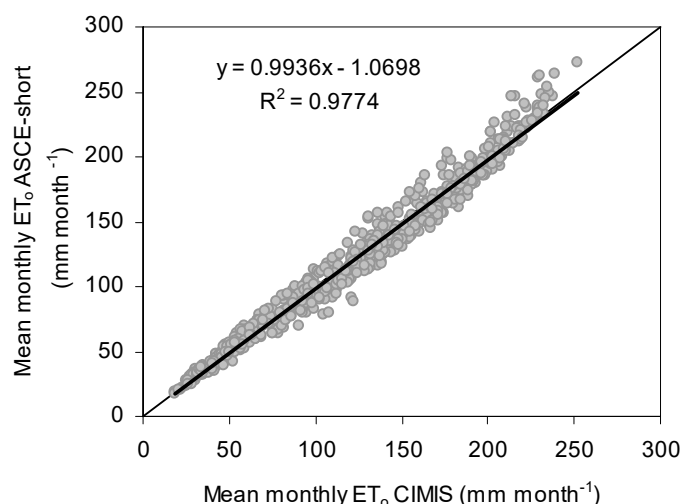


**Fig.S1** Comparison between the mean monthly  $ET_o$  values of ASCE-short method using the final clean climatic data from CIMIS database versus the provided mean monthly values of  $ET_o$  by the database using the CIMIS evapotranspiration method.

**General statistics of meteorological stations data (validation data) and comparison with the raster data (calibration data) used for developing the global maps of  $ET_o$  with ASCE method.**

**Table S1.** General statistics\* of the mean monthly observed values of climatic parameters from the 140 stations of California-USA and Australia that participate in the estimation of reference evapotranspiration with the ASCE method.

Parameter	$T_{max}$	$T_{min}$	$R_s$	$RH$	$u_2$	$P$	$ET_o$ ASCE-short	$ET_o$ ASCE-tall
Unit	°C	°C	MJ m <sup>-2</sup> d <sup>-1</sup>	%	m s <sup>-1</sup>	mm month <sup>-1</sup>	mm month <sup>-1</sup>	mm month <sup>-1</sup>
Average	25.3	11.4	18.8	56.4	2.6	41.5	138.4	190.5
Minimum	5.3	-7.2	4.9	19.0	0.9	0.0	17.9	26.2
Lower quartile	19.7	6.5	13.5	45.5	1.8	11.7	82.2	112.7
Upper quartile	31.1	15.8	24.4	68.2	3.2	50.6	186.9	254.2
Maximum	41.2	26.3	30.1	90.3	6.8	470.4	377.5	563.8
Range	35.9	33.5	25.2	71.3	5.9	470.4	359.6	537.6
Standard deviation	7.1	6.4	6.5	15.4	1.0	51.5	69.5	98.9
Coeff. of variation %	28.11%	56.13%	34.32%	27.36%	37.05%	123.90%	50.17%	51.93%

\*The statistics are based on 1680 values (140 stations × 12 months)

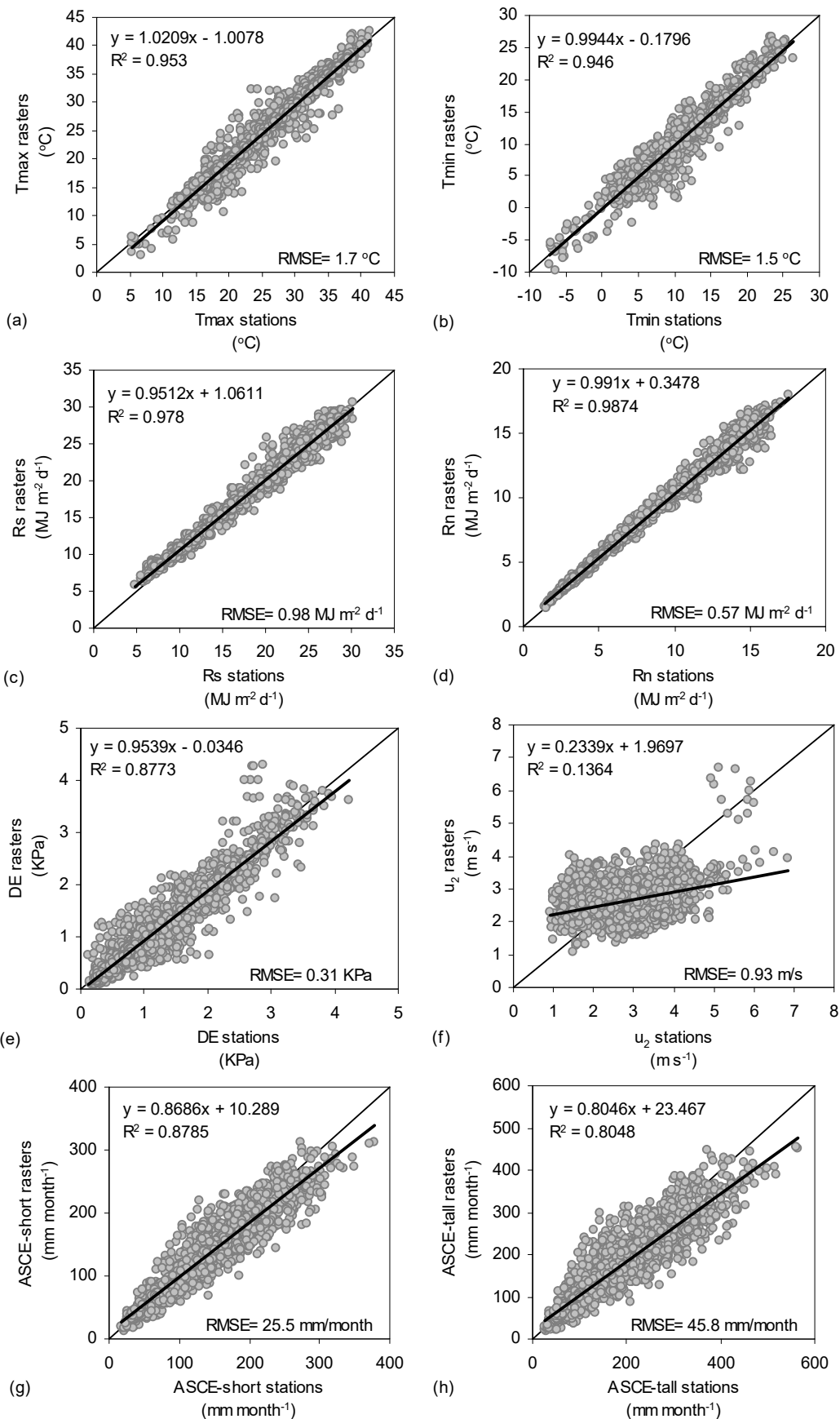


**Fig.S2** Comparison of  $T_{max}$ ,  $T_{min}$ ,  $R_s$ ,  $R_n$ ,  $DE$  (vapour pressure deficit),  $u_2$ ,  $ET_o$  ASCE-short, and  $ET_o$  ASCE-tall between the rasters (0.5 degree resolution) and the stations data.

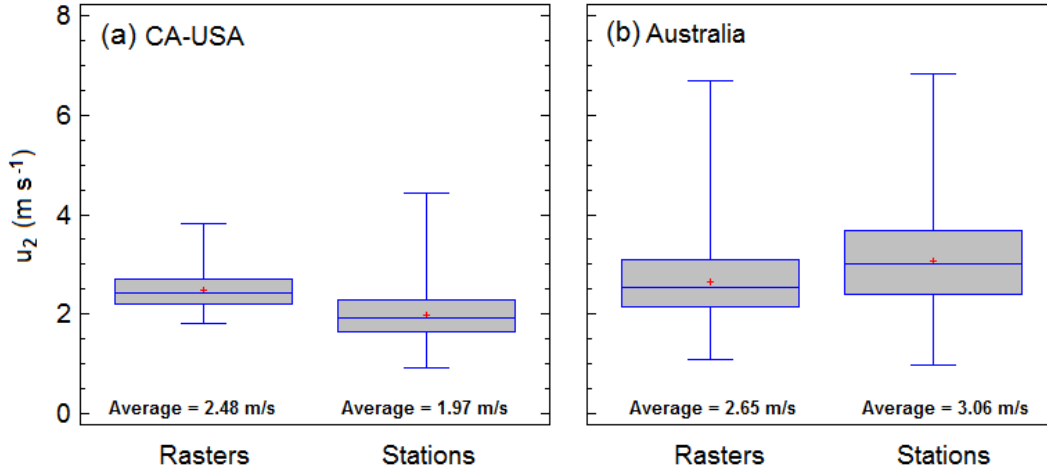


**Fig.S3** Comparison of total averages of mean monthly  $u_2$  values through Box-Whisker plots: a) between rasters (Sheffield et al., 2006) and California-USA stations, b) between rasters (Sheffield et al., 2006) and Australia stations.

*Extracted values of the p.w.a. coefficients for each station in the validation dataset.*

**Table S2.** Partial weighted averages of mean monthly coefficients ( $a_{pt}$ ,  $c_{hs2}$ ,  $K_{RS}$ ) for each station extracted by the 0.5 degree resolution maps.

No.	Code	Station	Country	$a_{pt}$ p.w.a.s. (0.5 deg)	$a_{pt}$ p.w.a.t. (0.5 deg)	$c_{hs2}$ p.w.a.s. (0.5 deg)	$c_{hs2}$ p.w.a.t. (0.5 deg)	$K_{RS}$ p.w.a. (0.5 deg)
CA-1	006	Davis	USA-CA	1.45	1.93	0.0022	0.0029	0.16
CA-2	002	FivePoints	USA-CA	1.53	2.06	0.0023	0.0030	0.16
CA-3	005	Shafter	USA-CA	1.48	1.97	0.0023	0.0031	0.16
CA-4	007	Firebaugh/Telles	USA-CA	1.48	1.99	0.0022	0.0029	0.15
CA-5	012	Durham	USA-CA	1.49	2.01	0.0024	0.0031	0.16
CA-6	008	Gerber	USA-CA	1.46	1.96	0.0023	0.0031	0.16
CA-7	015	Stratford	USA-CA	1.47	1.95	0.0023	0.0030	0.16
CA-8	019	Castroville	USA-CA	1.20	1.53	0.0023	0.0029	0.18
CA-9	021	Kettleman	USA-CA	1.49	1.99	0.0022	0.0030	0.15
CA-10	027	Zamora	USA-CA	1.45	1.93	0.0022	0.0029	0.16
CA-11	030	Nicolaus	USA-CA	1.45	1.93	0.0022	0.0029	0.16
CA-12	032	Colusa	USA-CA	1.49	2.01	0.0023	0.0030	0.15
CA-13	033	Visalia	USA-CA	1.48	1.96	0.0023	0.0031	0.16
CA-14	035	Bishop	USA-CA	1.71	2.38	0.0026	0.0036	0.15
CA-15	039	Parlier	USA-CA	1.45	1.92	0.0023	0.0030	0.16
CA-16	041	Calipatria/Mulberry	USA-CA	1.79	2.50	0.0025	0.0036	0.15
CA-17	043	McArthur	USA-CA	1.31	1.70	0.0022	0.0029	0.15
CA-18	044	U.C.Riverside	USA-CA	1.68	2.35	0.0025	0.0035	0.16
CA-19	047	Brentwood	USA-CA	1.45	1.94	0.0023	0.0030	0.16
CA-20	049	Oceanside	USA-CA	1.62	2.26	0.0029	0.0040	0.18
CA-21	054	Blackwells Corner	USA-CA	1.49	1.99	0.0022	0.0030	0.15
CA-22	056	Los Banos	USA-CA	1.47	1.95	0.0023	0.0030	0.16
CA-23	061	Orland	USA-CA	1.45	1.94	0.0023	0.0030	0.16
CA-24	062	Temecula	USA-CA	1.62	2.26	0.0029	0.0040	0.18
CA-25	064	Santa Ynez	USA-CA	1.36	1.81	0.0024	0.0032	0.17
CA-26	068	Seeley	USA-CA	1.93	2.76	0.0026	0.0037	0.15
CA-27	070	Manteca	USA-CA	1.43	1.89	0.0023	0.0030	0.16
CA-28	071	Modesto	USA-CA	1.43	1.89	0.0023	0.0030	0.16

CA-29	077	Oakville	USA-CA	1.37	1.82	0.0023	0.0030	0.16
CA-30	075	Irvine	USA-CA	1.65	2.29	0.0027	0.0038	0.17
CA-31	078	Pomona	USA-CA	1.72	2.39	0.0027	0.0038	0.16
CA-32	080	Fresno State	USA-CA	1.45	1.92	0.0023	0.0030	0.16
CA-33	083	Santa Rosa	USA-CA	1.24	1.63	0.0021	0.0027	0.16
CA-34	084	Browns Valley	USA-CA	1.45	1.93	0.0024	0.0031	0.17
CA-35	085	Hopland F.S.	USA-CA	1.38	1.87	0.0021	0.0028	0.15
CA-36	086	Lindcove	USA-CA	1.48	1.96	0.0023	0.0031	0.16
CA-37	087	Meloland	USA-CA	1.91	2.71	0.0025	0.0036	0.14
CA-38	088	Cuyama	USA-CA	1.37	1.81	0.0025	0.0033	0.17
CA-39	091	Tulelake F.S.	USA-CA	1.39	1.81	0.0022	0.0029	0.15
CA-40	092	Kesterson	USA-CA	1.47	1.95	0.0023	0.0030	0.16
CA-41	094	Goletta foothills	USA-CA	1.37	1.81	0.0025	0.0033	0.17
CA-42	099	Santa Monica	USA-CA	1.63	2.24	0.0027	0.0037	0.17
CA-43	103	Windsor	USA-CA	1.28	1.68	0.0021	0.0028	0.16
CA-44	104	De Laveaga	USA-CA	1.20	1.53	0.0023	0.0029	0.18
CA-45	105	Westlands	USA-CA	1.48	1.97	0.0023	0.0030	0.16
CA-46	106	Sanel Valley	USA-CA	1.10	1.39	0.0019	0.0024	0.16
CA-47	57	Buntingville	USA-CA	1.55	2.11	0.0023	0.0031	0.15
CA-48	90	Alturas	USA-CA	1.33	1.74	0.0023	0.0030	0.15
CA-49	151	Ripley	USA-CA	2.01	2.88	0.0028	0.0040	0.16
CA-50	183	Owens Lake North	USA-CA	1.43	1.89	0.0026	0.0034	0.17
CA-51	147	Otay Lake	USA-CA	1.71	2.39	0.0026	0.0037	0.15
CA-52	175	Palo Verde II	USA-CA	1.98	2.84	0.0027	0.0038	0.15
CA-53	135	Blynthe NE	USA-CA	2.01	2.88	0.0028	0.0040	0.16
CA-54	155	Bryte	USA-CA	1.45	1.93	0.0022	0.0029	0.16
CA-55	159	Monrovia	USA-CA	1.72	2.39	0.0027	0.0038	0.16
CA-56	161	Patterson	USA-CA	1.48	1.98	0.0023	0.0030	0.16
CA-57	174	Long Beach	USA-CA	1.52	2.08	0.0029	0.0040	0.20
CA-58	173	Torrey Pines	USA-CA	1.62	2.26	0.0029	0.0040	0.18
CA-59	150	Miramar	USA-CA	1.62	2.26	0.0029	0.0040	0.18
CA-60	153	Escondido SPV	USA-CA	1.62	2.24	0.0025	0.0035	0.16
A-1	32040	Townsville Aero	Australia	1.28	1.66	0.0026	0.0033	0.19
A-2	33307	Woolshed	Australia	1.28	1.66	0.0026	0.0033	0.19
A-3	2056	Kununurra Aero	Australia	1.56	2.11	0.0025	0.0034	0.18
A-4	35264	Emerald	Australia	1.29	1.63	0.0021	0.0027	0.16
A-5	24024	Loxton R.C.	Australia	1.63	2.21	0.0024	0.0032	0.15
A-6	74037	Yanco AG.I.	Australia	1.48	1.95	0.0023	0.0031	0.16
A-7	74258	Deniliquin Airp.AWS	Australia	1.49	1.99	0.0023	0.0030	0.16
A-8	75041	Griffith Airp.AWS	Australia	1.51	2.02	0.0024	0.0032	0.16
A-9	76031	Mildura Airp.	Australia	1.67	2.30	0.0025	0.0034	0.16
A-10	24048	Renmark Apt.1	Australia	1.63	2.21	0.0024	0.0032	0.15
A-11	40082	University of QLD G.	Australia	1.27	1.63	0.0021	0.0027	0.16
A-12	40922	Kingaroy Airp.	Australia	1.23	1.56	0.0021	0.0026	0.16
A-13	41359	Oakey Aero	Australia	1.23	1.55	0.0021	0.0026	0.16
A-14	41522	Dalby Airp.	Australia	1.26	1.60	0.0021	0.0026	0.16
A-15	41525	Warwick	Australia	1.22	1.55	0.0021	0.0027	0.16
A-16	41529	Toowoomba Airp.	Australia	1.25	1.58	0.0021	0.0026	0.16
A-17	80091	Kyabram	Australia	1.43	1.88	0.0022	0.0030	0.16
A-18	81049	Tatura I.S.A.	Australia	1.43	1.88	0.0022	0.0030	0.16
A-19	81124	Yarrawonga	Australia	1.39	1.80	0.0022	0.0028	0.15
A-20	81125	Shepparton Airp.	Australia	1.43	1.88	0.0022	0.0030	0.16
A-21	41175	Applethorpe	Australia	1.20	1.49	0.0021	0.0026	0.16
A-22	81123	Bendigo Airp.	Australia	1.43	1.89	0.0023	0.0030	0.15
A-23	85072	East sale Airp.	Australia	1.34	1.80	0.0023	0.0031	0.16
A-24	85279	Bairnsdale Airp.	Australia	1.40	1.88	0.0024	0.0032	0.16
A-25	85280	Morwell L.V.Airp.	Australia	1.38	1.86	0.0023	0.0031	0.15

A-26	85296	Mount Moornapa	Australia	1.43	1.94	0.0023	0.0031	0.15
A-27	90035	Colac	Australia	1.46	2.00	0.0024	0.0033	0.16
A-28	9538	Dwellingup	Australia	1.36	1.80	0.0023	0.0031	0.17
A-29	9617	Bridgetown	Australia	1.32	1.73	0.0022	0.0029	0.16
A-30	23373	Nuriootpa Pirs	Australia	1.54	2.07	0.0024	0.0032	0.16
A-31	26021	Mount Gambier Aero	Australia	1.38	1.85	0.0024	0.0032	0.16
A-32	26091	Coonawarra	Australia	1.49	2.03	0.0023	0.0032	0.15
A-33	66062	Sydney (Obs.Hill)	Australia	1.18	1.52	0.0022	0.0029	0.17
A-34	33002	Ayr DPI Res.St.	Australia	1.22	1.54	0.0023	0.0029	0.18
A-35	7176	Newman Aero	Australia	2.04	2.94	0.0031	0.0044	0.18
A-36	13017	Giles	Australia	2.18	3.20	0.0032	0.0046	0.17
A-37	11052	Forrest	Australia	1.78	2.52	0.0027	0.0038	0.15
A-38	11003	Eucla	Australia	1.68	2.39	0.0029	0.0041	0.17
A-39	12071	Salmon Gums	Australia	1.65	2.28	0.0027	0.0038	0.16
A-40	7045	Meekatharra Airp.	Australia	1.98	2.84	0.0031	0.0044	0.18
A-41	1025	Doongan	Australia	1.38	1.82	0.0027	0.0035	0.19
A-42	2012	Halls Creek Airp.	Australia	1.72	2.39	0.0025	0.0034	0.17
A-43	13015	Carnegie	Australia	2.12	3.09	0.0030	0.0044	0.17
A-44	3080	Curtin Aero	Australia	1.59	2.17	0.0026	0.0036	0.18
A-45	6022	Gascoyne Junction	Australia	1.97	2.83	0.0029	0.0041	0.17
A-46	9789	Esperance	Australia	1.53	2.12	0.0027	0.0038	0.17
A-47	91223	Marrawah	Australia	1.10	1.47	0.0023	0.0030	0.19
A-48	18106	Nullarbor	Australia	1.77	2.52	0.0027	0.0039	0.16
A-49	16090	Coober Pedy Airp.	Australia	2.05	2.98	0.0030	0.0044	0.17
A-50	16085	Marla Police St.	Australia	2.05	2.98	0.0030	0.0044	0.17
A-51	13011	Warburton Airfield	Australia	2.19	3.22	0.0031	0.0046	0.17
A-52	15528	Yuendumu	Australia	2.14	3.13	0.0032	0.0046	0.17
A-53	15666	Rabbit Flat	Australia	2.15	3.14	0.0029	0.0042	0.16
A-54	14829	Lajamanu Airp.	Australia	1.85	2.63	0.0026	0.0036	0.17
A-55	15135	Tennant Creek Airp.	Australia	2.05	2.98	0.0031	0.0045	0.18
A-56	37010	Camooweal Township	Australia	1.93	2.78	0.0027	0.0038	0.16
A-57	14707	Wollogorang	Australia	1.56	2.12	0.0028	0.0037	0.19
A-58	14938	Mango Farm	Australia	1.37	1.79	0.0023	0.0030	0.17
A-59	69134	Batemans Bay	Australia	1.19	1.51	0.0021	0.0027	0.16
A-60	14198	Jabiru Airp.	Australia	1.28	1.60	0.0023	0.0028	0.18
A-61	28008	Lockhart River Airp.	Australia	1.27	1.63	0.0026	0.0033	0.19
A-62	34084	Charters Towers Airp.	Australia	1.27	1.60	0.0022	0.0028	0.17
A-63	29038	Kowanyama Airp.	Australia	1.29	1.65	0.0024	0.0030	0.19
A-64	32078	Ingham Composite	Australia	1.34	1.76	0.0025	0.0032	0.18
A-65	40854	Logan City W.T.P.	Australia	1.33	1.79	0.0023	0.0031	0.17
A-66	8095	Mullewa	Australia	1.78	2.51	0.0027	0.0038	0.16
A-67	8251	Kalbarri	Australia	1.58	2.18	0.0028	0.0038	0.18
A-68	8225	Eneabba	Australia	1.82	2.60	0.0029	0.0041	0.17
A-69	7139	Paynes Find	Australia	1.81	2.54	0.0027	0.0038	0.17
A-70	10007	Bencubbin	Australia	1.61	2.20	0.0025	0.0034	0.16
A-71	10092	Merredin	Australia	1.62	2.21	0.0025	0.0035	0.16
A-72	12038	Kalgoorlie-Boulder Airp.	Australia	1.79	2.52	0.0028	0.0040	0.17
A-73	16098	Tarcoola Aero	Australia	1.95	2.80	0.0028	0.0041	0.16
A-74	18195	Minnipa Pirs	Australia	1.73	2.44	0.0027	0.0038	0.16
A-75	46126	Tibooburra Airp.	Australia	2.02	2.92	0.0029	0.0042	0.17
A-76	48245	Boorke Airp. AWS	Australia	1.68	2.30	0.0025	0.0034	0.16
A-77	55325	Tamworth Airp. AWS	Australia	1.21	1.48	0.0020	0.0024	0.15
A-78	38026	Birdsville Airp.	Australia	2.36	3.52	0.0032	0.0047	0.16
A-79	30161	Richmond Airp.	Australia	1.64	2.25	0.0024	0.0033	0.16
A-80	33013	Collinsville Airp.	Australia	1.38	1.81	0.0024	0.0031	0.17

**Table S3.** Ranking of models for each criterion (1 is the best, 12 is the worst).

Model	MAE	RMSE	NRMSE%	PBIAS%	R <sup>2</sup>	bR <sup>2</sup>	NSE	d	KGE
P-T (Eq.2) with $a_{pt}=1.26$	12	12	12	12	12	12	12	12	12
P-T (Eq.2) with $a_{pt}=p.w.a.s.$	9	7	5	7	10	6	5	6	4
H-S (Eq.4b) with $c_{hs2}=0.0023$	7	9	9	9	9	10	9	9	9
H-S (Eq.4b) with $c_{hs2}=p.w.a.s.$	4	4	4	2	6	4	4	4	2
DRAL1 (Eq.8)	5	6	7	5	8	8	7	7	6
DRAL2 (Eq.9)	10	8	8	3	11	9	8	8	3
Copais (Eq.10)	3	3	3	6	4	5	3	3	7
VAL1 (Eq.11)	8	10	11	10	7	11	11	10	11
VAL2 (Eq.12)	2	2	2	4	3	2	2	2	5
VAL3 (Eq.13)	1	1	1	1	2	1	1	1	1
AKJ1 (Eq.14)	6	5	6	8	1	3	6	5	8
AKJ2 (Eq.15)	11	11	10	11	5	7	10	11	10

*Analysis of Dc (distance from the coastline) and DT (difference between max and min monthly temperature) effects on  $K_{RS}$  coefficient.*

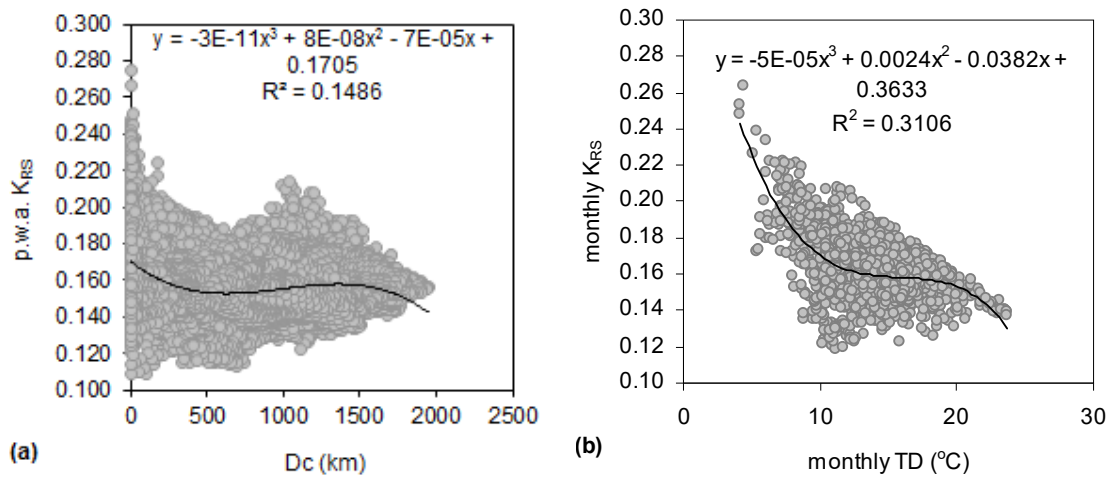


**Fig.S4** Correlation between (a) p.w.a.  $K_{RS}$  and  $Dc$  (59031 observations derived by 0.5 degree resolution maps, all regions included except Greenland that showed extremely high  $K_{RS}$  values in inland areas, see Fig.7 in the manuscript) and (b) monthly  $K_{RS}$  and monthly  $TD$  values (1680 mean monthly observations derived by the 140 stations of Table 1 in the manuscript).

**Example case using the Hargreaves-Samani method of evapotranspiration for the stations of California with revised coefficients.**

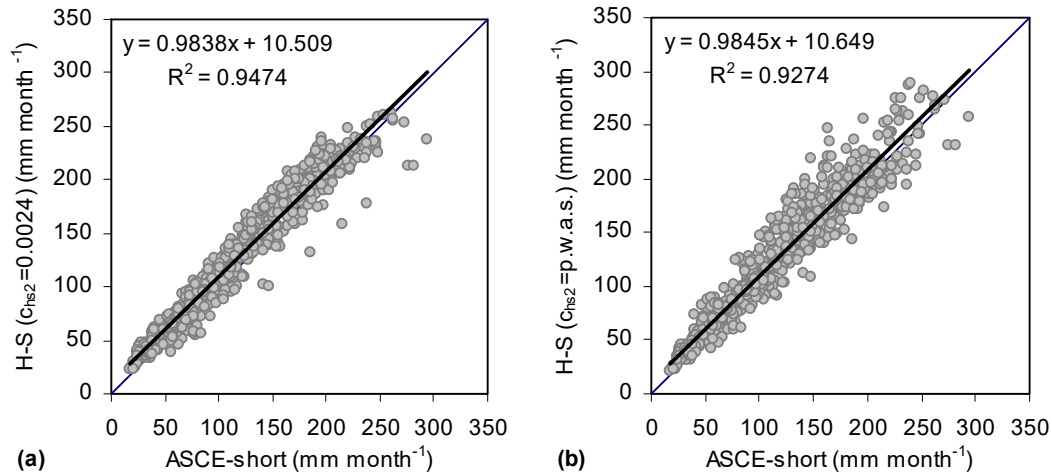


**Fig.S5** Comparative 1:1 plots between the results of ASCE-short versus **(a)** the H-S method with  $c_{hs2}=0.0024$  (mean value of p.w.a.s.  $c_{hs2}$  coefficients of all California stations obtained from Table S.2), **(b)** the H-S method using the individual values of  $c_{hs2}=p.w.a.s.$  for each station of California stations (Table S.2).

**Table S4.** Statistical criteria from the respective comparisons given in Fig.S5.

Criterion	Optimum value	H-S vs. ASCE-short	
		H-S (Eq.4b) with $c_{hs2}=0.0024$	H-S (Eq.4b) with $c_{hs2}=p.w.a.s.$
MAE	0	13.237*	14.297
RMSE	0	16.693*	19.119
NRMSE%	0	26.900*	30.500
PBIAS%	0	-7.100*	-7.200
$R^2$	1	0.947*	0.927
$bR^2$	1	0.887*	0.863
NSE	1	0.928*	0.907
d	1	0.982*	0.976
KGE	1	0.924*	0.916

\*The asterisk is used to indicate the best value of each criterion.

**Attributes of the datasets provided in the context of this study**

**Table S5.** Contents of the database produced in this study (all five resolutions are included: 30 arc-sec, 2.5 arc-min, 5 arc-min, 10 arc-min, 0.5 deg.). The order of contents follows the alphabetical order of file names as they are stored in PANGAEA (<https://doi.pangaea.de/10.1594/PANGAEA.868808>)

No.	Content/resolution	File name	Method	Comment
1	Re-adjusted Priestley-Taylor coefficient for short ref.crop ETo (rescaled $\times 100$ ) (unitless)/(30 arc-sec)	apts1_30s.zip	Re-calibration of Priestley-Taylor coefficient $apt=1.26$ for ETo method (Priestley and Taylor, 1972) using ASCE-EWRI method (Allen et al., 2005) for short ref.crop	the zip contains 1 raster (ESRI-grid) (partial weighted average of mean monthly values). For zero values use the closest non-zero value.
2	Re-adjusted Priestley-Taylor coefficient for tall ref.crop ETo (rescaled $\times 100$ ) (unitless)/(30 arc-sec)	aptt1_30s.zip	Re-calibration of Priestley-Taylor coefficient $apt=1.26$ for ETo method (Priestley and Taylor, 1972) using ASCE-EWRI method (Allen et al., 2005) for tall ref.crop	the zip contains 1 raster (ESRI-grid) (partial weighted average of mean monthly values). For zero values use the closest non-zero value.
3	Re-adjusted Hargreaves-Samani coefficient for short ref.crop ETo (rescaled $\times 100,000$ ) (unitless)/(30 arc-sec)	chs2s1_30s.zip	Re-calibration of Hargreaves-Samani coefficient $chs2=0.0023$ for ETo method (Hargreaves and Samani, 1982, 1985) using ASCE-EWRI method (Allen et al., 2005) for short ref.crop	the zip contains 1 raster (ESRI-grid) (partial weighted average of mean monthly values). For zero values use the closest non-zero value.
4	Re-adjusted Hargreaves-Samani coefficient for tall ref.crop ETo (rescaled $\times 100,000$ ) (unitless)/(30 arc-sec)	chs2t1_30s.zip	Re-calibration of Hargreaves-Samani coefficient $chs2=0.0023$ for ETo method (Hargreaves and Samani, 1982, 1985) using ASCE-EWRI method (Allen et al., 2005) for tall ref.crop	the zip contains 1 raster (ESRI-grid) (partial weighted average of mean monthly values). For zero values use the closest non-zero value.
5	Hargreaves-Samani versus Priestley-Taylor (comparison between original methods versus ASCE-short) (DMADhp) (%) (30 arc-sec)	dmadhp1_30s.zip	$abs(madhs)-abs(madpt)$ , higher negative values suggest better performance of original Hargreaves-Samani ETo method while higher positive values suggest better performance of original Priestley-Taylor ETo method using as reference the ASCE-short	the zip contains 1 raster (ESRI-grid)
6	Mean monthly ASCE-ETo for short reference crop (clipped grass) (mm/month)/(30 arc-sec)	etos1_30s.zip	ASCE-EWRI method (Allen et al., 2005) using climatic data from Hijmans et al. (2005) and Sheffield et al. (2006)	the zip contains 12 rasters (ESRI-grids) for each month (January is the first month)
7	Mean monthly ASCE-ETo for tall reference crop (alfalfa) (mm/month)/(30 arc-sec)	etot1_30s.zip	ASCE-EWRI method (Allen et al., 2005) using climatic data from Hijmans et al. (2005) and Sheffield et al. (2006)	the zip contains 12 rasters (ESRI-grids) for each month (January is the first month)
8	Re-adjusted coefficient for solar radiation formula of Hargreaves-Samani (rescaled $\times 1000$ ) (unitless)/(30 arc-sec)	krs1_30s.zip	Re-calibration of Hargreaves-Samani coefficient $krs=0.16-0.19$ for solar radiation formula (Hargreaves and Samani, 1982, 1985) using solar radiation data (from Sheffield et al., 2006)	the zip contains 1 raster (ESRI-grid) (partial weighted average of mean monthly values)

9	Expected Mean Annual Difference/Error (MAD%) between original Hargreaves-Samani ETo and ASCE-ETo for short ref.crop (%) / (30 arc-sec)	madhs1_30s.zip	$100 * [(Annual\ ETo\ H-S) - (Annual\ ETo\ ASCE-short)] / (Annual\ ETo\ ASCE-short)$ , Annual ETo H-S is estimated with the typical value $chs2=0.0023$	the zip contains 1 raster (ESRI-grid)
10	Expected Mean Annual Difference/Error (MAD%) between original Priestley-Taylor ETo and ASCE-ETo for short ref.crop (%) / (30 arc-sec)	madpt1_30s.zip	$100 * [(Annual\ ETo\ P-T) - (Annual\ ETo\ ASCE-short)] / (Annual\ ETo\ ASCE-short)$ , Annual ETo P-T is estimated with the typical value $apt=1.26$	the zip contains 1 raster (ESRI-grid)
11	Expected Mean Annual Difference/Error (MAD%) between original Hargreaves-Samani radiation formula versus solar radiation data (%) / (30 arc-sec)	madrs1_30s.zip	$100 * [(Annual\ RS\ of\ H-S) - (Annual\ RS\ data)] / (Annual\ RS\ data)$ , Annual RS H-S is estimated with the typical value $krs=0.17$ and RS obtained from Sheffield et al. (2006)	the zip contains 1 raster (ESRI-grid)
12	Re-adjusted Priestley-Taylor coefficient for short ref.crop ETo (rescaled $\times 100$ ) (unitless) / (2.5 arc-min)	apts2_2-5m.zip	Re-calibration of Priestley-Taylor coefficient $apt=1.26$ for ETo method (Priestley and Taylor, 1972) using ASCE-EWRI method (Allen et al., 2005) for short ref.crop	the zip contains 1 raster (ESRI-grid) (partial weighted average of mean monthly values)
13	Re-adjusted Priestley-Taylor coefficient for tall ref.crop ETo (rescaled $\times 100$ ) (unitless) / (2.5 arc-min)	aptt2_2-5m.zip	Re-calibration of Priestley-Taylor coefficient $apt=1.26$ for ETo method (Priestley and Taylor, 1972) using ASCE-EWRI method (Allen et al., 2005) for tall ref.crop	the zip contains 1 raster (ESRI-grid) (partial weighted average of mean monthly values)
14	Re-adjusted Hargreaves-Samani coefficient for short ref.crop ETo (rescaled $\times 100,000$ ) (unitless) / (2.5 arc-min)	chs2s2_2-5m.zip	Re-calibration of Hargreaves-Samani coefficient $chs2=0.0023$ for ETo method (Hargreaves and Samani, 1982, 1985) using ASCE-EWRI method (Allen et al., 2005) for short ref.crop	the zip contains 1 raster (ESRI-grid) (partial weighted average of mean monthly values)
15	Re-adjusted Hargreaves-Samani coefficient for tall ref.crop ETo (rescaled $\times 100,000$ ) (unitless) / (2.5 arc-min)	chs2t2_2-5m.zip	Re-calibration of Hargreaves-Samani coefficient $chs2=0.0023$ for ETo method (Hargreaves and Samani, 1982, 1985) using ASCE-EWRI method (Allen et al., 2005) for tall ref.crop	the zip contains 1 raster (ESRI-grid) (partial weighted average of mean monthly values)
16	Hargreaves-Samani versus Priestley-Taylor (comparison between original methods versus ASCE-short) (DMADhp) (%) / (2.5 arc-min)	dmdhp2_2-5m.zip	$abs(madhs) - abs(madpt)$ , higher negative values suggest better performance of original Hargreaves-Samani ETo method while higher positive values suggest better performance of original Priestley-Taylor ETo method using as reference the ASCE-short	the zip contains 1 raster (ESRI-grid)
17	Mean monthly ASCE-ETo for short reference crop (clipped grass) (mm/month) / (2.5 arc-min)	etos2_2-5m.zip	ASCE-EWRI method (Allen et al., 2005) using climatic data from Hijmans et al. (2005) and Sheffield et al. (2006)	the zip contains 12 rasters (ESRI-grids) for each month (January is the first month)

18	Mean monthly ASCE-ETo for tall reference crop (alfalfa) (mm/month)/(2.5 arc-min)	etot2_2-5m.zip	ASCE-EWRI method (Allen et al., 2005) using climatic data from Hijmans et al. (2005) and Sheffield et al. (2006)	the zip contains 12 rasters (ESRI-grids) for each month (January is the first month)
19	Re-adjusted coefficient for solar radiation formula of Hargreaves-Samani (rescaled $\times 1000$ ) (unitless)/(2.5 arc-min)	krs2_2-5m.zip	Re-calibration of Hargreaves-Samani coefficient $krs=0.16-0.19$ for solar radiation formula (Hargreaves and Samani, 1982, 1985) using solar radiation data (from Sheffield et al., 2006)	the zip contains 1 raster (ESRI-grid) (partial weighted average of mean monthly values)
20	Expected Mean Annual Difference/Error (MAD%) between original Hargreaves-Samani ETo and ASCE-ETo for short ref.crop (%) (2.5 arc-min)	madhs2_2-5m.zip	$100 * [(Annual\ ETo\ H-S) - (Annual\ ETo\ ASCE-short)] / (Annual\ ETo\ ASCE-short)$ , Annual ETo H-S is estimated with the typical value $chs2=0.0023$	the zip contains 1 raster (ESRI-grid)
21	Expected Mean Annual Difference/Error (MAD%) between original Priestley-Taylor ETo and ASCE-ETo for short ref.crop (%) (2.5 arc-min)	madpt2_2-5m.zip	$100 * [(Annual\ ETo\ P-T) - (Annual\ ETo\ ASCE-short)] / (Annual\ ETo\ ASCE-short)$ , Annual ETo P-T is estimated with the typical value $apt=1.26$	the zip contains 1 raster (ESRI-grid)
22	Expected Mean Annual Difference/Error (MAD%) between original Hargreaves-Samani radiation formula versus solar radiation data (%) (2.5 arc-min)	madrs2_2-5m.zip	$100 * [(Annual\ RS\ of\ H-S) - (Annual\ RS\ data)] / (Annual\ RS\ data)$ , Annual RS H-S is estimated with the typical value $krs=0.17$ and RS obtained from Sheffield et al. (2006)	the zip contains 1 raster (ESRI-grid)
23	Re-adjusted Priestley-Taylor coefficient for short ref.crop ETo (rescaled $\times 100$ ) (unitless)/(5 arc-min)	apts3_5m.zip	Re-calibration of Priestley-Taylor coefficient $apt=1.26$ for ETo method (Priestley and Taylor, 1972) using ASCE-EWRI method (Allen et al., 2005) for short ref.crop	the zip contains 1 raster (ESRI-grid) (partial weighted average of mean monthly values)
24	Re-adjusted Priestley-Taylor coefficient for tall ref.crop ETo (rescaled $\times 100$ ) (unitless)/(5 arc-min)	aptt3_5m.zip	Re-calibration of Priestley-Taylor coefficient $apt=1.26$ for ETo method (Priestley and Taylor, 1972) using ASCE-EWRI method (Allen et al., 2005) for tall ref.crop	the zip contains 1 raster (ESRI-grid) (partial weighted average of mean monthly values)
25	Re-adjusted Hargreaves-Samani coefficient for short ref.crop ETo (rescaled $\times 100,000$ ) (unitless)/(5 arc-min)	chs2s3_5m.zip	Re-calibration of Hargreaves-Samani coefficient $chs2=0.0023$ for ETo method (Hargreaves and Samani, 1982, 1985) using ASCE-EWRI method (Allen et al., 2005) for short ref.crop	the zip contains 1 raster (ESRI-grid) (partial weighted average of mean monthly values)
26	Re-adjusted Hargreaves-Samani coefficient for tall ref.crop ETo (rescaled $\times 100,000$ ) (unitless)/(5 arc-min)	chs2t3_5m.zip	Re-calibration of Hargreaves-Samani coefficient $chs2=0.0023$ for ETo method (Hargreaves and Samani, 1982, 1985) using ASCE-EWRI method (Allen et al., 2005) for tall ref.crop	the zip contains 1 raster (ESRI-grid) (partial weighted average of mean monthly values)

27	Hargeaves-Samani versus Priestley-Taylor (comparison between original methods versus ASCE-short) (DMADhp) (%) / (5 arc-min)	dmadhp3_5m.zip	abs(madhs)-abs(madpt), higher negative values suggest better performance of original Hargreaves-Samani ETo method while higher positive values suggest better performance of original Priestley-Taylor ETo method using as reference the ASCE-short	the zip contains 1 raster (ESRI-grid)
28	Mean monthly ASCE-ETo for short reference crop (clipped grass) (mm/month) / (5 arc-min)	etos3_5m.zip	ASCE-EWRI method (Allen et al., 2005) using climatic data from Hijmans et al. (2005) and Sheffield et al. (2006)	the zip contains 12 rasters (ESRI-grids) for each month (January is the first month)
29	Mean monthly ASCE-ETo for tall reference crop (alfalfa) (mm/month) / (5 arc-min)	etos3_5m.zip	ASCE-EWRI method (Allen et al., 2005) using climatic data from Hijmans et al. (2005) and Sheffield et al. (2006)	the zip contains 12 rasters (ESRI-grids) for each month (January is the first month)
30	Re-adjusted coefficient for solar radiation formula of Hargreaves-Samani (rescaled $\times 1000$ ) (unitless) / (5 arc-min)	krs3_5m.zip	Re-calibration of Hargreaves-Samani coefficient krs=0.16-0.19 for solar radiation formula (Hargreaves and Samani, 1982, 1985) using solar radiation data (from Sheffield et al., 2006)	the zip contains 1 raster (ESRI-grid) (partial weighted average of mean monthly values)
31	Expected Mean Annual Difference/Error (MAD%) between original Hargreaves-Samani ETo and ASCE-ETo for short ref.crop (%) / (5 arc-min)	madhs3_5m.zip	$100 * [(Annual\ ETo\ H-S) - (Annual\ ETo\ ASCE-short)] / (Annual\ ETo\ ASCE-short)$ , Annual ETo H-S is estimated with the typical value chs2=0.0023	the zip contains 1 raster (ESRI-grid)
32	Expected Mean Annual Difference/Error (MAD%) between original Priestley-Taylor ETo and ASCE-ETo for short ref.crop (%) / (5 arc-min)	madpt3_5m.zip	$100 * [(Annual\ ETo\ P-T) - (Annual\ ETo\ ASCE-short)] / (Annual\ ETo\ ASCE-short)$ , Annual ETo P-T is estimated with the typical value apt=1.26	the zip contains 1 raster (ESRI-grid)
33	Expected Mean Annual Difference/Error (MAD%) between original Hargreaves-Samani radiation formula versus solar radiation data (%) / (5 arc-min)	madrs3_5m.zip	$100 * [(Annual\ RS\ of\ H-S) - (Annual\ RS\ data)] / (Annual\ RS\ data)$ , Annual RS H-S is estimated with the typical value krs=0.17 and RS obtained from Sheffield et al. (2006)	the zip contains 1 raster (ESRI-grid)
34	Re-adjusted Priestley-Taylor coefficient for short ref.crop ETo (rescaled $\times 100$ ) (unitless) / (10 arc-min)	apts4_10m.zip	Re-calibration of Priestley-Taylor coefficient apt=1.26 for ETo method (Priestley and Taylor, 1972) using ASCE-EWRI method (Allen et al., 2005) for short ref.crop	the zip contains 1 raster (ESRI-grid) (partial weighted average of mean monthly values)
35	Re-adjusted Priestley-Taylor coefficient for tall ref.crop ETo (rescaled $\times 100$ ) (unitless) / (10 arc-min)	aptt4_10m.zip	Re-calibration of Priestley-Taylor coefficient apt=1.26 for ETo method (Priestley and Taylor, 1972) using ASCE-EWRI method (Allen et al., 2005) for tall ref.crop	the zip contains 1 raster (ESRI-grid) (partial weighted average of mean monthly values)

36	Re-adjusted Hargreaves-Samani coefficient for short ref.crop ETo (rescaled $\times 100,000$ ) (unitless)/(10 arc-min)	chs2s4_10m.zip	Re-calibration of Hargreaves-Samani coefficient chs2=0.0023 for ETo method (Hargreaves and Samani, 1982, 1985) using ASCE-EWRI method (Allen et al., 2005) for short ref.crop	the zip contains 1 raster (ESRI-grid) (partial weighted average of mean monthly values)
37	Re-adjusted Hargreaves-Samani coefficient for tall ref.crop ETo (rescaled $\times 100,000$ ) (unitless)/(10 arc-min)	chs2t4_10m.zip	Re-calibration of Hargreaves-Samani coefficient chs2=0.0023 for ETo method (Hargreaves and Samani, 1982, 1985) using ASCE-EWRI method (Allen et al., 2005) for tall ref.crop	the zip contains 1 raster (ESRI-grid) (partial weighted average of mean monthly values)
38	Hargreaves-Samani versus Priestley-Taylor (comparison between original methods versus ASCE-short) (DMADhp) (%) (10 arc-min)	dmadhp4_10m.zip	abs(madhs)-abs(madpt), higher negative values suggest better performance of original Hargreaves-Samani ETo method while higher positive values suggest better performance of original Priestley-Taylor ETo method using as reference the ASCE-short	the zip contains 1 raster (ESRI-grid)
39	Mean monthly ASCE-ETo for short reference crop (clipped grass) (mm/month)/(10 arc-min)	etos4_10m.zip	ASCE-EWRI method (Allen et al., 2005) using climatic data from Hijmans et al. (2005) and Sheffield et al. (2006)	the zip contains 12 rasters (ESRI-grids) for each month (January is the first month)
40	Mean monthly ASCE-ETo for tall reference crop (alfalfa) (mm/month)/(10 arc-min)	etot4_10m.zip	ASCE-EWRI method (Allen et al., 2005) using climatic data from Hijmans et al. (2005) and Sheffield et al. (2006)	the zip contains 12 rasters (ESRI-grids) for each month (January is the first month)
41	Re-adjusted coefficient for solar radiation formula of Hargreaves-Samani (rescaled $\times 1000$ ) (unitless)/(10 arc-min)	krs4_10m.zip	Re-calibration of Hargreaves-Samani coefficient krs=0.16-0.19 for solar radiation formula (Hargreaves and Samani, 1982, 1985) using solar radiation data (from Sheffield et al., 2006)	the zip contains 1 raster (ESRI-grid) (partial weighted average of mean monthly values)
42	Expected Mean Annual Difference/Error (MAD%) between original Hargreaves-Samani ETo and ASCE-ETo for short ref.crop (%) (10 arc-min)	madhs4_10m.zip	$100 * [(Annual\ ETo\ H-S) - (Annual\ ETo\ ASCE-short)] / (Annual\ ETo\ ASCE-short)$ , Annual ETo H-S is estimated with the typical value chs2=0.0023	the zip contains 1 raster (ESRI-grid)
43	Expected Mean Annual Difference/Error (MAD%) between original Priestley-Taylor ETo and ASCE-ETo for short ref.crop (%) (10 arc-min)	madpt4_10m.zip	$100 * [(Annual\ ETo\ P-T) - (Annual\ ETo\ ASCE-short)] / (Annual\ ETo\ ASCE-short)$ , Annual ETo P-T is estimated with the typical value apt=1.26	the zip contains 1 raster (ESRI-grid)
44	Expected Mean Annual Difference/Error (MAD%) between original Hargreaves-Samani radiation formula versus solar radiation data (%) (10 arc-min)	madrs4_10m.zip	$100 * [(Annual\ RS\ of\ H-S) - (Annual\ RS\ data)] / (Annual\ RS\ data)$ , Annual RS H-S is estimated with the typical value krs=0.17 and RS obtained from Sheffield et al. (2006)	the zip contains 1 raster (ESRI-grid)

45	Re-adjusted Priestley-Taylor coefficient for short ref.crop ETo (rescaled $\times 100$ ) (unitless)/(0.5 deg)	apts5_0-5d.zip	Re-calibration of Priestley-Taylor coefficient $apt=1.26$ for ETo method (Priestley and Taylor, 1972) using ASCE-EWRI method (Allen et al., 2005) for short ref.crop	the zip contains 1 raster (ESRI-grid) (partial weighted average of mean monthly values)
46	Re-adjusted Priestley-Taylor coefficient for tall ref.crop ETo (rescaled $\times 100$ ) (unitless)/(0.5 deg)	aptt5_0-5d.zip	Re-calibration of Priestley-Taylor coefficient $apt=1.26$ for ETo method (Priestley and Taylor, 1972) using ASCE-EWRI method (Allen et al., 2005) for tall ref.crop	the zip contains 1 raster (ESRI-grid) (partial weighted average of mean monthly values)
47	Re-adjusted Hargreaves-Samani coefficient for short ref.crop ETo (rescaled $\times 100,000$ ) (unitless)/(0.5 deg)	chs2s5_0-5d.zip	Re-calibration of Hargreaves-Samani coefficient $chs2=0.0023$ for ETo method (Hargreaves and Samani, 1982, 1985) using ASCE-EWRI method (Allen et al., 2005) for short ref.crop	the zip contains 1 raster (ESRI-grid) (partial weighted average of mean monthly values)
48	Re-adjusted Hargreaves-Samani coefficient for tall ref.crop ETo (rescaled $\times 100,000$ ) (unitless)/(0.5 deg)	chs2t5_0-5d.zip	Re-calibration of Hargreaves-Samani coefficient $chs2=0.0023$ for ETo method (Hargreaves and Samani, 1982, 1985) using ASCE-EWRI method (Allen et al., 2005) for tall ref.crop	the zip contains 1 raster (ESRI-grid) (partial weighted average of mean monthly values)
49	Hargeaves-Samani versus Priestley-Taylor (comparison between original methods versus ASCE-short) (DMADhp) (%) / (0.5 deg)	dmdhp5_0-5d.zip	$abs(madhs)-abs(madpt)$ , higher negative values suggest better performance of original Hargreaves-Samani ETo method while higher positive values suggest better performance of original Priestley-Taylor ETo method using as reference the ASCE-short	the zip contains 1 raster (ESRI-grid)
50	Mean monthly ASCE-ETo for short reference crop (clipped grass) (mm/month)/(0.5 deg)	etos5_0-5d.zip	ASCE-EWRI method (Allen et al., 2005) using climatic data from Hijmans et al. (2005) and Sheffield et al. (2006)	the zip contains 12 rasters (ESRI-grids) for each month (January is the first month)
51	Mean monthly ASCE-ETo for tall reference crop (alfalfa) (mm/month)/(0.5 deg)	etot5_0-5d.zip	ASCE-EWRI method (Allen et al., 2005) using climatic data from Hijmans et al. (2005) and Sheffield et al. (2006)	the zip contains 12 rasters (ESRI-grids) for each month (January is the first month)
52	Re-adjusted coefficient for solar radiation formula of Hargreaves-Samani (rescaled $\times 1000$ ) (unitless)/(0.5 deg)	krs5_0-5d.zip	Re-calibration of Hargreaves-Samani coefficient $krs=0.16-0.19$ for solar radiation formula (Hargreaves and Samani, 1982, 1985) using solar radiation data (from Sheffield et al., 2006)	the zip contains 1 raster (ESRI-grid) (partial weighted average of mean monthly values)
53	Expected Mean Annual Difference/Error (MAD%) between original Hargreaves-Samani ETo and ASCE-ETo for short ref.crop (%) / (0.5 deg)	madhs5_0-5d.zip	$100 * [(Annual\ ETo\ H-S) - (Annual\ ETo\ ASCE-short)] / (Annual\ ETo\ ASCE-short)$ , Annual ETo H-S is estimated with the typical value $chs2=0.0023$	the zip contains 1 raster (ESRI-grid)

54	Expected Mean Annual Difference/Error (MAD%) between original Priestley-Taylor ETo and ASCE-ETo for short ref.crop (%)/(0.5 deg)	madpt5_0-5d.zip	100*[(Annual ETo P-T)-(Annual ETo ASCE-short)]/(Annual ETo ASCE-short), Annual ETo P-T is estimated with the typical value apt=1.26	the zip contains 1 raster (ESRI-grid)
55	Expected Mean Annual Difference/Error (MAD%) between original Hargreaves-Samani radiation formula versus solar radiation data (%)/(0.5 deg)	madr5_0-5d.zip	100*[(Annual RS of H-S)-(Annual RS data)]/(Annual RS data), Annual RS H-S is estimated with the typical value krs=0.17 and RS obtained from Sheffield et al. (2006)	the zip contains 1 raster (ESRI-grid)